ABSTRACT

Title of Document:	GOLD DISTRIBUTION IN THE ARCHEAN TANZANIAN CRATON: EVALUATING THE EFFECTS OF INTRACRUSTAL DIFFERENTIATION
	Kristy Jeanne Long, Master of Science, 2013
Directed By:	Professor Roberta L. Rudnick, Geology Professor William F. McDonough, Geology

This study evaluates the vertical distribution of gold in the continental crust. Implementing a recently published method by Pitcairn et al. (2006a) for the chromatographic separation of gold from acid-digested rocks using diisobutyl ketone (DIBK), followed by analysis using standard addition inductively coupled plasma mass spectrometry (ICP-MS), high- and low-grade metamorphic rocks of the Tanzanian Craton, representative of the lower and upper crust, respectively, are analyzed to determine the distribution of gold in the crust. Greenstone belt basalts have the highest gold concentrations (ave.=60 (+193/-19) ng/g), followed by greenstone belt andesites (ave.=1.4 (+3.6/-0.6) ng/g). The lowest concentrations are observed in granulite-facies lower-crustal xenoliths (ave.=0.4 (+1.0/-0.1) ng/g). Gold is incompatible in silicates and can partition into hydrothermal and/or magmatic fluid during high-grade metamorphic dehydration reactions or partial melting, particularly

if sulfides break down during these processes. Rise of buoyant mobile phases may explain the depletion of gold in the lower crust.

GOLD DISTRIBUTION IN THE ARCHEAN TANZANIAN CRATON: EVALUATING THE EFFECTS OF INTRACRUSTAL DIFFERENTIATION

By

Kristy Jeanne Long

Thesis submitted to the Faculty of the Graduate School of the
University of Maryland, College Park, in partial fulfillment
of the requirements for the degree of
Master of Science
2013

Advisory Committee:
Professor Roberta L. Rudnick, Co-Chair
Professor William F. McDonough, Co-Chair
Professor Philip A. Candela
Research Associate Richard Gaschnig

Acknowledgements

I would like to acknowledge my thesis committee, including Dr. Roberta L. Rudnick, Dr. William F. McDonough, Dr. Philip Candela, and Dr. Richard Gaschnig, for their insight and patience. I would like to thank Dr. Philip Candela for conversations about metamorphic fluids, Dr. Richard Gaschnig for continuous help with all of my questions and help in the plasma lab, Dr. Richard Ash for constant help trouble-shooting in the plasma lab, and Dr. Philip Piccoli for finding the time to help me with my SEM work. I would also like to show my utmost appreciation for the help received by Dr. Shukrani Manya in supplying powdered rock samples at short notice, and the email support from Dr. Iain Pitcairn as I tried to develop his method here at the University of Maryland. Finally, I would like to thank my fellow graduate students and my family and friends for their encouragement.

This research was funded in part by the Society of Economic Geologists Canada Foundation, Graduate Student Fellowship.

Table of Contents

List of Tables

List of Figures

Chapter 1: Introduction

1.1

Gold is a precious metal with a market value oscillating around $1600 USD per troy ounce (31.1 g) over the past year. Gold's primary uses are as a store of value, due to its stable market value, and as jewelry. It is also used in electronics due to its high electrical conductivity and chemical stability. The economic importance of gold has led to numerous studies on the formation of gold deposits. Studying the behaviour of gold during intracrustal differentiation and metamorphic and hydrothermal processes, particularly in the continental crust, is thus of interest to the mineral resources industry.

Gold is a highly siderophile element and, as such, is of interest as a tracer of planetary differentiation and evolution. Information on the distribution and behavior of gold in the Earth can help to further inform the study of planetary formation. Gold has a distribution coefficient between iron metal and silicate melt ($D^{\text{iron metal / silicate melt}}$) of ~300 at core/mantle boundary conditions (2588 K and fO_2 IW -2) (e.g., Brenan and McDonough 2009). Whereas the partitioning experiments of Brenan and McDonough (2009) were performed at 2 GPa, experiments performed from 0.1MPa to 23 GPa (Borisov and Palme, 1996; Danielson et al., 2005) agree with the results from Brenan and McDonough (2009) and indicate that pressure does not play a significant role in metal-silicate partitioning of gold. Due to gold's preference for Fe-metal, it is assumed to be concentrated in the Earth's core at a concentration of 500 nanograms per gram (ng/g) (McDonough, 2003). Gold is much less abundant in the Earth's silicate mantle and crust, in comparison to the core, at a concentration of approximately 1 ng/g (McDonough and Sun, 1995; Rudnick and Gao, 2003). The distribution coefficient for gold between olivine and basaltic melt, used as a proxy for the main phases present during mantle/crust differentiation, is $D^{\text{olivine/basaltic melt}} = \sim 0.002$ (1573 K and fO_2 FMQ), but gold can be retained in the mantle in the presence of phases such as sulfides that have a high affinity for gold (Brenan et al., 2005). Due to gold's preference for sulfur over silicate, it is also defined as a chalcophile element with a distribution coefficient between sulfide melt and silicate melt of $D^{\text{sulfide melt / silicate melt}} = \sim 15{,}000$ at partial melting conditions associated with the formation of mid-ocean ridge basalts (1473 K and fO_2 FMQ) (Peach et al., 1990). The sulfur concentration of the primitive upper mantle is suggested to be 250 μg/g (McDonough and Sun, 1995), which translates to a modal sulfide content in the upper mantle of approximately 0.07 wt% (based on the composition of pyrrhotite; $Fe_{(1-x)}S$ (x=0 to 0.2)). If the olivine content of the primitive upper mantle is approximately 60 wt% (e.g., Harris et al., 1967; McDonough, 1990), then the bulk distribution coefficient for gold between primitive mantle and basaltic melt would be $D^{\text{olivine and sulfide / silicate melt}} = \sim 15$. However, sulfur is an incompatible element during mantle melting (Morgan, 1986), and sulfides will melt preferentially. Thus, gold may become increasingly incompatible with degree of melting and may therefore be transferred to the continental crust during crust-mantle differentiation.

Gold distribution in the continental crust is of particular interest since it is the most accessible location for extracting gold as a resource. Average gold concentrations for the upper, middle, and lower continental crust are estimated to be 1.5 ng/g, 0.66 ng/g, and 1.6 ng/g, respectively (Rudnick and Gao, 2003, and references therein). These estimates are based on composite sampling of representative rocks taken over large areas in the Canadian Shield (Shaw et al., 1976, n=5 composites) and Central East China (Gao et al., 1998, n=17 composites). Other, more localized sampling has provided further gold concentration data in crustal rocks, as presented in Table A.1 (see Appendix) and Fig. 1.1. The majority of the data in Table A.1 are averages of gold data from a variety of crustal rock types from around the world representing more than 13,000 individual samples. A table of gold data for individual samples (Table A.2) from a subset of the literature sources for Table A.1 is included in Appendix A. Table A.2 represents this much more limited set of samples (n=654) compared to the more extensive average gold concentration data (Table A.1). Gold concentration data for crustal rocks follow an approximate log-normal distribution, yielding an average gold concentration of 2.6 (+11.3 / -0.6) ng/g with mean ln[Au] = 0.94 and median ln[Au] = 0.88 (Fig. 1a, n=180, based on averages of more than 13,000 analyses from around the world), whereas the average of the gold concentration for individual crustal samples in Table A.2 is 1.4 (+7.9 / -0.3) ng/g with mean ln[Au] = 0.18 and median ln[Au] = -0.09, indicating that the distribution in this case is more skewed (Fig. 1b, n=654).

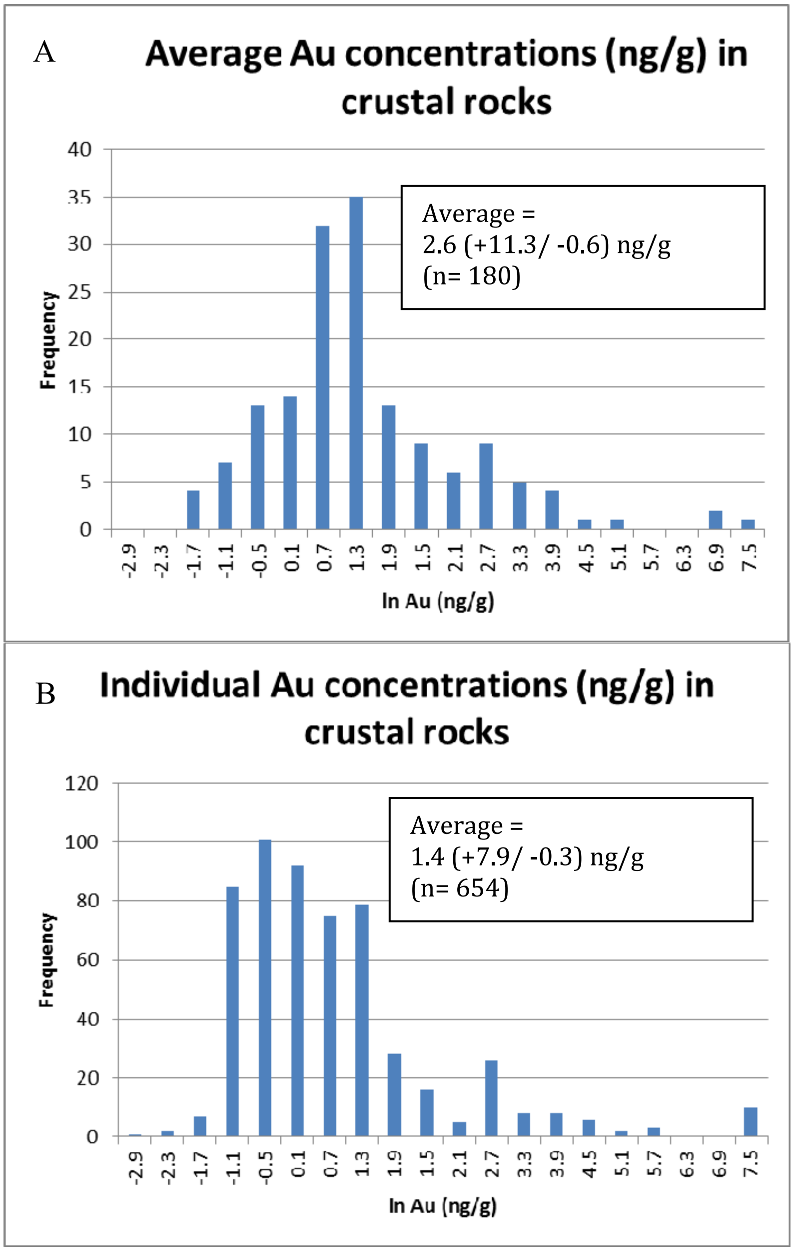

Figure 1.1: Approximate log-normal distribution of averaged and individual gold concentrations (A) and skewed log distribution of gold concentrations for individual crustal samples only (B). A: The average gold concentration of the crust based on all gold data is 2.6 (+11.3, -0.6) ng/g (n=180), representing averages of more than 13,000 analyses from around the world. B: Gold concentrations in individual samples; includes metamorphic, sedimentary, and igneous rocks ranging in composition from felsic to ultramafic. Average gold concentration is 1.4 (+7.9, -0.3) ng/g (n=654). Data and sources are in Tables A.1 and A.2 (see the Appendix).

Previous studies by Pitcairn et al. (2006b) and Cameron (1989, 1994), have suggested that gold may be depleted in the lower crust as a result of metamorphism.

Fluids produced during metamorphic dehydration reactions or partial melting associated with metamorphism may transport gold and other elements upward in the crust (e.g., Seward, 1973; Newton et al., 1980; Cameron 1988; Kerrich and Wyman, 1990; Phillips, 1993; Pitcairn et al., 2006b). Gold can be transported in mobile phases as thio- and chloro-complexes (Seward, 1973), and the solubility of gold is greatly increased with increasing sulfur content in the mobile phase (Seward, 1973; Boyle and Jonasson, 1984). Increasing fO_2, due to the presence of oxidizing H_2O-CO_2-rich fluids, can cause the dissolution of sulfide minerals, and the dissolved sulfide can then complex with Au^+ to create aqueous thio-gold-complexes (Seward, 1973; Cameron, 1989).

For example, the oxidized, H_2O-CO_2–rich fluids released during dehydration that accompanies the conversion of amphibolite-facies rocks to granulite-facies rocks, may ascend through the lower crust, causing depletion of large ion lithophile elements, such as Cs, K, Rb. Such fluids may also cause depletion of gold (Clough and Field, 1980; Cameron, 1989), since gold will complex with sulfur in fluids containing H_2S-H_2O-CO_2 (Phillips and Grove, 1983; Groves et al., 1984; Ho, 1984; Ho et al., 1985; Robert and Kelly, 1987; Phillips and Powell, 2010) under appropriate fO_2. The oxygen fugacity of gold-bearing fluids is thought to lie within the oxidized carbon/reduced sulfur field (Phillips and Powell, 2009, 2010) and concentrations of reduced sulfur in gold-bearing fluids from gold deposit sites have been calculated to be between 300 μg/g (Neall and Phillips, 1987) and 300 000 μg/g (Mikucki and Ridley, 1993). These observations suggest that gold may complex with sulfur in such metamorphic fluids and be lost to the rocks upon removal of the fluid.

Gold depletion may also occur at lower grades of metamorphism. Rocks at the transition between greenschist- to amphibolite-facies metamorphic conditions can yield fluids rich in H_2O-CO_2 during mineral break down (Fyfe et al., 1973; Clough and Field, 1980; Cameron, 1989; Phillips and Powell, 2010). Furthermore a decrease in modal sulfide has been observed with increasing metamorphic grade (Ferry, 1980; 1981; Binns et al., 1976; Ridley, 1995; Hughes et al., 1997; Pitcairn et al., 2006b). The devolatilization of mafic rocks during metamorphism from greenschist- to amphibolite-facies can, thus, produce H_2S-H_2O-CO_2-bearing fluids, in which gold can complex with bisulfide and be removed from the rocks (Phillips and Powell, 2010)

The movement of H_2S-H_2O-CO_2–rich fluids at lower-crustal depths can also lower the melting point of rocks and cause partial melting, which could also transport incompatible elements in the melt phase (Fyfe 1973; Cameron, 1988). Infiltration of meteoric or magmatic fluids into the deep crust is limited to zones of higher permeability (e.g., shear zones, extensional zones), and may be difficult to achieve in the ductile lower crust (Walther and Orville, 1982; Etheridge et al., 1984; Manning and Ingebritsen, 1999; Ague, 2003). Pervasive, as opposed to localized, depletion of gold in the lower crust may, therefore, be linked to generation of internally-derived metamorphic fluids (Fyfe et al., 1978; Walther and Orville, 1982, 1986; Etheridge et al., 1984; Yardley, 1986; Pitcairn et al., 2006b) or partial melts (Fyfe 1973). Transport of internally-derived metamorphic fluids or partial melts may occur along grain boundaries, and exploit metamorphic fabric development, such as foliation. Such fluids may eventually enter zones of higher permeability, such as shear zones or extensional zones (Walther and Orville, 1982; Cartwright and Oliver, 2000; Pitcairn et al., 2006b). If gold is dissolved in these oxidized metamorphic fluids or melts, which ascend upwards, this could lead to depletion of gold in the lower crust as a result of high-grade metamorphism.

Depletion of gold in the lower continental crust has been observed in the Bamble Belt of south Norway (Cameron, 1989), a major ductile shear zone. Here former lower crustal, mafic intrusive rocks exhibit an order of magnitude depletion in gold concentration compared to the crustal average (1-4 ng/g, Crocket, 1974; Korobeynikov, 1986; Rudnick and Gao, 2003), as well as a depletion in Rb, Sb, As, Cu and S (Cameron, 1989). The depletion of large ion lithophile elements (LILEs), such as rubidium in the Bamble Belt, however, has been associated with a separate depletion event than that which caused depletion of the gold (Cameron, 1994). Similarly, depletion of gold was found in the higher-grade metamorphic rocks of the Otago and Alpine schists of New Zealand, compared to their unmetamorphosed protoliths (Pitcairn et al., 2006b, Table 1.2).

When the metamorphic rocks from Table A.1 are separated by metamorphic grade, no relationship between gold concentration and metamorphic grade is observed (Table 1.1). However, Pitcairn et al. (2006b) showed that gold concentrations in metamorphosed rocks are lower than in their unmetamorphosed protoliths by a factor of 3.5 (Table 1.2). This would suggest gold depletion in the lower crust relative to the upper crust due to high-grade metamorphism.

Table 1.1: Gold concentration of metamorphic rocks. The average compositions show no discernible trend with gold concentration and increasing metamorphic grade. The average gold concentrations for each metamorphic grade are calculated based on the log-normal distribution.

	n	Range Au (ng/g)	Ave. Au (ng/g)	Error (1σ)	Author, Year
Low Grade Metamorphic Rocks					
Argillite and Slate	135	0.34 - 10	1	0.95	Crocket, 1974
Quartzofeldspathic Lower greenschist	12	0.01 - 1.31	0.34	0.41	Pitcairn et al., 2006b
Quartzofeldspathic Chlorite greenschist	17	0.06 - 0.38	0.23	0.11	Pitcairn et al., 2006b
Quartzofeldspathic Biotite greenschist	6	0.14 - 0.55	0.36	0.36	Pitcairn et al., 2006b
Quartzofeldspathic Garnet greenschist	7	0.07 - 0.6	0.21	0.21	Pitcairn et al., 2006b
Quartzofeldspathic Lower Greenschist	9	0.18 - 0.4	0.29	0.08	Pitcairn et al., 2006b
Quartzofeldspathic Chlorite Greenschist	9	0.15 - 0.19	0.15	0.01	Pitcairn et al., 2006b
Slate	10	<0.5 - 1.8	0.56	0.47	White and Goodwin, 2011
Average			**0.3**	**+ 0.6 / - 0.2**	
Medium Grade Metamorphic Rocks					
Schists	114	0.38 - 9	2.2	0.87	Crocket, 1974
Quartzofeldspathic Gar-Olig Amphibolite	8	0.13 - 0.38	0.22	0.10	Pitcairn et al., 2006b
Archean amphibolites	165		8.21		Gao et al., 1998
Amphibolite, Laget	11		0.37	0.25	Alirezaei&Cameron, 2002
Amphibolite, Tvedstrand	4		0.43	0.08	Alirezaei&Cameron, 2002
Amphibolite, Hisoy	3		0.38	0.09	Alirezaei&Cameron, 2002
Average			**0.8**	**+ 3.2 / - 0.2**	
High Grade Metamorphic Rocks					
Gneisses	37	0.2 - 22	3.9	3.55	Crocket, 1974
Mixed gniess, Hinnebu	32		0.15		Crocket, 1974; Korobeynikov, 1986
Tonalite gneiss, Tromoy	51		0.24		Crocket, 1974; Korobeynikov, 1986
Garnet gneiss, Arendal	13		0.37		Crocket, 1974; Korobeynikov, 1986
Felsic granulites (Charnockites)	5	<0.6 - 4.6	1.9	1.66	Sighinolfi and Gorgoni, 1977
Felsic granulites (Stronalithes)	5	1.4 - 6.7	3	2.15	Sighinolfi and Gorgoni, 1977
Mica-garnet gneiss	1		1.8		Degrazi and Haskin, 1964
Archean felsic granulites	116		1		Gao et al., 1998
Archean intermediate granulites	115		1.35		Gao et al., 1998
Archean mafic granulites	93		0.99		Gao et al., 1998
Acid granulites	42		0.57		Sighinolfi and Santos, 1976
Intermediate granulites	51		1.58		Sighinolfi and Santos, 1976
Mafic granulites	8		0.73		Sighinolfi and Santos, 1976
Average			**0.9**	**+ 2.5 / - 0.4**	

Table 1.2: Gold concentrations of protoliths and metamorphic equivalents from the Alpine and Otago schist, Torlesse and Caples terranes, New Zealand (Pitcairn et al., 2006b). The average gold concentrations are calculated using a log-normal distribution. The unmetamorphosed protoliths have higher gold contents by a factor of 3.5.

	n	Range Au (ng/g)	Ave. Au (ng/g)	Error (1σ)
Protoliths				
Quartzofeldspathic Protolith, Torlesse	13	0.22 - 1.7	0.56	0.4
Quartzofeldspathic Protolith, Caples	9	0.2 - 7	1.24	2.16
Average			**0.9**	**+ 1.5 / - 0.5**
Metamorphic Rocks				
Quartzofeldspathic Lower greenschist, Torlesse	12	0.01 - 1.31	0.34	0.41
Quartzofeldspathic Chlorite greenschist, Torlesse	17	0.06 - 0.38	0.23	0.11
Quartzofeldspathic Biotite greenschist, Torlesse	6	0.14 - 0.55	0.36	0.21
Quartzofeldspathic Garnet greenschist, Torlesse	7	0.07 - 0.6	0.21	0.17
Quartzofeldspathic Gar-Olig Amphibolite, Torlesse	8	0.13 - 0.38	0.22	0.1
Quartzofeldspathic Lower Greenschist, Caples	9	0.18 - 0.4	0.29	0.08
Quartzofeldspathic Chlorite Greenschist, Caples-Torlesse	9	0.15 - 0.19	0.15	0.01
Average			**0.26**	**+ 0.34 / - 0.18**

Data from Pitcairn et al. (2006b)

In this study, lower- and upper-crustal rocks from the Tanzanian craton and neighbouring Mozambique belt are analyzed to test the hypothesis that there is a difference in the gold concentration between the upper and the lower crust, which may be due to high-grade metamorphism and accompanying partial melting and dehydration processes. Gold concentrations in compositionally similar rocks derived from different depths in the continental crust from the same geographic region in Tanzania are analyzed: the deeper crust is sampled by granulite-facies xenoliths, whereas the upper crust is represented by greenstone belt basalts and andesites. The new data provide insight into the behaviour of gold during intracrustal differentiation and the process attending granulite-facies metamorphism of the deep crust.

Chapter 2: Samples

2.1

The samples investigated in this study include greenstone belt basalts and andesites (n=12) from the Archean Tanzanian Craton (comprising samples from the Musoma-Mara and Sukumaland greenstone belts, respectively, Figure 2.1 and Figure 2.2), and geographically-associated mafic lower crustal granulite-facies xenoliths (n=16) (Figure 2.1) carried in young basalts associated with the East African Rift. The xenoliths come from two volcanic vents, the on-craton Labait tuff-cone and the off-craton Naibor Soito basaltic tuff-cone (Figure 2.1). A genetic association has been proposed for the upper- and lower-crustal rocks due to their spatial relationship (Figure 2.1), similar major and trace element compositions, and coincident U-Pb ages (i.e., ca. 2660 Ma, within error of each other, Figure 2.3 (Manya et al., 2006; Mansur, 2008)).

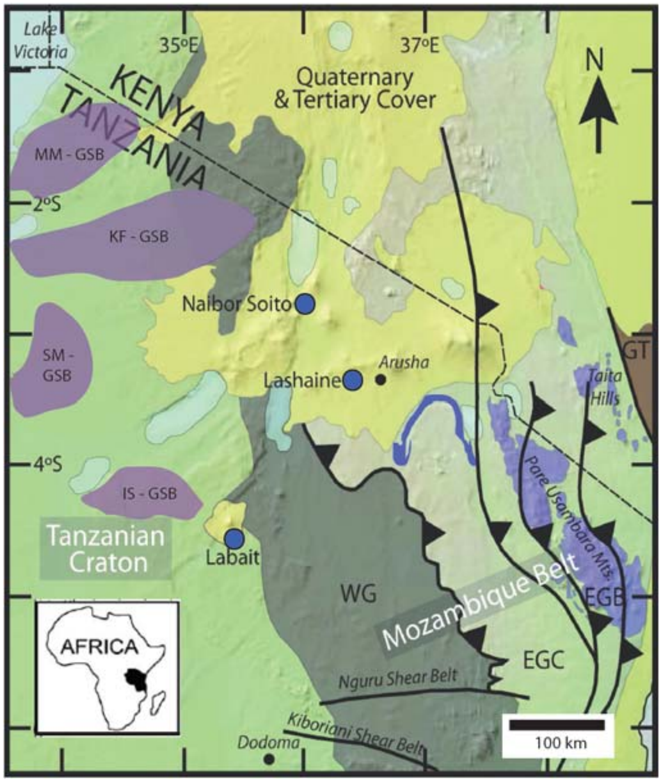

Figure 2.1: Geologic map of the northern area of the Tanzanian Craton. The blue dots indicate the xenolith locations, of which Labait and Naibor Soito samples were analyzed in this study. Purple areas labelled GSB indicate the locations of some of the greenstone belts in the area (MM-Musoma Mara, KF-Kilimafedha, SM-Shinyanga-Malita, IS-Irama Sekenke). Greenstone belt basalt and andesite samples analyzed in this study are from the Musoma-Mara (pictured here and Figure 2.2), and the Rwamagaza area in the Sukumaland (Figure 2.2) greenstone belts. (Image adapted from Blondes et al., 2013, and Mansur, 2008; greenstone belt locations from Manya, et al., 2006).

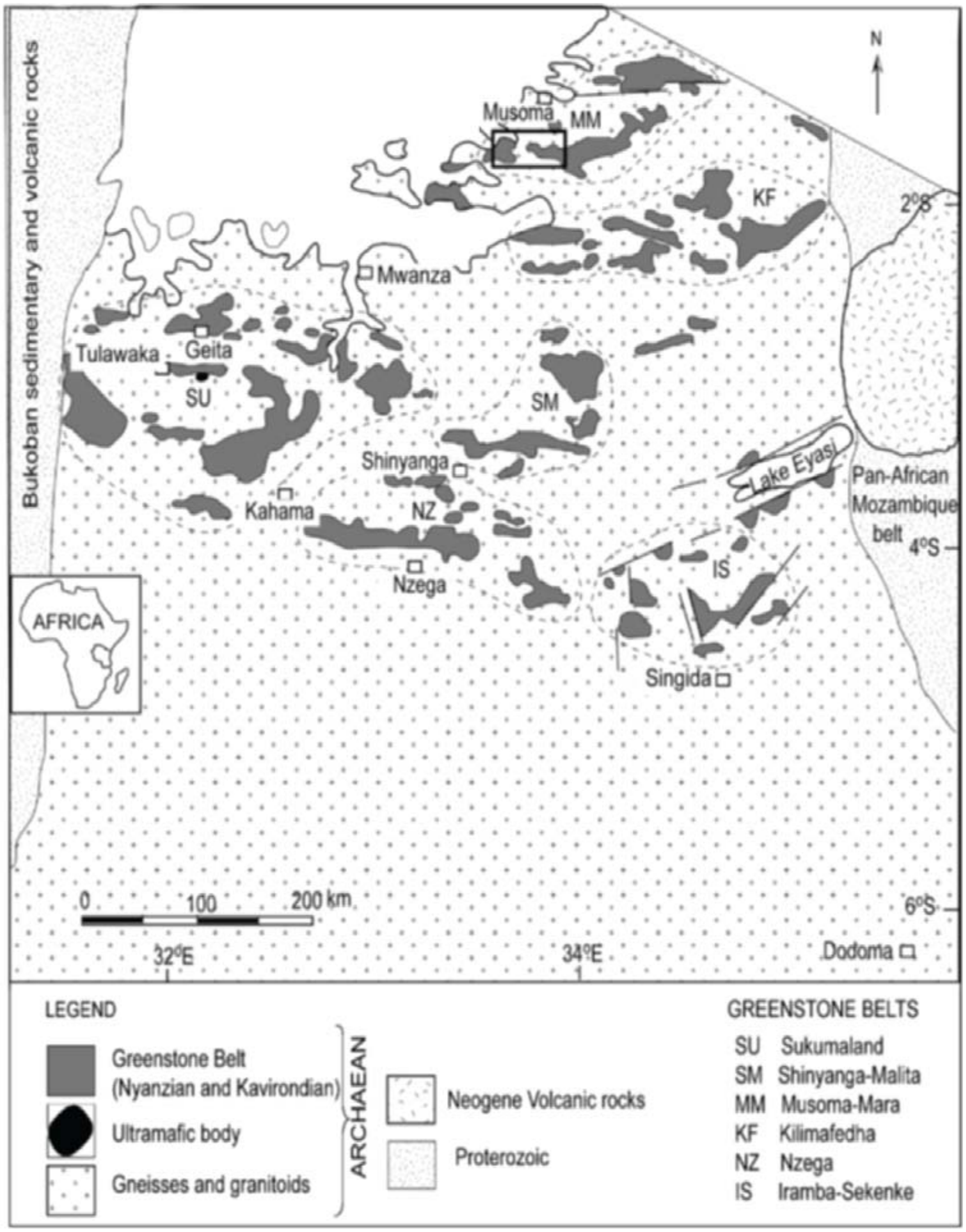

Figure 2.2: Detailed map of the greenstone belts (grey areas) of Northern Tanzania. Samples analyzed in this study are from Sukumaland (SU) and Musoma-Mara (MM) greenstone belts, from Manya et al., 2006.

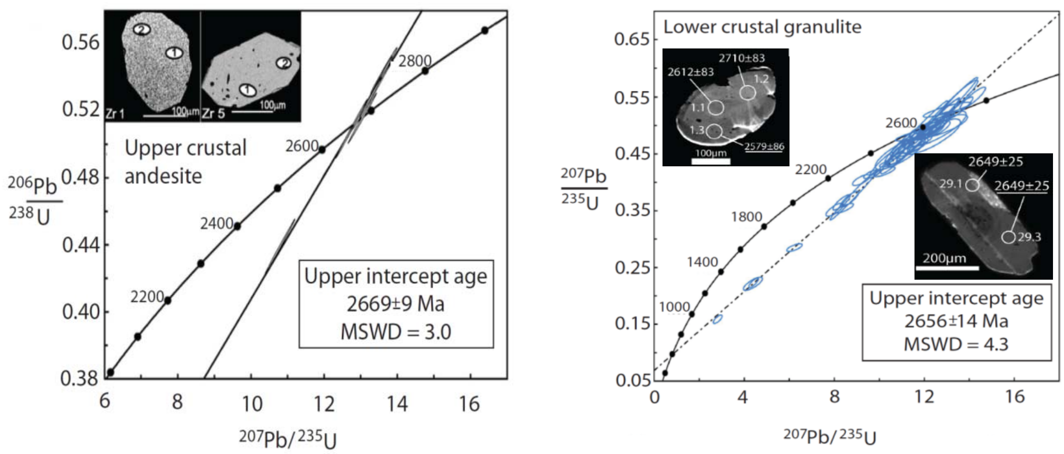

Figure 2.3: Concordia plots for zircons from an upper-crustal andesite from the Musoma-Mara greenstone belt (left) and a lower-crustal Naibor Soito two-pyroxene mafic granulite (right). (Figures from Manya et al., 2006 and Mansur, 2008 respectively).

The basalts (R 8, 9, 11, and 67) are sampled from the Rwamagaza area of the Sukumaland Greenstone Belt. They are part of a suite of basalts and basaltic andesites that include pillow basalts, which indicate sub-aqueous eruption (Manya and Maboko, 2003; Manya, 2004). The basalts and basaltic andesites show signs of mixed geochemical affinities and are interpreted to be derived from the partial melting of a heterogeneous mantle consisting of a mixture of two distinct components (Manya, 2004). A flat REE pattern associated with these rocks indicates shallow melting outside of the garnet stability field (Manya, 2004). The basalts and basaltic andesites have undergone greenschist-facies metamorphism, exhibited by the presence of chlorite and epidote (Quennell et al., 1956; Naylor, 1961; Manya and Maboko, 2003; Manya, 2004), as well as some hydrothermal alteration. All samples with loss on ignition (LOI) values greater than 3.5 wt% were discarded, so the selected samples represent the samples that are most likely to retain information of primary processes

(Manya, 2004). Further details concerning the basaltic samples can be found in Manya (2004), and Manya and Maboko (2003).

The andesites (TA 18, 20-23, 26, 41, and 96) come from the Musoma-Mara Greenstone Belt. They contain rare olivines, pyroxenes and hornblende, which have been altered to chlorite and epidote during greenschist-facies metamorphism (Manya et al., 2006). As was the case with the basaltic samples, all samples with LOI values greater than 3.5 wt% were discarded (Manya, et al., 2007). The high MgO content of some of the Musoma-Mara Greenstone Belt andesites compared to average island arc andesites, as well as their high Cr and Ni content, indicates that the magma was in equilibrium with mantle peridotite (Yogodzinski et al., 1995, Manya et al., 2007). The andesites also exhibit high heavy rare earth element (HREE) contents, which is inconsistent with partial melting of the subducting slab in equilibrium with residual garnet ± amphibole that would lead to depleted HREE patterns (Martin, 1999; Katz et al., 2004, Manya et al., 2007). The geochemical evidence thus suggests that the andesites were derived from flux-melting of the peridotitic mantle wedge due to slab-generated hydrous fluids (Manya, et al. 2007). The ε_{Nd} values for the andesites (+0.44 to +1.81, Manya et al., 2007) are lower than depleted mantle values (3.50, DePaolo et al., 1991) at 2.69 Ga, indicating that they may have experienced a small amount of contamination by older felsic crust (Manya et al., 2007). Further information about the Musoma-Mara samples can be found in Manya et al. (2006, 2007).

The lower-crustal granulite xenoliths derive from the craton-margin Labait melilitite tuff cone and the off-craton Naibor Soito basaltic tuff-cone. Xenoliths from Labait consist of mafic two-pyroxene granulites (LB04-19, 36, 52, 53, 65, and 93), one hornblende-bearing two-pyroxene granulite (LB04-82), and one garnet-orthopyroxene granulite (LB04-91) (Mansur, 2008). The two-pyroxene Labait granulites contain antiperthite (or plagioclase), orthopyroxene, clinopyroxene, ilmenite (± biotite, apatite, zircon, and monazite), with some alteration along grain boundaries and within the plagioclase, and some samples contain a weak foliation defined by pyroxene crystals (Mansur, 2008). The hornblende-bearing two-pyroxene granulite (LB04-82) has the same mineralogy, with the addition of hornblende that is in textural equilibrium with the pyroxenes and plagioclase (Mansur, 2008). The garnet-orthopyroxene granulite (LB04-91) contains plagioclase, garnet, quartz and orthopyroxene in mm-scale bands of garnet and plagioclase+quartz+orthopyroxene (Mansur, 2008).

The Naibor Soito tuff-cone is situated just off the Tanzanian Craton, in the Mozambique Belt. The samples consist of quartz-bearing (NS04-01, 05, 13, 73, 91, and 98) and quartz-free (NS04-61 and 82) mafic granulite xenoliths. The quartz-bearing granulites contain felsic bands of plagioclase, quartz, orthopyroxene, and minor clinopyroxene, and mafic bands of plagioclase, pyroxene, hornblende, biotite, garnet, and minor quartz (Mansur, 2008). The quartz-free granulites, however, are not banded and contain abundant ortho- and clino-pyroxene, and some plagioclase, garnet and ilmenite (Mansur, 2008). More information regarding both the Naibor Soito and Labait granulite xenolith suites can be found in Mansur (2008).

Granulites from both suites were examined for sulfides by reflected light microscopy. No sulfides were observed in the Labait granulites and the majority of the Naibor Soito granulites. Trace millimeter- to sub-millimeter-scale sulfide phases were observed in four samples from Naibor Soito (NS04 05, NS04 61, NS04 94, and NS04 150). Of these samples, only one (NS04 05) was analyzed for gold in this study. The sulfide-bearing granulites were imaged using back-scatter electron (BSE) imaging (Fig. 2.4). Energy dispersive x-ray spectroscopy (EDS) revealed that the sulfides are pyrite ringed with a thin rim of magnetite.

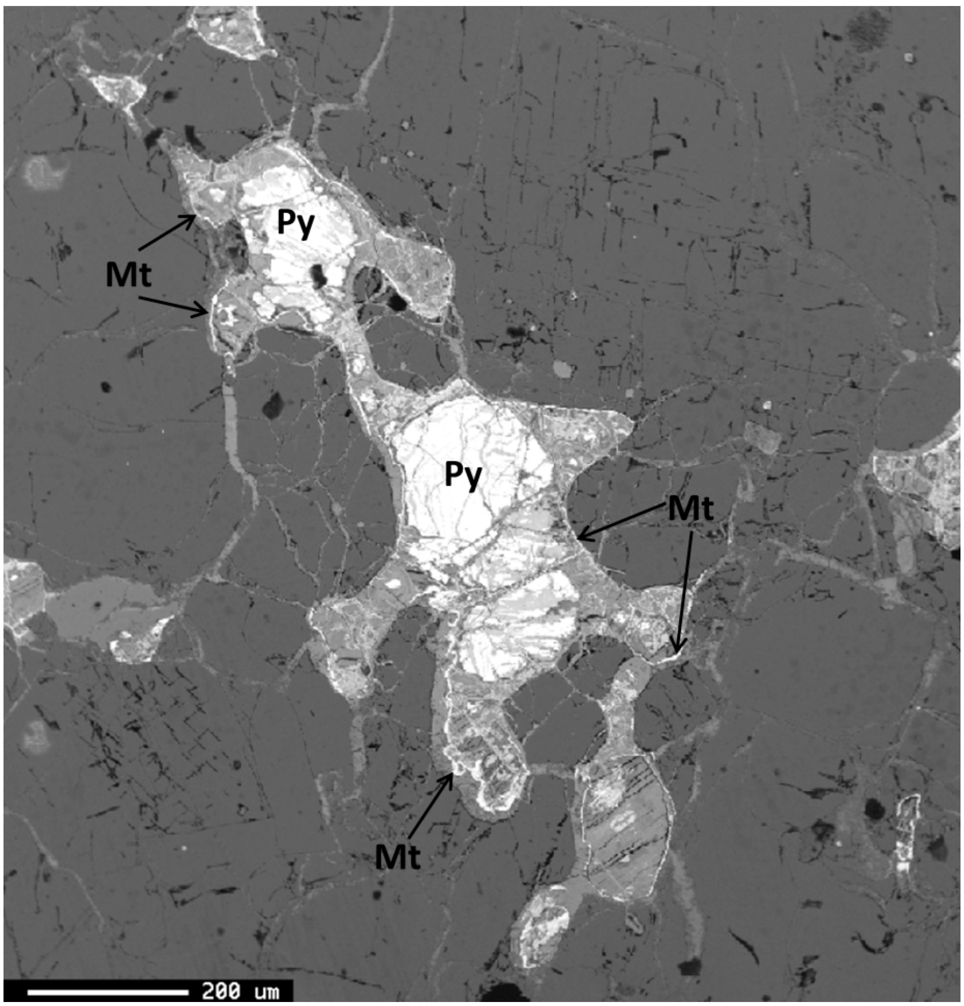

Fig 2.4: Back-scatter electron image of a fractured pyrite (Py) grain with a very thin rim (~5 µm thick) of magnetite (Mt) in sample NS04-05 a two-pyroxene mafic granulite xenolith from the Naibor Soito crater. The magnetite is the lighter coloured material on the outermost edge of the sulfide patch. The image is overexposed, minimizing the difference in brightness between pyrite and magnetite.

The upper- and lower-crustal rocks share similar trace element compositions (Mansur, 2008; Mtoro et al., 2009) (Figure 2.5). The greenstone belt andesites exhibit trace element patterns showing a relationship of increasing concentrations of the most highly incompatible lithophile elements during mantle melting (Figure 2.5). The lower crustal granulite xenoliths exhibit similar trace element patterns with increasing concentrations from the heavy rare earth elements (HREE) to the light rare earth elements (LREE), however, the granulite samples are significantly depleted in the highly incompatible elements Cs, Th, U, and sometimes Rb, by 1-2 orders of magnitude. This preferential depletion of some highly incompatible elements seen in the lower crustal mafic granulite xenoliths is unlike any signature seen in the volcanic rocks and could be related to partial melting or dehydration reactions associated with granulite-facies metamorphism (Mansur et al., 2008). This project seeks to determine whether gold is similarly depleted in the granulites, as some previous studies on metamorphic rocks have suggested (Cameron, 1989; Pitcairn et al., 2006b).

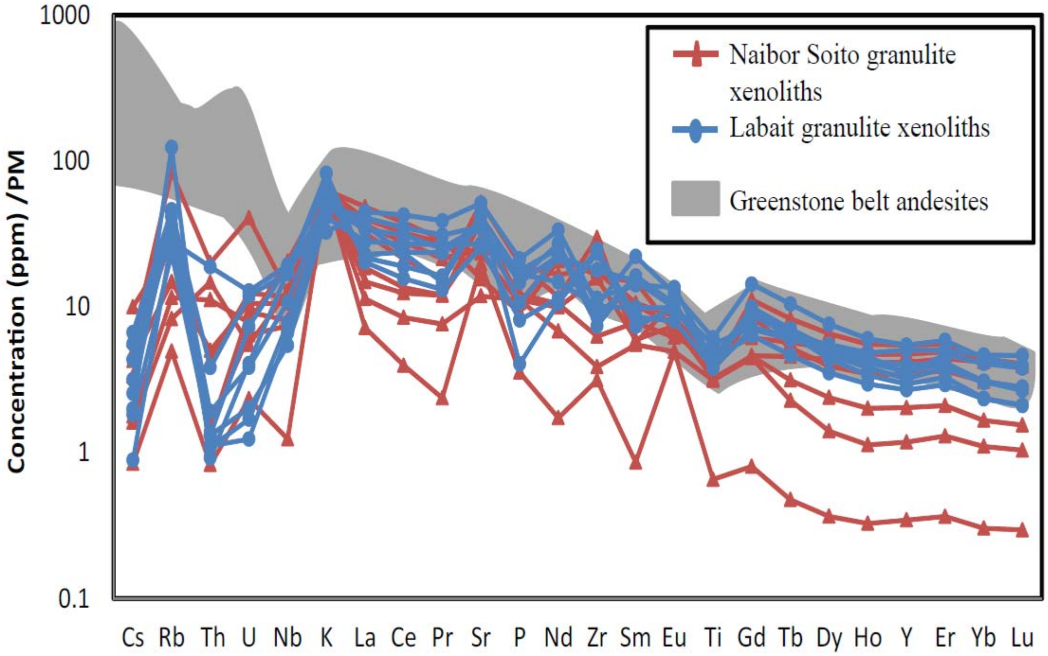

Figure 2.5: Primitive mantle normalized trace element plot of the upper-crustal greenstone belt lavas from Musoma-Mara greenstone belt (grey field; data from Manya et al., 2007) and lower-crustal mafic granulite xenoliths Naibor Soito (red; data from Mansur, 2008) and Labait (blue; data from Mansur, 2008) in the Archean Tanzanian Craton and adjacent Mozambique Belt.

The lithophile element compositions of the lower crustal xenoliths do not appear to have been altered by the rift basalts that entrained them (Mansur et al., 2008). The young rift basalts are enriched in incompatible lithophile elements and, had there been significant contamination of the xenoliths during their ascent, the xenoliths would not have maintained the strong and selective incompatible element depletion they exhibit (Mansur et al., 2008). By contrast, the magnetite rims around the pyrite grains in the Naibor Soito crater granulite xenoliths are evidence for oxidative breakdown of the sulfides. If this occurred as a consequence of the xenoliths' entrainment into the rift basalts, entrainment may have affected the chalcophile and siderophile element concentrations of the xenoliths, as discussed below.

Chapter 3: Methods

3.1: Introduction

The analytical method adopted here to determine the gold content of rocks and Certified Reference Materials (CRM) is modified from Pitcairn et al. (2006a). Whole rock powders were dissolved according to the sequence outlined in Table 3.1 and gold was extracted using diisobutyl ketone (DIBK) coated resin (see Table 3.2 for resin preparation method) in a chromatographic column (Table 3.3; Pitcairn et al., 2006a). Gold concentrations were analyzed using standard addition via inductively coupled plasma mass spectrometry (ICP-MS).

3.2: Cleaning, blanks, and acids

Gold is believed to be heterogeneously distributed in crustal rocks, which have a nominal concentration of 0.1-10 ng/g (see Table 1.1 in the Appendix). To address the potential problems of the "nugget effect" (i.e., high gold concentrations in micron-size and smaller discrete phases that are heterogeneously distributed in the sample powder), between 200 and 400 mg of whole rock powder was digested in each powder aliquot in order to determine whether differences in sample size affect the reproducibility of the analyses.

The amounts of reagents used in the treatment of this amount of sample will introduce a processing blank, which is foreign gold added to the sample before analyses. It is important to address issues of blank contribution by analyzing the total analytical blank that has undergone all of the analytical procedural steps associated with this method, (see Table 3.1). Average total analytical blank, based on 60 repeat analyses of 6 separate preparations of the total analytical blank is 3 picograms (pg) +/- 1 pg (1 σ). The 3 σ limit of detection using this method is therefore 6 pg Au. Sample solutions in this study are diluted 25 to 50 times, and the range of gold being analyzed in the samples is 5 ng to 8 pg, with most granulites containing ~15 pg. Total analytical blank TAB 2 was found to be anomalously high in gold (~30 pg) and was not processed during the preparation of any of the samples discussed in this study. It has therefore been excluded from the total analytical blank average.

Table 3.1: Gold concentration for the total analytical blank.

TAB #	Date prepared	Date analyzed	Au (ng/g)	1σ
TAB 1	18-Jun-12	19-Sep-12	0.0011	0.0002
TAB 1	18-Jun-12	11-Oct-12	0.0020	0.0002
TAB 1	18-Jun-12	01-Feb-13	0.0012	0.0002
TAB 1	18-Jun-12	01-Feb-13	0.0015	0.0003
TAB 1	18-Jun-12	01-Feb-13	0.0011	0.0002
TAB 1	18-Jun-12	01-Feb-13	0.0011	0.0002
TAB 1	18-Jun-12	10-Feb-13	0.0013	0.0003
TAB 1	18-Jun-12	10-Feb-13	0.0012	0.0002
TAB 1	18-Jun-12	10-Feb-13	0.0010	0.0002
TAB 1	18-Jun-12	11-Feb-13	0.0012	0.0003
TAB 3	14-Nov-12	28-Nov-12	0.0033	0.0007
TAB 3	14-Nov-12	14-Dec-12	0.0036	0.0004
TAB 3	14-Nov-12	14-Dec-12	0.0031	0.0004
TAB 3	14-Nov-12	14-Dec-12	0.0031	0.0004
TAB 3	14-Nov-12	14-Dec-12	0.0031	0.0006
TAB 3	14-Nov-12	14-Dec-12	0.0029	0.0005
TAB 3	14-Nov-12	14-Dec-12	0.0031	0.0004
TAB 3	14-Nov-12	14-Dec-12	0.0034	0.0003
TAB 3	14-Nov-12	14-Dec-12	0.0031	0.0006
TAB 3	14-Nov-12	14-Dec-12	0.0030	0.0003
TAB 3	14-Nov-12	30-Jan-13	0.0030	0.0004
TAB 3	14-Nov-12	30-Jan-13	0.0030	0.0003

TAB 3	14-Nov-12	30-Jan-13	0.0028	0.0004
TAB 3	14-Nov-12	30-Jan-13	0.0026	0.0003
TAB 3	14-Nov-12	30-Jan-13	0.0030	0.0005
TAB 3	14-Nov-12	30-Jan-13	0.0029	0.0003
TAB 3	14-Nov-12	30-Jan-13	0.0032	0.0005
TAB 3	14-Nov-12	30-Jan-13	0.0030	0.0007
TAB 3	14-Nov-12	01-Feb-13	0.0030	0.0004
TAB 3	14-Nov-12	01-Feb-13	0.0030	0.0004
TAB 3	14-Nov-12	01-Feb-13	0.0026	0.0003
TAB 3	14-Nov-12	05-Feb-13	0.0026	0.0004
TAB 3	14-Nov-12	05-Feb-13	0.0028	0.0004
TAB 4	30-Nov-12	05-Feb-13	0.0037	0.0005
TAB 4	30-Nov-12	05-Feb-13	0.0030	0.0004
TAB 4	30-Nov-12	10-Feb-13	0.0028	0.0005
TAB 4	30-Nov-12	11-Feb-13	0.0030	0.0005
TAB 5	03-Jan-13	01-Feb-13	0.0026	0.0003
TAB 5	03-Jan-13	01-Feb-13	0.0025	0.0003
TAB 5	03-Jan-13	01-Feb-13	0.0025	0.0003
TAB 5	03-Jan-13	10-Feb-13	0.0033	0.0004
TAB 5	03-Jan-13	10-Feb-13	0.0031	0.0004
TAB 5	03-Jan-13	10-Feb-13	0.0028	0.0005
TAB 5	03-Jan-13	10-Feb-13	0.0028	0.0004
TAB 5	03-Jan-13	10-Feb-13	0.0026	0.0005
TAB 5	03-Jan-13	11-Feb-13	0.0027	0.0004
TAB 5	03-Jan-13	11-Feb-13	0.0027	0.0004
TAB 5	03-Jan-13	17-Feb-13	0.0033	0.0003
TAB 5	03-Jan-13	20-Feb-13	0.0033	0.0003
TAB 5	03-Jan-13	20-Feb-13	0.0030	0.0002
TAB 6	18-Jan-13	17-Feb-13	0.0025	0.0002
TAB 6	18-Jan-13	20-Feb-13	0.0026	0.0002
TAB 6	18-Jan-13	20-Feb-13	0.0030	0.0003
TAB 6	18-Jan-13	20-Feb-13	0.0029	0.0004
TAB 6	18-Jan-13	27-Feb-13	0.0028	0.0002
TAB 7	06-Feb-13	20-Feb-13	0.0034	0.0006
TAB 7	06-Feb-13	20-Feb-13	0.0036	0.0005
TAB 7	06-Feb-13	20-Feb-13	0.0032	0.0004
TAB 7	06-Feb-13	27-Feb-13	0.0037	0.0008
TAB 7	06-Feb-13	03-Mar-13	0.0035	0.0004
TAB 7	06-Feb-13	03-Mar-13	0.0035	0.0004
Average			**0.003**	**0.001**

All labware and acids are cleaned before introducing them to the sample. Teflon digestion vials are thoroughly cleaned with 6 M HNO_3 and Milli-Q H_2O (i.e., 18MΩ water), first by soaking in boiling 6M HNO_3 for two days, rinsing in Milli-Q H_2O three times, repeating these two steps again with fresh nitric acid and Milli-Q H_2O, and finally boiling the beakers in Milli-Q H_2O for one day. All pipette tips, centrifuge tubes, and chromatographic columns used throughout the method are cleaned by soaking in room temperature 6 M HCl for at least 1 day prior to use, followed by rinsing three times with Milli-Q H_2O. Twice quartz distilled, once Teflon distilled, ultra-pure HCl and HNO_3 is used in all sample digestions, whereas the HF acid is ultra-pure Seastar acid from their line of Baseline acids (http://wwwsci.seastarchemicals.com/products.asp?pg=BL05_HydrofluoricAcid)

3.3: Sample and reference material preparation and digestion

Whole rocks were fragmented using a rock hammer and unweathered and unaltered rock chips from the interior of the rock sample were selected to be pulverized in an agate or alumina ring mill (Mansur, 2008; Mtoro et al., 2009). Extended milling (>2 minutes) yields powders having grain sizes of ~50 microns (200 mesh) and finer.

Following the method of Pitcairn et al. (2006a), 200 to 400 mg aliquots of a certified reference material (CRM) and whole rock powders are digested according to the procedure outlined in Table 3.2. The CRM TDB-1 was selected as a low gold (certified Au concentration of 6.3 ng/g ± 1.0 ng/g) reference material to test the accuracy and precision of the analytical method. TDB-1 is a whole rock powder (200 mesh) of a diabase dike from Tremblay Lake, Saskatchewan, Canada, containing grains of titaniferous magnetite and ilmenite with associated chalcopyrite and bornite (Certificate of Analysis, Natural Resources Canada, 1994). The TDB-1 reference material was selected for use in this study based on the reproducibility of the gold concentration of the CRM in the literature and also based on a recommendation from Pitcairn through personal correspondence.

Table 3.2: Rock digestion method

Step	Amount/Time	Action or acid addition
weighing	200-400 mg	rock powder placed into 15 mL round-bottom Savillex screw-top beaker
add acid	1 mL	16M HNO_3*
digest	2 hours	at 160°C closed lid, then an open vial dry down
add acid	3 mL	concentrated HF**
digest	24 hours	at 180°C closed lid, then an open vial dry down
add acid	2 mL	6 M HCl*
digest	12 hours	at 160°C closed lid, then an open vial dry down
add acid	2 mL	aqua regia (16M HNO_3*/12M HCl* 1:1 v/v)
digest	2 hours	at 180°C closed lid
add acid	4.5mL	Milli-Q H_2O
digest	12 hours	at 160°C closed lid, then an open vial dry down
finish	3 mL	take up the residue in 3 mL of 2 M HCl*

(Adapted from Pitcairn et al., 2006a)
* HCl, HNO_3 are twice quartz distilled, once Teflon distilled, ultra-pure acid.
**HF acid is ultra-pure Seastar
(http://wwwsci.seastarchemicals.com/products.asp?pg=BL05_HydrofluoricAcid)

If the gold in the rock is present at very low levels in the silicate phases, the HF will dissolve the silicate phases and allow for complete dissolution of trace gold (Pitcairn et al., 2006a). Addition of aqua regia will oxidize any sulfides present in the rock powder and will leach out gold as an $AuCl_4^-$ complex (Pitcairn et al., 2006a). To ensure that gold is entirely present as a chloro-complex, the aqua regia digestion is dried down and the sample residue is taken up in 0.5 mL of 12 M HCl, which is diluted with 2.5 mL of Milli-Q H_2O to a solution with a final concentration of 2 M HCl.

3.4: Chromatography

After sample digestion, gold is extracted from the samples by chromatographic column separation. An inert resin, Amberchrom CG71 polyacrylamide resin (50-100 μm), is coated with an organic solvent, diisobutyl ketone (DIBK), suitable for the extraction of gold-chloro-complexes. Diisobutyl ketone is added to the resin at a ratio of 1 g resin to 1.6 g DIBK (Table 3.3: Step 2; adapted from Pitcairn et al., 2006a). The dry powder-like mixture is then made into a slurry with the addition of 6M HCl (Table 3.3: Step 3; adapted from Pitcairn et al., 2006a). The HCl and DIBK must be added drop by drop to the resin with constant stirring in order to coat the resin beads evenly with DIBK. The slow addition of DIBK also prevents the production of a hydrophobic solid that may not hold the gold on the resin. The resin should be used immediately after preparation in order to minimize evaporation of the DIBK from the resin beads. Econo-Pac 12 x 1.5 cm disposable columns from Bio-Rad were prepared by carefully adding approximately 2 g of the inert resin, DIBK, and HCl slurry, which is held in place with acid-washed Si-wool. The resin preparation method is described in Table 3.3.

Table 3.3: Resin preparation method

1	dry 4 mL of inert resin, Amberchrom CG71 polyacrylamide resin (50-100 μm), which is shipped in a mixture of ethanol and water, by first centrifuging the resin aliquot, decanting the liquid, then placing the damp resin in a Teflon beaker and letting it air-dry for 48 hours
2	1.6 g (2 mL) of diisobutyl ketone (DIBK) is added very slowly drop by drop to the ~1 g of resin that remains after drying down resulting in a dry-looking powder
3	add 2 ml of 6 M HCl drop by drop to the powder to create a slurry
4	pour 2 g of the suspended resin into the disposable column carefully to ensure that there are no bubbles in the resin

(Adapted from Pitcairn et al., 2006a)

The chromatographic column method, including gold extraction onto the column using DIBK and subsequent elution of gold using NH_4OH, is outlined in Table 3.4. The DIBK was found to extract gold when the sample was loaded in 2 M HCl, whereas less than 5% of Fe^{3+} and other matrix elements such as Ta, Gd, As, Sb, and Hg were extracted onto the DIBK coated resin (Morrison and Freiser, 1962; Pitcairn et al., 2006a). Elution using 4% NH_4OH followed by Milli-Q H_2O was found to be more effective at eluting gold compared to HNO_3, aqua regia, or ethyl acetate (Pitcairn et al., 2006a).

Table 3.4: Chromatographic column method

Step	Procedure
1	add 5 mL of 6 M HCl to wash the resin; collect in a 50 mL beaker
2	add 3 mL of sample solution (equivalent to 200 mg of rock) in 2 M HCl
3	add 10 mL of 6 M HCl to wash the resin
4	discard the wash and sample elutants and replace the waste beaker with a clean 60 mL Teflon screw-top container
5	elute the column with 20 mL of 4% NH_4OH
6	elute with 20 mL of Milli-Q H_2O
7	elute with 10 mL of 4% NH_4OH
8	elute with 10 mL of Milli-Q H_2O
9	place Teflon container on a hot plate at 160°C and dry down
10	add 1mL 12 M HNO_3 and 1mL 12 M HCl and heat at 160°C in closed Teflon screw-top container for 1hour, then dry down at 160°C
11	add 0.5 mL of 12 M HCl and wash around the container before adding 2.5 mL of Milli-Q H_2O to dissolve remaining solute
12	dilute to 10 mL with Milli-Q H_2O

(Adapted from Pitcairn et al., 2006a)

3.5: ICP-MS method

Samples were analyzed on an Element 2 Thermo Finnigan single-collector inductively coupled plasma mass spectrometer (SC-ICP-MS) using the parameters listed in Table 3.5. An Apex desolvating nebulizer was used for sample introduction at an approximate uptake rate of 100 µL/min. Washout with 5% HCl between samples was found to remove gold more effectively than HNO_3 (Pitcairn et al., 2006a). Wash time between samples should be at least 10 minutes because it takes approximately 500 s for gold counts to return to background levels (typically 600 cps, i.e., maximum count rate on a single mass peak) after a sample run. Gold concentrations of the standards and samples were determined using a standard addition protocol after subtraction of the background signal.

Table 3.5: Element 2 Thermo Finnigan SC-ICP-MS parameters

Forward power	1260 W
HV	8 kV
Scan optimization	Mass Accuracy
Number of pre-scans	1
Active dead time	20 ns
Guard electrode	Enabled
Mass resolution (M/ ΔM)	300
Mass window	150%
Dwell time (per isotope)	10 ms
Samples per peak	10
Search window	120%
Integration window	80%
Scan type	Escan
Detection mode	Both
Runs and passes	100 x 1
Sampler cone	1.0 mm Ni or Al
Skimmer cone	0.4 mm Ni or Al
Cool gas flow	16 L min^{-1} Ar
Auxiliary gas flow	1.05 L min^{-1} Ar
Sample gas flow	0.9 L min^{-1} Ar

The gold concentrations for the samples are determined using a standard addition protocol (see description at http://zimmer.csufresno.edu/~davidz/Chem106/StdAddn/StdAddn.html). Standard addition is carried out by adding a constant volume (1 mL, or 1.5 mL in the case of the granulite samples) of a sample solution with unknown gold concentration to three sample vials (Figure 3.1). A stock solution with a known gold concentration (1 ng/g in this study) is added in incrementally increasing volumes to sample vial 2 and 3 (0.5 mL and 1 mL respectively, or 0.25 mL and 0.5 mL in the case of the granulites) (Figure 3.1). Sample vial 1 and 2 are then diluted to 2 mL with 5% HCl to match the volume of sample vial 3.

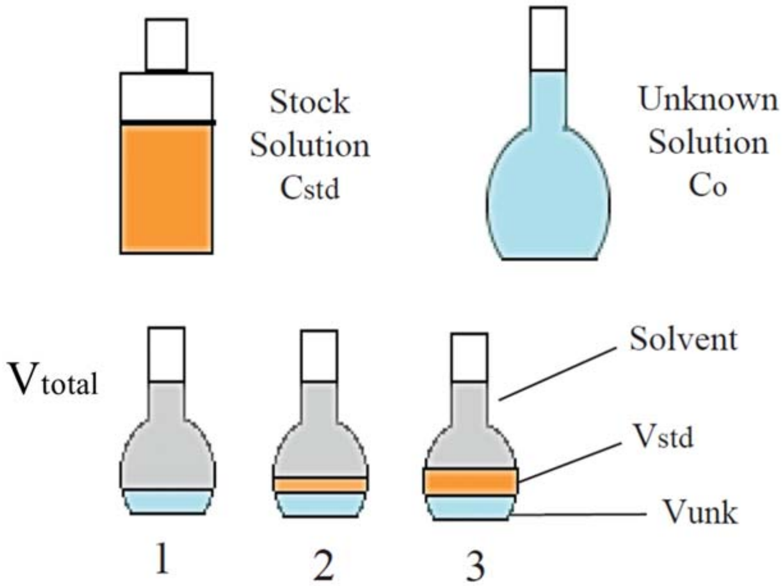

Fig. 3.1: Standard addition schematic diagram (Image adapted from http://zimmer.csufresno.edu/~davidz/Chem106/StdAddn/StdAddn.html).

The concentration of the standard solution, 1 ng/g Au, is corrected for the additional volume introduced during the sample solution mixing (Equation 1 from http://zimmer.csufresno.edu/~davidz/Chem106/StdAddn/StdAddn.html) and it can then be plotted against the counts per second (cps) recorded by the ICP-MS (Figure 3.2). In Equation 1 below, C_{sa} corresponds to the corrected concentration of the 1 ng/g standard gold solution (C_{std}), V_{std} corresponds to the volume of the 1 ng/g standard gold solution added, and V_{total} corresponds to the total volume of each sample vial (2 mL in this study).

$$C_{sa} = \frac{C_{std} \; V_{std}}{V_{total}} \quad \textbf{(E 1)}$$

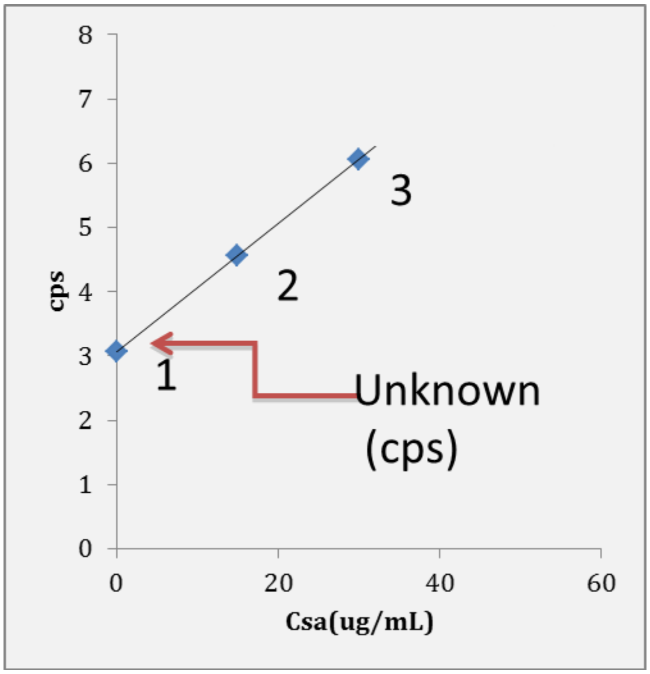

Fig. 3.2: Schematic plot of the corrected concentration of the standard Au solution against the counts per second (cps) recorded by the ICP-MS. (Image adapted from http://zimmer.csufresno.edu/~davidz/Chem106/StdAddn/StdAddn.html).

The concentration of gold in the unknown sample solution can then be calculated by extrapolating the x-intercept of the linear fit to find the negative gold concentration corresponding to the unknown solution. A volume correction is then applied to the negative gold concentration (C_{sa}) to determine the concentration of gold in the sample ($C_{unknown}$) (Equation 2 from http://zimmer.csufresno.edu/~davidz/Chem106/StdAddn/StdAddn.html).

$$C_{unknown} = - C_{sa} \frac{V_{total}}{V_{unknown}} \qquad \textbf{(E 2)}$$

3.6: Precision and Accuracy

The precision and accuracy of the method was determined by analyzing the CRM TDB-1. Repeat analysis of TDB-1 yields an average gold concentration of 6.5 ng/g ± 1.4 ng/g (1 σ) (Figure 3.3 and Table 3.6). The certified gold concentration value for TDB-1 is 6.3 ng/g ± 1.0 ng/g.

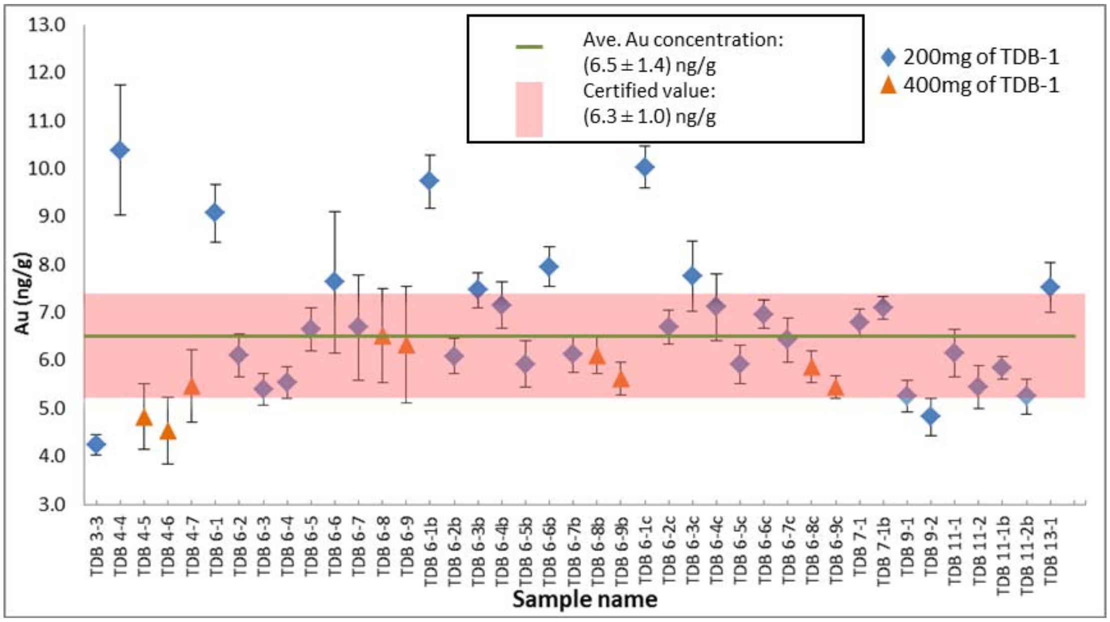

Fig. 3.3: Plot of repeat analyses of the CRM TDB-1, executed over a six month time period. Average gold concentration is 6.5 ng/g ± 1.4 ng/g (green line indicates the average). The certified value from the CRM TDB-1 is 6.3 ng/g ± 1.0 ng/g (pink field). The sample numbers in this plot represent aliquots and repeat analyses of the CRM TDB-1. The first number in the sample name represents the round of aliquots that were dissolved at the same time in the same group of samples. The second number in the sample name represents successive aliquots within a given dissolution round. The letter attached to the end of certain sample names indicates that a given solution has been re-analyzed on the ICP-MS on a different day.

Table 3.6: Gold concentration for aliquots of CRM TDB-1.

Sample name	Date dissolved	Date analyzed	Au (ng/g)	±1σ (ng/g)	Sample size (mg)
TDB 3-4	15-Aug-12	25-Oct-12	4.2	0.2	200
TDB 4-4	06-Sep-12	04-Nov-12	10.4	1.4	200
TDB 4-5	06-Sep-12	04-Nov-12	4.8	0.7	400
TDB 4-6	06-Sep-12	04-Nov-12	4.5	0.7	400
TDB 4-7	06-Sep-12	04-Nov-12	5.5	0.7	400
TDB 6-1	24-Sep-12	28-Nov-12	9.1	0.6	200
TDB 6-2	24-Sep-12	28-Nov-12	6.1	0.4	200
TDB 6-3	24-Sep-12	28-Nov-12	5.4	0.3	200
TDB 6-4	24-Sep-12	28-Nov-12	5.5	0.3	200
TDB 6-5	24-Sep-12	28-Nov-12	6.6	0.4	200
TDB 6-6	24-Sep-12	28-Nov-12	7.6	2.9	200
TDB 6-7	24-Sep-12	28-Nov-12	6.7	1.1	200
TDB 6-8	24-Sep-12	28-Nov-12	6.5	1.0	400
TDB 6-9	24-Sep-12	28-Nov-12	6.3	1.3	400
TDB 6-1b	24-Sep-12	14-Dec-12	9.7	0.5	200
TDB 6-2b	24-Sep-12	14-Dec-12	6.1	0.6	200
TDB 6-3b	24-Sep-12	14-Dec-12	7.5	0.4	200
TDB 6-4b	24-Sep-12	14-Dec-12	7.1	0.5	200
TDB 6-5b	24-Sep-12	14-Dec-12	5.9	0.5	200
TDB 6-6b	24-Sep-12	14-Dec-12	7.9	0.6	200
TDB 6-7b	24-Sep-12	14-Dec-12	6.1	0.4	200
TDB 6-8b	24-Sep-12	14-Dec-12	6.1	0.4	400
TDB 6-9b	24-Sep-12	14-Dec-12	5.6	0.3	400
TDB 6-1c	24-Sep-12	30-Jan-13	10.0	0.4	200
TDB 6-2c	24-Sep-12	30-Jan-13	6.7	0.4	200
TDB 6-3c	24-Sep-12	30-Jan-13	7.7	0.7	200
TDB 6-4c	24-Sep-12	30-Jan-13	7.1	0.7	200
TDB 6-5c	24-Sep-12	30-Jan-13	5.9	0.4	200
TDB 6-6c	24-Sep-12	30-Jan-13	7.0	0.5	200
TDB 6-7c	24-Sep-12	30-Jan-13	6.4	0.5	200
TDB 6-8c	24-Sep-12	30-Jan-13	5.9	0.3	400
TDB 6-9c	24-Sep-12	30-Jan-13	5.4	0.2	400
TDB 7-1	07-Dec-12	14-Dec-12	6.8	0.3	200
TDB 7-1b	07-Dec-12	05-Feb-13	7.1	0.2	200
TDB 9-1	03-Jan-13	11-Feb-13	5.3	0.3	200
TDB 9-2	03-Jan-13	11-Feb-13	4.8	0.4	200
TDB 11-1	16-Jan-13	10-Feb-13	6.2	0.5	200
TDB 11-2	16-Jan-13	10-Feb-13	5.4	0.5	200
TDB 11-1b	16-Jan-13	11-Feb-13	5.8	0.2	200
TDB 11-2b	16-Jan-13	11-Feb-13	5.2	0.4	200
TDB 13-1	05-Feb-13	17-Feb-13	7.5	0.5	200

Repeat analyses of the same TDB-1 aliquots are shown in Figure 3.4. Most of the repeat analyses are in good agreement with each other. For the CRM TDB-1, the gold concentrations determined for 200 mg aliquots are reproducible within 22% (n=32), whereas 400 mg aliquots are reproducible within 12% (n=9). For comparison, Pitcairn et al. (2006a), found that 2 g sample aliquots of whole rock certified reference materials having gold concentrations between 300-3300 ng/g were reproducible to within 5%. They also ran unknown rock samples in the 0.3-0.9 ng/g range and found that the gold concentrations were externally reproducible within 33%.

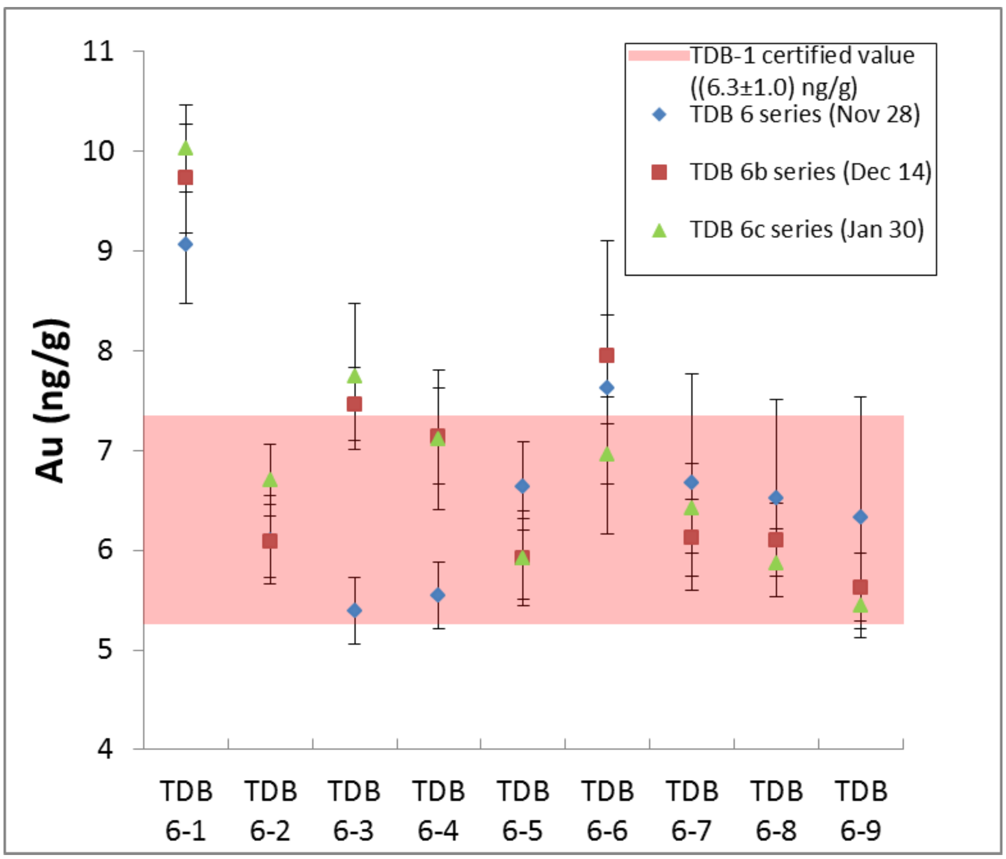

Fig. 3.4: Repeat analyses of CRM TDB-1. All but two of the repeat analyses of the digested aliquots fall within uncertainty of each other. Repeats were run on different days. TDB 6-8 and 6-9 represent 400 mg dissolutions; the remainder are 200 mg dissolutions.

Chapter 4: Results

<u>*4.1*</u>

A higher gold background in the ICP-MS following the CRM TDB-1 analyses and before the upper- and lower-crustal rock sample analyses resulted in a greatly decreased signal to noise ratio during the analyses of the unknowns (signal to noise ranged from 10:1 to 2:1 for the andesites, and 15:1 to 1.5:1 for the granulites). To compensate for this challenge, the signal to noise ratio was increased for the granulites by diluting the samples by a factor of two less, as compared to the reference material and upper-crustal samples, for standard addition analyses. The results are reproducible, after subtracting the steady background signal, to within 20% for the andesites, 14% for the basalts, and 33% for the granuilites.

Analysis of andesites (Fig. 4.1 and 4.2, blue) and basalts (Fig. 4.1 and 4.2, green) from the Musoma-Mara greenstone belt and Rwamagaza area in the Sukumaland greenstone belt, respectively, reveals a somewhat skewed log-normal distribution of gold concentrations between 0.2 to 143 ng/g (Table 4.1). The basalts have an average gold concentration of 60 (+193 / -19) ng/g, with mean ln[Au] = 4.1 and median ln[Au] = 3.7, whereas the average gold concentration of the andesites is 2.2 (+12 / -0.4) ng/g, with mean ln[Au] = 0.79 and median ln[Au] = 0.26, or 1.2 (+3.6 / -0.6) ng/g, with mean ln[Au] = 0.22 and median ln[Au] = 0.25 if the outlier TA 18 is excluded (an outlier is defined in this study as a sample that falls beyond two sigma uncertainty of the average). Concentrations of gold in mafic granulite xenoliths from

Naibor Soito and Labait (Fig. 4.1 and 4.2, red symbols and purple symbols, respectively), Tanzania, also show an approximate log-normal distribution, with gold concentrations ranging from <0.15 ng/g to 5 ng/g (Table 4.1), and an average concentration of 0.4 (+1.3/-0.1) ng/g, with mean ln[Au] = -0.82 and median ln[Au] = -1.1, or 0.3 (+0.7 / -0.07) ng/g, with mean ln[Au] = -1.2 and median ln[Au] = -1.2, if the outlier NS04 01 is excluded from the Naibor Soito granulite xenoliths and 0.6 (+0.8 / -0.5) ng/g, with mean ln[Au] = -0.52 and median ln[Au] = -0.46, for the Labait granulite xenoliths. The two granulite populations are statistically identical, and the average gold concentration of all granulite samples is 0.5 (+1.2 / -0.2) ng/g, with mean ln[Au] = -0.70 and median ln[Au] = -0.89, or 0.4 (+1.0 / -0.1) ng/g, with mean ln[Au] = -0.90 and median ln[Au] = -0.95, if the outlier NS04 01 is excluded. Averages for the granulite populations do not include four samples (three from Labait and one from Naibor Soito) that were found to be below the detection limit for gold (<0.150 ng/g) and, thus, this average value constitutes a maximum estimate of the gold concentration of the lower-crustal rocks. The gold concentrations of the lower-crustal granulites are statistically different from those of the upper-crustal andesites and basalts, as discussed in the next section. The data are consistent with gold depletion in lower-crustal rocks compared to upper-crustal rocks (Fig. 4.1 and 4.2. See Table 4.2 for individual gold analyses).

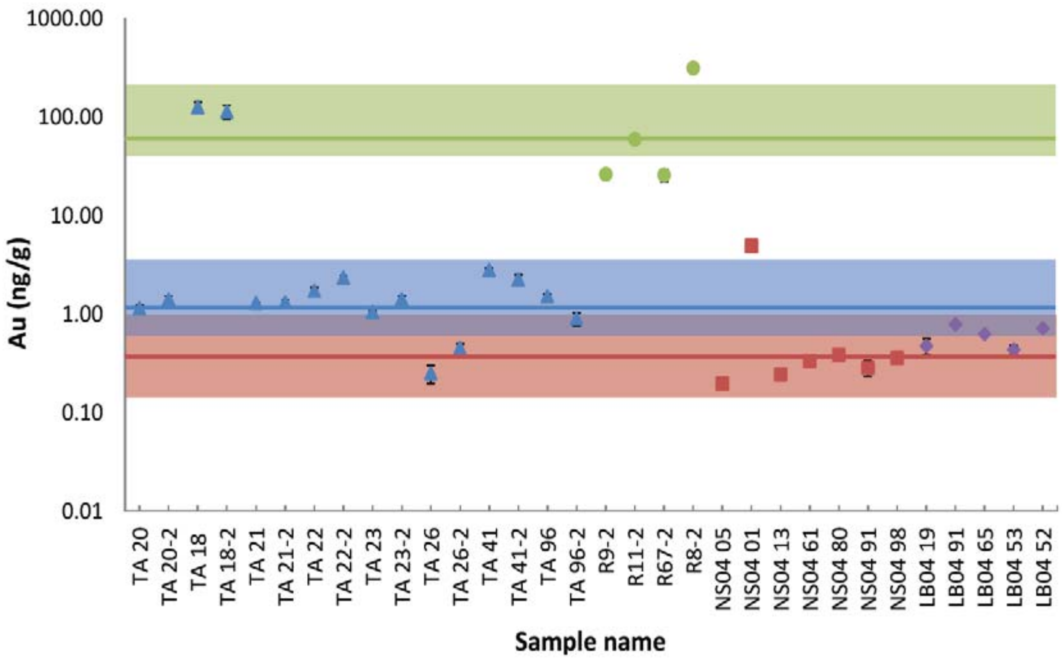

Fig. 4.1: Average gold concentrations for individual dissolutions of samples (data points) and average gold concentrations (excluding outliers) of andesite samples (blue triangles: TA samples = andesites; blue line: ave. Au = 1.2 (+3.6 / -0.6) ng/g) and basalt samples (green circles: R samples = basalts; green line: ave. Au = 60 (+193/-19) ng/g) from the Musoma-Mara greenstone belt and the Rwamagaza area in the Sukumaland greenstone belt, respectively and mafic granulite xenoliths from Naibor Soito and Labait (red field: average gold concentration field contains both Naibor Soito and Labait samples, ave. Au = 0.4 (+1.0 / -0.1) ng/g), Tanzania (red squares: NS samples = Naibor Soito; purple diamonds: LB samples = Labait) on a log scale. Three Labait granulites and one Naibor Soito granulite have gold concentrations below the detection limit (<0.150 ng/g) and are not included in this plot. The majority of the lower crustal granulite xenoliths contain less gold than the upper-crustal rocks: between 0.3 to 3 orders of magnitude lower gold contents.

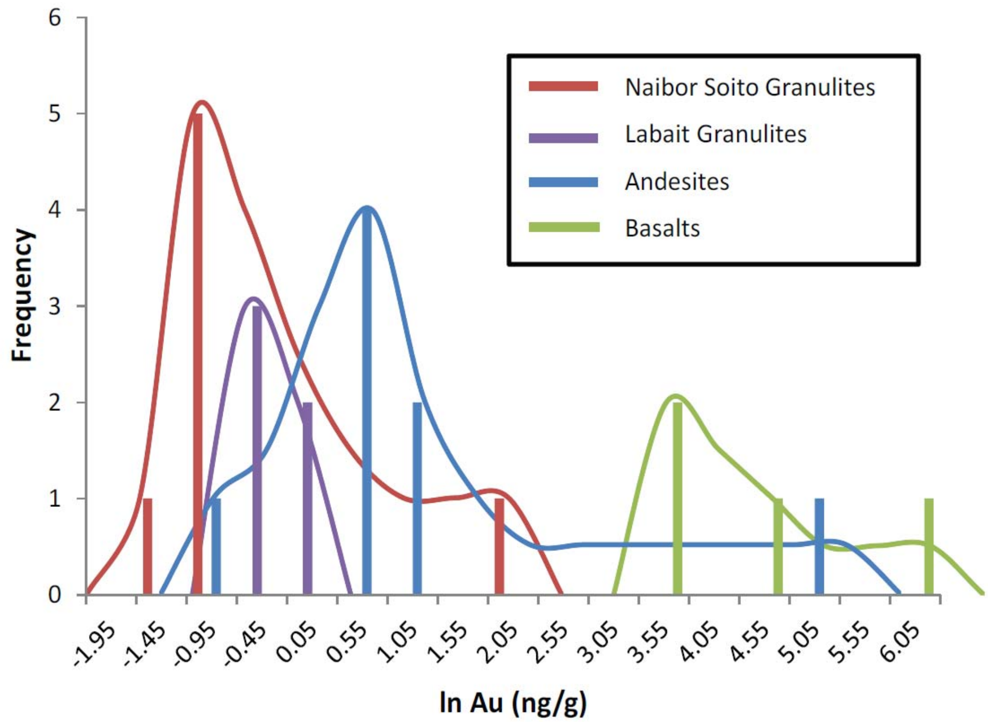

Fig. 4.2: Log-normal plot of individual gold concentrations of andesites (blue) and basalts (green) from the Musoma-Mara greenstone belt and the Rwamagaza area in the Sukumaland greenstone belt, respectively, and mafic granulite xenoliths from Naibor Soito (red) and Labait (purple) craters, Tanzania. Three Labait granulites and one Naibor Soito granulite have gold concentrations below the detection limit (<0.150 ng/g) and are not shown on this diagram.

Table 4.1: Average gold concentration for each sample (plotted in Fig. 4.1) used to calculate average gold concentrations for each rock type. Errors for sample aliquots with only one analysis are based on the associated analytical uncertainty. The average gold concentration for the granulites does not include four samples that were found to be below the detection limit (<0.150 ng/g) and thus constitutes a maximum.

Sample name	**Au(ng/g)**	**n**	**±1σ (ng/g)**
Andesites			
TA 20	1.28	3	0.09
TA 18	120	2	15.5
TA 21	1.31	3	0.03
TA 22	2.04	3	0.14
TA 23	1.24	3	0.05
TA 26	0.35	3	0.05
TA 41	2.52	3	0.12
TA 96	1.21	3	0.09
Average andesite	**2.2**		**+12/-0.4**
Average andesite (excluding outlier)	**1.2**		**+3.6/-0.6**
Basalts			
R9-2	26.3	4	1.54
R11-2	59.6	3	3.03
R67-2	25.9	3	3.60
R8-2	314	3	10.5
Average basalt	**60**		**+193/-19**
Granulites			
NS04 05	0.155	4	0.050
NS04 01	4.941	4	0.038
NS04 13	0.213	3	0.066
NS04 61	0.333	3	0.033
NS04 73	<0.150	2	
NS04 80	0.386	3	0.053
NS04 91	0.287	2	0.015
NS04 98	0.361	4	0.085
LB04 19	0.476	2	0.009
LB04 91	0.790	1	0.035
LB04 65	0.629	2	0.049
LB04 53	0.437	2	0.016
LB04 52	0.720	2	0.018
LB04 36	<0.150		
LB04 82	<0.150		
LB04 93	<0.150		
Average granulite	**0.5**		**+1.2/-0.2**
Average granulite (excluding outlier)	**0.4**		**+1.0/-0.1**

Table 4.2: Individual data collected from repeat analyses of single aliquots of andesites (TA samples) and basalts (R samples) from the Musoma-Mara greenstone belt and the Rwamagaza area in the Sukumaland greenstone belt, Tanzania, and mafic granulite xenoliths from Naibor Soito (NS samples) and Labait (LB samples), Tanzania. The letter given at the end of the name indicates successive repeat analyses of the same sample aliquot.

Sample name	Au (ng/g)	±1σ (ng/g)	Sample size (mg)	Date run
Andesites				
TA 20	1.28	0.25	400	Feb-20
TA 20b	1.13	0.05	400	Feb-27
TA 20c	1.08	0.07	400	Mar-05
TA 20d	1.11	0.10	400	Mar-12
TA 20-2	1.41	0.11	400	Mar-12
TA 18	122	11.4	200	Feb-20
TA 18b	144	8.88	400	Mar-05
TA 18-2	114	17.9	400	Mar-12
TA 21	1.35	0.80	400	Feb-11
TA 21b	1.30	0.10	400	Feb-17
TA 21c	1.27	0.09	400	Feb-20
TA 21d	1.30	0.05	400	Feb-27
TA 21e	1.26	0.06	400	Mar-12
TA 21-2	1.32	0.09	200	Mar-12
TA 22	1.88	0.13	400	Feb-17
TA 22b	1.79	0.12	400	Feb-20
TA 22c	1.80	0.07	400	Feb-27
TA 22d	1.59	0.08	400	Mar-05
TA 22e	1.58	0.11	400	Mar-12
TA 22-2	2.35	0.12	200	Mar-12
TA 23	1.12	0.08	400	Feb-20
TA 23b	1.02	0.05	400	Feb-27
TA 23c	1.07	0.07	400	Mar-05
TA 23d	1.03	0.09	400	Mar-12
TA 23-2	1.42	0.11	200	Mar-12
TA 26	0.27	0.03	400	Feb-17
TA 26b	0.30	0.11	400	Feb-20
TA 26c	0.19	0.01	400	Feb-27
TA 26-2	0.45	0.04	200	Mar-12
TA 41	2.89	0.23	400	Feb-17
TA 41b	2.88	0.35	400	Feb-20
TA 41c	2.79	0.09	400	Feb-27
TA 41d	2.60	0.18	400	Mar-05
TA 41e	2.82	0.13	400	Mar-12
TA 41-2	2.25	0.26	200	Mar-12
TA 96	1.45	0.30	400	Feb-20
TA 96b	1.66	0.07	400	Feb-27

TA 96c	1.51	0.19	400	Mar-05
TA 96d	1.48	0.12	400	Mar-12
TA 96-2	0.90	0.13	200	Mar-12
Basalts				
R9-2	23.7	1.00	200	Dec-14
R9-2b	24.7	1.95	200	Feb-05
R9-2c	28.3	1.69	200	Feb-17
R9-2d	26.7	0.90	200	Feb-20
R9-2e	27.0	0.51	200	Feb-27
R9-2f	26.8	0.52	200	Mar-05
R9-2g	26.7	0.91	200	Mar-12
R11-2	57.6	2.88	200	Dec-14
R11-2b	55.2	1.55	200	Feb-05
R11-2c	61.6	3.94	200	Feb-17
R11-2d	61.2	0.91	200	Feb-27
R11-2e	62.2	2.37	200	Mar-12
R67-2	22.1	2.14	200	Dec-14
R67-2b	21.8	0.88	200	Feb-05
R67-2c	28.7	1.82	200	Feb-17
R67-2d	27.9	0.54	200	Feb-27
R67-2e	28.8	1.52	200	Mar-12
R8-2	329	33.2	200	Dec-14
R8-2b	316	12.6	200	Feb-05
R8-2c	302	12.1	200	Feb-17
R8-2d	301	4.24	200	Feb-27
R8-2e	318	4.42	200	Mar-05
R8-2f	317	5.65	200	Mar-12
Mafic Granulite Xenoliths, Naibor Soito crater				
NS04 05	<0.150	0.014	400	Feb-08
NS04 05b	<0.150	0.013	400	Feb-10
NS04 05c	0.187	0.018	400	Mar-03
NS04 05d	0.209	0.029	400	Mar-12
NS04 01	4.88	0.20	400	Feb-10
NS04 01b	4.95	0.18	400	Feb-11
NS04 01c	4.95	0.16	400	Mar-03
NS04 01d	4.97	0.17	400	Mar-05
NS04 01e	4.97	0.20	400	Mar-12
NS04 13	<0.150	0.015	400	Feb-10
NS04 13b	0.223	0.032	400	Mar-03
NS04 13c	0.263	0.030	400	Mar-05
NS04 13d	0.248	0.020	400	Mar-12
NS04 61	0.300	0.029	400	Mar-03
NS04 61b	0.333	0.032	400	Mar-05
NS04 61c	0.366	0.034	400	Mar-12

NS04 73	<0.150	0.020	400	Feb-10
NS04 73b	<0.150	0.007	400	Mar-05
NS04 73c	<0.150	0.006	400	Mar-12
NS04 80	0.309	0.036	400	Feb-10
NS04 80b	0.455	0.045	400	Feb-20
NS04 80c	0.368	0.037	400	Mar-03
NS04 80d	0.403	0.038	400	Mar-05
NS04 80e	0.394	0.042	400	Mar-12
NS04 91	0.274	0.094	400	Mar-03
NS04 91b	0.283	0.030	400	Mar-05
NS04 91c	0.303	0.038	400	Mar-12
NS04 98	0.394	0.047	400	Feb-10
NS04 98b	0.311	0.035	400	Feb-11
NS04 98c	0.464	0.047	400	Mar-03
NS04 98d	0.275	0.019	400	Mar-05
Mafic Granulite Xenoliths, Labait crater				
LB04 19	0.481	0.040	400	Feb-20
LB04 19b	0.479	0.020	400	Mar-03
LB04 19c	0.480	0.020	400	Mar-05
LB04 19d	0.462	0.031	400	Mar-12
LB04 91	0.817	0.058	400	Feb-20
LB04 91b	0.804	0.040	400	Mar-03
LB04 91c	0.739	0.036	400	Mar-05
LB04 91d	0.802	0.047	400	Mar-12
LB04 65	0.676	0.051	400	Feb-20
LB04 65b	0.650	0.038	400	Mar-03
LB04 65c	0.562	0.033	400	Mar-05
LB04 65d	0.628	0.037	400	Mar-12
LB04 53	0.439	0.035	400	Mar-03
LB04 53b	0.420	0.018	400	Mar-05
LB04 53c	0.451	0.032	400	Mar-12
LB04 52	0.740	0.052	400	Feb-20
LB04 52b	0.721	0.044	400	Mar-03
LB04 52c	0.696	0.030	400	Mar-05
LB04 52d	0.725	0.045	400	Mar-12
LB04 36	<0.150		400	Feb-20
LB04 82	<0.150		400	Feb-20
LB04 93	<0.150		400	Feb-20

Chapter 5: Discussion

5.1: Statistical evaluation

A Kolmogorov-Smirnov (KS) test was used to determine whether or not there is a statistically significant difference between the gold concentrations of the upper-crustal andesites and the lower-crustal granulites. The maximum difference (D) between the cumulative distributions is 0.79, which is greater than the 99% confidence level maximum difference value of 0.36 for the number of samples in the population (n=20) (Fig. 5.1, determined using an online evaluation tool that can be found at http://www.physics.csbsju.edu/stats/KS-test.n.plot_form.html). This indicates that the gold concentrations of the upper-crustal andesites (dashed line in Fig. 5.1) compared to the lower-crustal granulites (solid line in Fig. 5.1) are statistically different. The Kolmogorov-Smirnov (KS) test also calculates a small corresponding P-value of <1E-04, indicating that there is a very low probability that the KS statistic was achieved by chance (the P-value was also determined using an online evaluation tool that can be found at http://www.physics.csbsju.edu/stats/KS-test.n.plot_form.html). A plot of the comparison of the cumulative fractions of the andesite (solid line) and granulite (dashed line) distributions of gold concentration values is shown in Fig. 5.1.

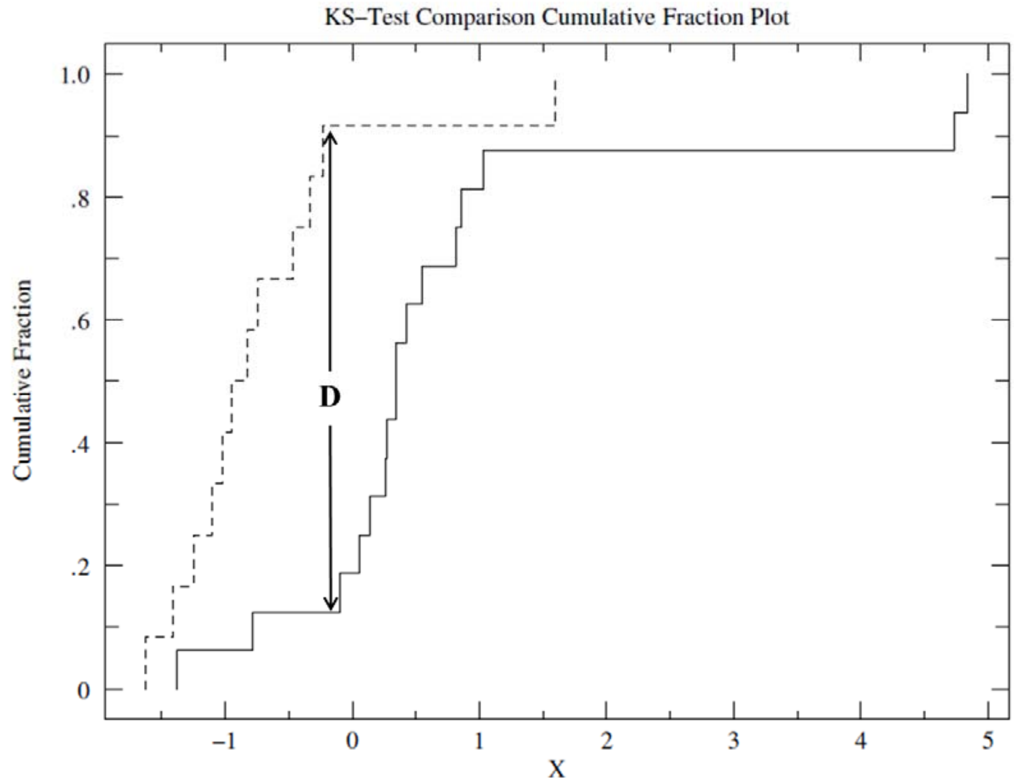

Fig. 5.1: Kolmogorov-Smirnov test comparison of ln[Au] (x-axis) in cumulative fractions between the andesite population (solid line) and the granulite population (dashed line). The maximum difference (D) between the cumulative distributions is 0.79 with a small corresponding P-value indicating that the difference is real. (Determined using an online evaluation tool at: http://www.physics.csbsju.edu/stats/KS-test.n.plot_form.html).

5.2: Gold depletion in the lower crust

The lower-crustal rocks from the Archean Tanzanian Craton and neighboring Mozambique Belt show depletions in Au as well as Cs, Th, U and often Rb compared to upper-crustal rocks in the same area. Similar depletions in gold were found in metamorphic rocks in the Otago and Alpine schists, New Zealand, when compared to their unmetamorphosed protoliths (Pitcairn et al., 2006b), as well as the granulite-facies lower crustal rocks in Bamble Belt, Norway (Cameron, 1989). Depletions in

LILEs were also found in the lower crustal rocks from the Bamble Belt. However, the LILE depletion there has been associated with a separate event than that of the gold depletion in the rocks (Cameron, 1994). The depletion of gold, as well as LILEs, in the northern Tanzanian lower crust could potentially be due to metamorphic dehydration or partial melting events occurring during high-grade, granulite-facies metamorphism.

The average gold concentrations of the greenstone belt lavas are 2.2 (+11.6 / -0.4) ng/g, or 1.2 (+3.6 / -0.6) ng/g if the outlier TA 18 is excluded, for the andesites and 60 (+193 / -19) ng/g for the basalts (Fig. 4.1). The average gold concentration of the lower-crustal granulites is 0.5 (+1.2 / -0.2) ng/g, or 0.4 (+1.0 / -0.1) ng/g if the outlier NS04 01 is excluded (Fig. 4.1), and samples from the two granulite locations are statistically indistinguishable, as noted above. The mean gold concentrations of the upper and lower crustal rock types are distinct, yet their insoluble lithophile element compositions are similar (Fig. 2.5), suggesting that gold, like the LILEs, was depleted in the lower crust.

The depletion of gold may have been caused by removal of gold by oxidizing fluids or melts produced during high-grade metamorphism. To investigate whether the depletions in gold are correlated with those observed in U, Rb, Cs, and Th, the depletions for these elements are plotted against gold depletions (Fig. 5.2). Element depletions are calculated by dividing the concentration of the element of interest in a granulite xenolith sample by the log-normal mean concentration of the element in the andesite population. A weak correlation exists between Au depletion and U, Th, and Rb depletions (Fig. 5.2); however, the trendline is controlled by the single high gold granulite sample (NS04-01) in all cases. If the anomalously high gold granulite sample is removed from the plots (Fig. 5.3), there is no correlation between the gold depletion and the depletion of U, and Th, and an extremely weak correlation is observed between rubidium depletion and gold depletion. There is no trend between gold depletion and caesium depletion in either plot (Fig. 5.2 and Fig. 5.3). It appears as though there is no real relationship between the gold depletion and the depletions of the other elements. This suggests that these depletions are controlled by different factors or processes (e.g., depletion of gold is dependent on redox, and likely linked to the fate of primary sulfides, whereas Th, Rb, and Cs are not influenced by redox and are all contained within silicates).

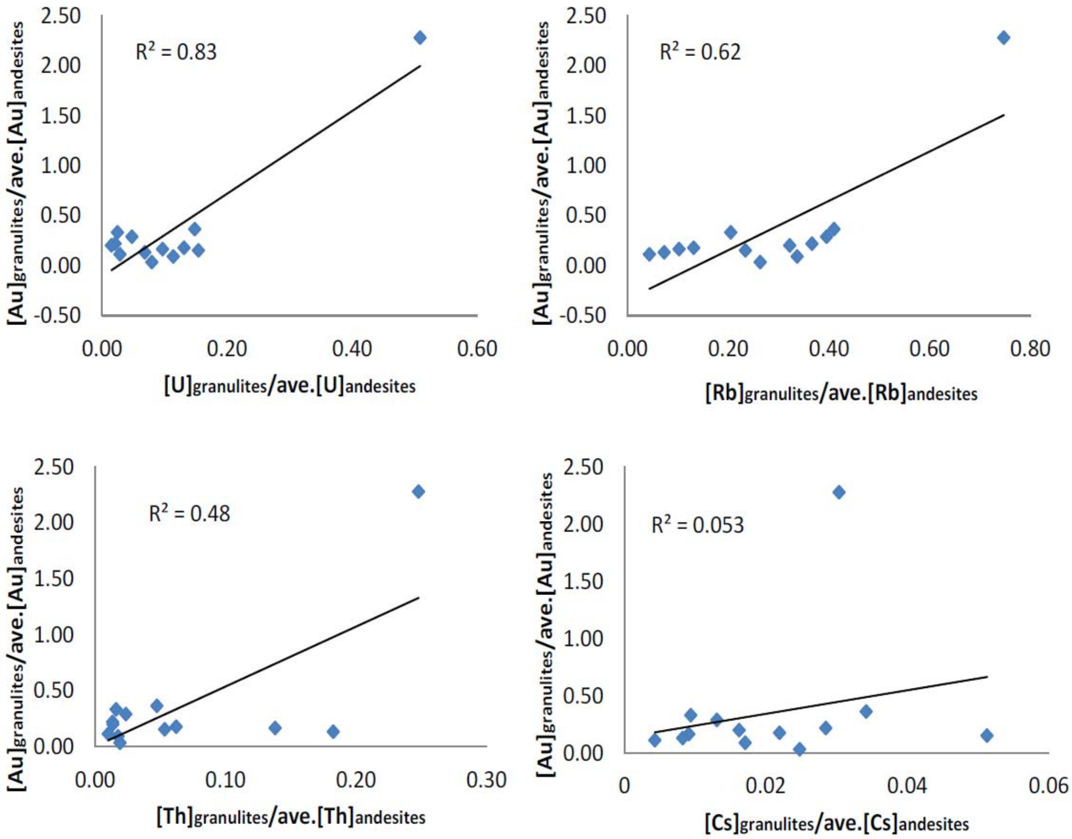

Fig. 5.2: Plots of gold depletion in the lower-crustal granulites from both Naibor Soito and Labait compared to depletion of U, Rb, Cs, and Th (clockwise) in the granulites from both locations. Depletion is calculated by dividing the concentration of the element of interest in a granulite-facies-sample by the log-normal mean concentration of the element in the andesite population. The linear correlation is heavily influenced by the high gold sample NS04-01.

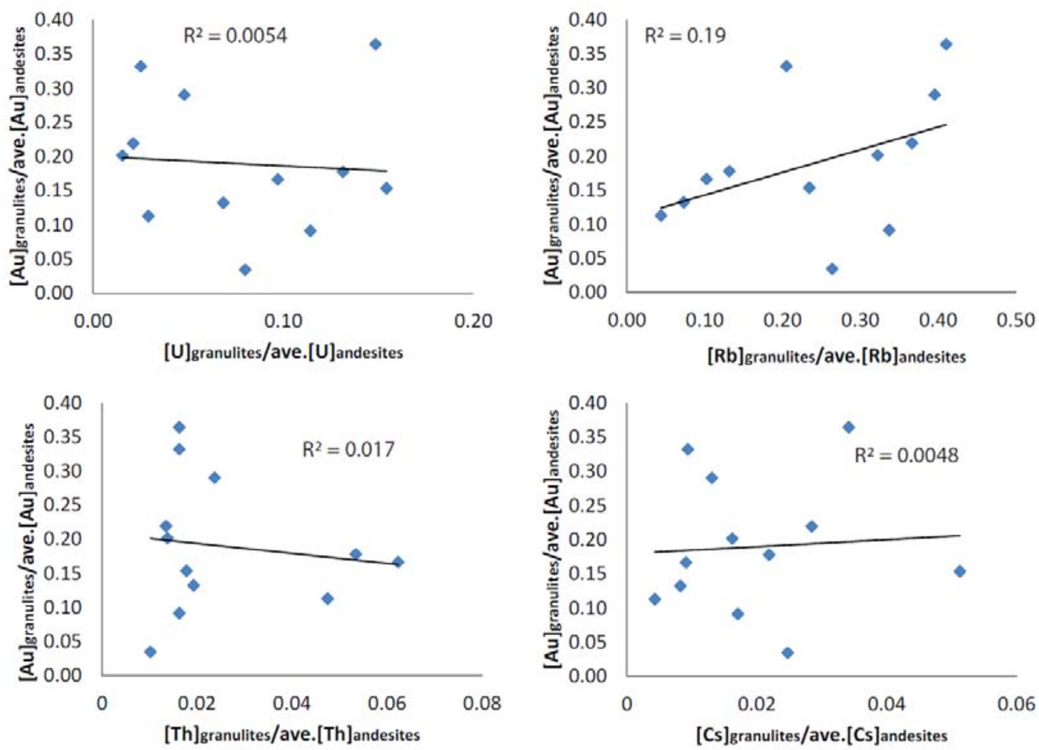

Fig 5.3: Plots of gold depletion in the lower-crustal granulites from both Naibor Soito and Labait and depletion of U, Rb, Cs, and Th (clockwise) in the granulites from both locations after the removal of the anomalously high gold granulite sample (NS04-01). Depletion is calculated by dividing the concentration of the element of interest in a granulite-facies-sample by the log-normal mean concentration of the element in the andesite population.

Greater than 93% of the lower-crustal granulites are depleted in gold compared to the upper-crustal rocks. The prevalent nature of this depletion suggests that the leaching of gold from the lower crustal rocks is likely pervasive and could be the result of metamorphic dehydration or partial melting. Oxidizing fluids associated with metamorphic reactions could cause the breakdown of sulfide phases resulting in the release of gold as gold-thio-complexes into the fluid phase, thus leaching the lower crust of its gold (Harlov et al., 1997).

Indeed, evidence for such a process is apparent in the Naibor Soito granulites where pyrite appears to have reacted with an oxidizing fluid to create a thin magnetite rim (Fig. 2.4). Pyrite rimmed with magnetite has been observed in the most highly oxidized Archean-aged granulite-facies quartzofeldspathic garnet charnockites of the Shevaroy Hills of Northern Tamil Nadu, southern India (Harlov et al., 1997), as well as in a granulite-facies terrane in the central area of the Nordre Stromford shear zone in West Greenland (Glassley, 1982; 1983), and in high-grade charnockites from the Bamble Belt, Norway (Cameron et al., 1993). Both Harlov et al. (1997) and Cameron et al. (1993) suggest that the replacement of pyrite by magnetite was caused by highly oxidizing fluids at high pressure (0.7-0.8 GPa) and temperature (700-800^{o}C) conditions applicable to the lower crust. Cameron et al. (1993) go on to suggest that the depletion of Au, Sb, and As in the high-grade lower-crustal charnockites of Bamble Belt, Norway, could have been caused by the infiltration of the highly-oxidized, sulfur-bearing fluids present at some stage during metamorphism.

The breakdown of pyrite to magnetite observed in the Naibor Soito xenoliths could potentially have occurred 1) during entrainment of the xenoliths in the host basalt, or 2) during high-grade metamorphic reactions in the lower crust (as described above). The available data do not allow one to determine which of the above scenarios is most likely. However, if the oxidative breakdown of sulfides observed in thin section were responsible for the pervasive depletion of gold in the xenolith suites, one would expect to see a correlation between the presence of sulfides and gold concentration, yet such a correlation is not apparent. For example, sample NS04 01 has anomalously high gold concentration (4 ng/g) and yet the thin section of this sample contains no sulfides. By contrast, sample NS04 05, which contains sulfides in thin section (Fig. 2.4), has low gold concentration (0.155 ng/g). This lack of correlation between gold content and visible sulfides suggests that the sulfides do not contain appreciable gold and that the gold depletion likely occurred prior to the growth of the pyrite and therefore before the entrainment of the xenoliths in the host basalts. If correct, the pervasive gold depletion observed in the xenoliths must have also occurred prior to xenolith entrainment and, thus, the gold contents of the xenoliths can be taken as representative of the gold content of the lower crust, though the process of Au depletion remains obscure.

5.3: Estimate of gold concentration in the continental crust

The data from this study can be used to derive a new estimate for the gold concentration of the lower crust. This estimate, based on the log-normal average of the granulite xenoliths and excluding the outlier, is 0.4 (+1.0 / -0.1) ng/g Au in the lower crust. This is lower than the average of 1.6 ng/g Au suggested by Rudnick and Gao (2003), though nearly within uncertainty. The average gold concentration of all granulites from the literature is 1.1 (+2.0 / -0.6) ng/g. The average gold concentration in the Tanzanian granulite xenoliths is lower, but within one sigma. The gold depletion in the lower crust revealed in this study and Pitcairn et al. (2006b), both of which directly compared genetically similar upper crustal rocks to metamorphosed equivalents, indicate that the middle and lower crust could be pervasively depleted in gold, potentially as a result of high-grade metamorphism.

A new estimate can also be made for the gold concentration of the upper crust. The average gold concentration of the upper-crustal rocks in this study is 4.2 (+33 / -0.5) ng/g. By comparison, the average gold concentration of the upper crust in Rudnick and Gao (2003) is 1.5 ng/g. The greenstone belts of northeastern Tanzania contain gold deposits, and so the higher estimate provided here could be influenced by these deposits, or it could reflect an overall higher gold concentration in Archean upper crust, which has been shown to have a greater proportion of mafic rocks than post-Archean upper crust (Taylor and McLennan, 1985; Condie, 1993). The average gold concentration of upper-crustal rocks from the literature and including the upper-crustal andesites and basalts from this study is 1.2 (+4.3 / -0.3) ng/g.

5.4: Future work:

In the future, it would be useful to investigate sulfur content of these rocks. If gold is travelling with sulfur, there might be a correlation. To further investigate the sulfides in the granulites, and also in the upper-crustal lavas, it would be useful to establish the sulfide mineralogy and chemistry, using an electron probe microanalyzer, in order to determine if they are genetically similar and also to analyze the gold concentrations in the sulfides using laser ablation ICP-MS. Investigating the chemistry of the ilmenites present in the granulites to determine their hematite content would be useful for determining the oxygen fugacity. Also, examining the chemistry of the magnetites would be useful to see if their chemistry is consistent across the granulites indicating that the grains are genetically similar. As in Harlov et al. (1997), the oxygen fugacity of the granulites could be determined by investigating the hematite abundance in the ilmenite grains and the ferrosilite component in the orthopyroxene crystals. This may help to constrain the oxygen fugacity of the samples and determine whether or not they have interacted with a highly-oxidized fluid that might have caused the dissolution of the sulfide minerals and partitioning of gold into the mobile phase. Fluid or melt inclusion work could be performed on the granulites in order to investigate the composition of the potential mobile phases that could have resulted in the depletion of gold in the lower crust

In order to evaluate whether or not there was more gold present in Archean crustal rocks, global gold data could be plotted versus the age of the rocks. A higher gold content in Archean crustal rocks could be a result of deep-seated magmatism, or plume activity in the late Archean that accessed lower mantle reservoirs with higher gold concentrations. The higher gold content of the upper crustal rocks analyzed in this study could be a result of this temporal change in the abundance of gold delivered to the crust or it could be a result of the concentration of gold during ore deposit formation.

Chapter 6: Conclusions

6.1

The main conclusions from this study are as follows:

1) A statistically significant difference exists between the gold concentrations of the upper- and lower-crustal rocks from Tanzanian Craton.
2) This result agrees with the past studies conducted on metamorphic rock suites in the Bamble Belt, Norway, (Cameron, 1989), and in the Otago and Alpine schists, New Zealand (Pitcairn et al., 2006b).
3) The depletion of gold in the lower crust could be associated with high-grade metamorphism, either through dehydration or partial melting reactions during which sulfide phases break down in the presence of an oxidized mobile phase.
4) Using the data in this study a new estimate of 0.4 (+1.0 / -0.1) ng/g Au is derived for the gold concentration of the lower continental crust, and a new estimate of 1.2 (+4.3 / -0.3) ng/g (combining published data with the data for the greenstone belt lavas investigated here) is derived for the upper continental crust.

Appendix

Table A.1: Average Au concentration values for crustal rocks in the literature.

Rock type	Location	n	Ave. Au(ng/g)	Author, Year
Mantle				
Mantle	Mantle		1	McDonough and Sun, 1995
Igneous				
Ultramafic				
Peridotite	Webster, N. Car., U.S.A.	1	2.4	Degrazi and Haskin, 1964
Alpine type dunite	Balsam, N. Car., U.S.A.	1	2.2	Vincent and Crocket, 1960
Layered Group Ultramafics	Ivrea-Verbano Gabbroic complex, Western Alps, Italy	6	3.9	Sighinolfi and Gorgoni, 1977
Pyroxenite	Nir Wandh, Kutch rift basin, India	1	3.1	Crocket, 2008
Shoshonitic Lamprophyres	Yilgarn Block, Western Australia	8	1.9	Taylor et al., 1994
Mafic				
Gabbro	Laget,Bamble, Norway	9	0.25	Alirezaei and Cameron, 2002
Gabbro	Tromoy,Bamble, Norway	4	0.24	Alirezaei and Cameron, 2002
Gabbro	Tvedestrand, Bamble, Norway	5	0.59	Alirezaei and Cameron, 2002
Gabbro	Hisoy, Bamble, Norway	2	0.42	Alirezaei and Cameron, 2002
low-Mg Gabbro	Arendal, Bamble, Norway	3	1.04	Alirezaei and Cameron, 2002
Gabbro	Lakhpa, Kutch rift basin, India	1	5.2	Crocket, 2008
Norite	Bushveld complex	1	2.9	Degrazi and Haskin, 1964
Gabbro	Ironton, Mo., U.S.A.	1	2.4	Degrazi and Haskin, 1964
Layered Group Gabbros	Ivrea-Verbano Gabbroic complex, Western Alps, Italy	5	3.4	Sighinolfi and Gorgoni, 1977

Rock type	Location	n	Ave. Au(ng/g)	Author, Year
Main Gabbro	Ivrea-Verbano Gabbroic complex, Western Alps, Italy	5	1.4	Sighinolfi and Gorgoni, 1977
Mafic plutonic		580	4.8	Crocket, 1974
Diabase	W-1	1	8.4	Vincent and Crocket, 1960
Diabase	W-1	1	4.9	Hamaguchi et al., 1961
Dolerite dyke	Diveghat, Deccan Traps, India	1	5.3	Crocket, 2004
Dolerite dyke	Panvel, Deccan Traps, India	3	6.8	Crocket, 2004
I.R.D.P. dykes	Iceland	9	3.04	Zentilli et al., 1985
Mafic intrusives	Central East China	276	1.05	Gao et al., 1998
Cafemic rocks	Southwestern Quebec	Comp*	0.49	Shaw et al., 1976
Cafemic rocks	Baffin Island	Comp*	10.1	Shaw et al., 1976
Cafemic rocks	Northern Quebec-Ungava,Canadian Shield	Comp*	3.72	Shaw et al., 1976
Continental Basalts				
Mokulaevsky Basalt	Siberian Trap, Noril'sk area, Russia	10	1.6	Brugmann et al., 1993
Morongovsky Basalt	Siberian Trap, Noril'sk area, Russia	10	1.61	Brugmann et al., 1993
Nadezhdinsky Basalt	Siberian Trap, Noril'sk area, Russia	15	0.62	Brugmann et al., 1993
Tuklonsky Picrite	Siberian Trap, Noril'sk area, Russia	2	1.5	Brugmann et al., 1993
Tuklonsky Basalt	Siberian Trap, Noril'sk area, Russia	4	2.11	Brugmann et al., 1993
Gudchichinsky Picrite	Siberian Trap, Noril'sk area, Russia	4	1.93	Brugmann et al., 1993
Gudchichinsky Basalt	Siberian Trap, Noril'sk area, Russia	3	1.05	Brugmann et al., 1993
Siverminsky Basalt	Siberian Trap, Noril'sk area, Russia	5	0.61	Brugmann et al., 1993
Ivankinsky Basalt	Siberian Trap, Noril'sk area, Russia	5	0.8	Brugmann et al., 1993
Basalt	Ambaghat, Deccan Traps, India	5	3.8	Crocket, 2004
Basalt	Rat., Deccan Traps, India	1	5.5	Crocket, 2004
Basalt	Panvel, Deccan Traps, India	2	4.4	Crocket, 2004
Basalt	Bhorghat, Deccan Traps, India	2	1.8	Crocket, 2004

Rock type	Location	n	Ave. Au(ng/g)	Author, Year
Basalt	Koyna, Deccan Traps, India	2	3.5	Crocket, 2004
Basalt	Diveghat, Deccan Traps, India	1	2.3	Crocket, 2004
Basalt	Sing., Deccan traps, India	1	2.8	Crocket, 2004
Basalt	Lintz, Rhenish, Prussia	1	2.6	Degrazi and Haskin, 1964
Cont. Flood Basalt	Deccan, India	18	3.8	Crocket 2004
Cont. Flood Basalt	Parana, India	20	3.1	Crocket unpublished
Cont. Flood Basalt	Karoo	27	1.3	Maier et al., 2001
Cont. Flood Basalt	Noril'sk Lower Triassic	5	1.6	Brugmann et al., 1993
Cont. Flood Basalt	Noril'sk Lower Triassic to Upper Permian	6	1	Brugmann et al., 1993
Cont. Flood Basalt	Greenland	5	3.3	Nielsen and Brooks, 1995
Cont. Flood Basalt	North American mid-continent	2	1.7	Theriault et al., 1997
Basalt-basanite sill	Sadra sill, Kutch rift basin, India	2	1.4	Crocket, 2008
Alkali basalt	Keera, Kutch rift basin, India	1	0.56	Crocket, 2008
Deccan tholeiite	Pranpur, Kutch rift basin, India	1	5	Crocket, 2008
Deccan tholeiite	Dhanoi, Kutch rift basin, India	1	3.4	Crocket, 2008
Olivine norm. tholeiites	Iceland	25	1.45	Zentilli et al., 1985
Quartz norm. tholeiites	Iceland	21	2	Zentilli et al., 1985
Basaltic andesites and Icelandite	Iceland	5	4.1	Zentilli et al., 1985
I.R.D.P.(Icelandic Research Drilling Project) lava flows	Iceland	18	1.68	Zentilli et al., 1985
Holmatindur lava flows	Iceland	24	1.69	Zentilli et al., 1985
Post-Archean mafic Volcanics	Central East China	583	1.01	Gao et al., 1998
Oceanic basalts				
Basalt	Mid-Atlantic Ridge, GE-159	1	10.6	Degrazi and Haskin, 1964

Rock type	Location	n	Ave. Au(ng/g)	Author, Year
Basalt	Mid-Atlantic Ridge, GE-160	1	6.3	Degrazi and Haskin, 1964
Basalt	Mid-Atlantic Ridge, GE-260	1	14	Degrazi and Haskin, 1964
Olivine Basalt	Jefferson Co., Colorado, U.S.A.	1	4	Degrazi and Haskin, 1964
Tertiary olivine basalt	Morvern, Scotland	1	2.2	Vincent and Crocket, 1960
Tertiary tholeiitic basalt	N. Ireland	1	2	Vincent and Crocket, 1960
Tholeiitic olivine basalt	Mauna Loa, Hawaii	1	2.6	Vincent and Crocket, 1960
Oceanic island basalts		4	0.5	Crocket et al., 1973
Island arc tholeiitic basalts	Izu-Oshima volcanic area	30	1.9	Togashi and Terashima, 1997
Island arc tholeiitic basalts	Fuji volcanic area	22	0.98	Togashi and Terashima, 1997
Island arc tholeiitic basalts	Osoreyama volcanic area	5	0.34	Togashi and Terashima, 1997
Intermediate to mafic				
Post-Archean Diorite	Central East China	243	0.47	Gao et al., 1998
Archean TTG	Central East China	502	1.05	Gao et al., 1998
Post-Archean TTG	Central East China	596	0.51	Gao et al., 1998
Mafic volcanics		696	3.6	Crocket, 1974
Intermediate plutonics		261	3.2	Crocket, 1974
Felsic				
Archean granite	Central East China	369	0.41	Gao et al., 1998
Post-Archean granite	Central East China	1140	2.21	Gao et al., 1998
Biotite granite	Stone Mt., GA, U.S.A.	1	1.9	Degrazi and Haskin, 1964
Granite	Bridgelans Still	1	4.7	Degrazi and Haskin, 1964
Aplite	Boulder, Colorado, U.S.A.	1	3.3	Degrazi and Haskin, 1964
Red granite	Wausau, Wisconsin, U.S.A.	1	3.3	Degrazi and Haskin, 1964
Standard Granite	G-1	1	4.5	Vincent and Crocket, 1960
Nepheline syenite	Bancroft, Ontario, Canada	1	2.6	Degrazi and Haskin, 1964

Rock type	Location	n	Ave. Au(ng/g)	Author, Year
Nepheline syenite	Wausau, Wisconsin, U.S.A.	1	0.64	Degrazi and Haskin, 1964
Nepheline sodalite syenite	Red Hill, N.H., U.S.A.	1	0.98	Degrazi and Haskin, 1964
Granites		310	1.7	Crocket, 1974
Felsic volcanics	Central East China	895	0.67	Gao et al., 1998
Rhyolites		188	1.5	Crocket, 1974
Syenodioritic rocks	Southwestern Quebec	Comp*	0.45	Shaw et al., 1976
Syenodioritic rocks	Northern Quebec-Ungava,Canadian Shield	Comp*	2.42	Shaw et al., 1976
Carbonatites				
Carbonatite	Panda Hill, Tanganyika	1	1.6	Degrazi and Haskin, 1964
Volcanic glasses and volcaniclastics				
Obsidian	Rotorua, New Zealand	1	21	Degrazi and Haskin, 1964
Perlite	Queensland, Australia	1	1.5	Degrazi and Haskin, 1964
Volcaniclastic units	Iceland	3	5.23	Zentilli et al., 1985
Impact glasses				
Bediasite		1	3	Degrazi and Haskin, 1964
Philippinite	Phillippenes	1	6.7	Degrazi and Haskin, 1964
Sedimentary				
Greywacke	Gowganda Form., Ontario, Canada	1	2.3	Degrazi and Haskin, 1964
Sandstone	Kettleman Hills, California	8	41	Degrazi and Haskin, 1964
Sandstone	Keweenawan, Wisconsin, U.S.A.	1	11.6	Degrazi and Haskin, 1964
Sandstone	Berea Form., Ky. U.S.A.	1	2.6	Degrazi and Haskin, 1964
Sandstone and siltstone		105	3	Crocket, 1974
Tertiary sandstone	Kettleman Hills, California, U.S.A.	1	41	Degrazi and Haskin, 1964
Quartz-rich sediments	Southwestern Quebec	Comp*	1.37	Shaw et al., 1976

Rock type	Location	n	Ave. Au(ng/g)	Author, Year
Quartz-rich sediments	Northern Quebec-Ungava,Canadian Shield	Comp*	2.80	Shaw et al., 1976
Quartzofeldspathic	Southwestern Quebec	Comp*	0.41	Shaw et al., 1976
Quartzofeldspathic	Northern Saskatchewan	Comp*	0.3	Shaw et al., 1976
Quartzofeldspathic	Baffin Island	Comp*	2.7	Shaw et al., 1976
Quartzofeldspathic	Northern Quebec-Ungava,Canadian Shield	Comp*	3.97	Shaw et al., 1976
Quartzofeldspathic Rock	Torlesse Terrane, Alpine Schists, New Zealand	13	0.56	Pitcairn et al., 2006
Quartzofeldspathic Rock	Caples Terrane,Otago Schists, New Zealand	9	1.24	Pitcairn et al., 2006
Archean arenaceous rocks	Central East China		1.36	Gao et al., 1998
Arenaceous rocks	Central East China		2.12	Gao et al., 1998
Archean pelitic rocks	Central East China		1.76	Gao et al., 1998
Post-Archean pelitic rocks	Central East China		1.8	Gao et al., 1998
Shale	Muncie Creek Form., Kans., U.S.A.		7.2	Degrazi and Haskin, 1964
Shale	Homestake Form., S. Dak., U.S.A.		4.7	Degrazi and Haskin, 1964
Shale	Oklahoma, U.S.A.		18	Orth et al., 1988
Shale	Indiana, U.S.A.		7	Coveney and Glascock, 1989
Shale		28	2.5	Crocket, 1974
Black shales	Central U.S.A.	74	2.5	Coveney and Glascock, 1989
Black shales	China	6	8.2	Coveney et al., 1992
Black shales	China	2	120	Fan, 1983
Black shales	World values	9120	7	Ketris and Yudovich, 2009
Black shales	Background Au in Popovich and Roberts Mt. Form.	78	14	Large et al., 2011
Terrigenous Sediments	Japan	85	2.4	Terashima et al., 1995
Red clay	Brazil Basin, 343cm core depth	1	31	Degrazi and Haskin, 1964
Red clay	Brazil Basin, 664cm core depth	1	11.6	Degrazi and Haskin, 1964
Red clay	Brazil Basin, 887cm core depth	1	4.2	Degrazi and Haskin, 1964

Rock type	Location	n	Ave. Au(ng/g)	Author, Year
Lutite	Argentine Basin 100cm core depth	1	10.6	Degrazi and Haskin, 1964
Lutite	Argentine Basin 355cm core depth	1	3.1	Degrazi and Haskin, 1964
Lutite	Argentine Basin 675cm core depth	1	5.2	Degrazi and Haskin, 1964
Lutite	Argentine Basin 1045cm core depth	1	17.3	Degrazi and Haskin, 1964
Deep-sea sediments		28	3.4	Crocket, 1974
Pelagic Sediments	Central Pacific	139	1.4	Terashima et al., 1995
Coal	Kentucky, U.S.A.		2	Chyi, 1982
Mud	Pacific coast, near waste dump, California, U.S.A.		920	Koide et al., 1986
Anoxic mud	Pacific, near coast, Chile		2	Koide et al., 1986
Peat	Sri Lanka		610	Dissanayake and Kritsotakis, 1984
Algal mat	Sri Lanka		1100	Dissanayake and Kritsotakis, 1984
Archean carbonate rocks	Central East China		0.41	Gao et al., 1998
Carbonate rocks	Central East China		1.31	Gao et al., 1998
Limestone	Paola Form., Kans., U.S.A.	1	4.8	Degrazi and Haskin, 1964
Recent Carbonate	Florida Coast, U.S.A.	1	3.9	Degrazi and Haskin, 1964
Oolite	Cleeve Hill, Cheltenham, England	1	2.3	Degrazi and Haskin, 1964
Recent coral	Florida Keys, U.S.A.	1	0.8	Degrazi and Haskin, 1964
Carbonates		20	2	Crocket, 1974
Carbonates	Southwestern Quebec	Comp*	1.48	Shaw et al., 1976
Carbonates	Northern Quebec-Ungava,Canadian Shield	Comp*	8.75	Shaw et al., 1976
Metamorphic				
Mafic				
Mixed gneiss Hinnebu	Bamble belt, Norway	32	0.15	Crocket, 1974; Korobeynikov, 1986
Tonalite gneiss Tromoy		51	0.24	Crocket, 1974; Korobeynikov, 1986
Metabasite Tvedestrand		16	0.16	Crocket, 1974; Korobeynikov, 1986

Rock type	Location	n	Ave. Au(ng/g)	Author, Year
Metabasite Tromoy		16	0.17	Crocket, 1974; Korobeynikov, 1986
Archean amphibolites	Central East China		8.21	Gao et al., 1998
Amphibolite	Laget, Bamble Belt, Norway	11	0.37	Alirezaei and Cameron, 2002
Amphibolite	Tvedstrand, Bamble Belt, Norway	4	0.43	Alirezaei and Cameron, 2002
Amphibolite	Hisoy, Bamble Belt, Norway	3	0.38	Alirezaei and Cameron, 2002
Metafelsic volcanics	Central East China		0.25	Gao et al., 1998
Garnet gneiss Arendal		13	0.37	Crocket, 1974; Korobeynikov, 1986
Archean mafic granulites	Central East China	93	0.99	Gao et al., 1998
Mafic granulites	Bahia State, Brazil	8	0.73	Sighinolfi and Santos, 1976
Intermediate				
Intermediate granulites	Central East China	115	1.35	Gao et al., 1998
Felsic				
Archean felsic granulites	Central East China	116	1	Gao et al., 1998
Charnockite granulites	Ivrea-Verbano Gabbroic complex, Western Alps, Italy	5	1.9	Sighinolfi and Gorgoni, 1977
Acid granulites	Bahia State, Brazil	42	0.57	Sighinolfi and Santos, 1976
Intermediate granulites	Bahia State, Brazil	51	1.58	Sighinolfi and Santos, 1976
Stronalithe granulites	Ivrea-Verbano Gabbroic complex, Western Alps, Italy	5	3.0	Sighinolfi and Gorgoni, 1977
Metasediments				
Argillite and Slate		135	1	Crocket, 1974
Schists		114	2.2	Crocket, 1974
Gneisses		37	3.9	Crocket, 1974
Aluminous schist, gneiss	Baffin Island	Comp*	2.4	Shaw et al., 1976
Aluminous schist, gneiss	Northern Quebec-Ungava,Canadian Shield	Comp*	2.80	Shaw et al., 1976
Mica-garnet gneiss	New York City, U.S.A.	1	1.8	Degrazi and Haskin, 1964
Metasandstone	Taylor's Head, Goldenville and Halifax Group	4	0.4	White and Goodwin, 2011

Rock type	Location	n	Ave. Au(ng/g)	Author, Year
Lower greenschist	Torlesse Terrane,Otago and Alpine Schists	12	0.34	Pitcairn et al., 2006b
Chlorite greenschist	Torlesse Terrane,Otago and Alpine Schists	17	0.23	Pitcairn et al., 2006b
Biotite greenschist	Torlesse Terrane,Otago and Alpine Schists	6	0.36	Pitcairn et al., 2006b
Garnet greenschist	Torlesse Terrane,Otago and Alpine Schists	7	0.21	Pitcairn et al., 2006b
Garnet-Olig Amphibolite	Torlesse Terrane,Otago and Alpine Schists	8	0.22	Pitcairn et al., 2006b
Lower Greenschist	Caples Terrane,Otago Schists, New Zealand	9	0.29	Pitcairn et al., 2006b
Chlorite Greenschist	Caples Terrane,Otago Schists, New Zealand	9	0.15	Pitcairn et al., 2006b
Quartzite	Rib Mt., Wisconsin, U.S.A.	1	7.3	Degrazi and Haskin, 1964
Quartzite	Devils' Lake, Wisconsin, U.S.A.	1	2.4	Degrazi and Haskin, 1964
Metasandstone	Bluestone,Goldenville and Halifax Group, Canada	8	0.64	White and Goodwin, 2011
Metasiltstone	Beaverbank, Goldenville and Halifax Group, Canada	6	1.5	White and Goodwin, 2011
Metaliferous Black slates	Dukpyungri-A, Okcheon belt, Korea	14	22.1	Jeong, 2006
Metaliferous Black slates	Dukpyungri-B, Okcheon belt, Korea	1	71	Jeong, 2006
Metaliferous Black slates	Dukpyungri-C, Okcheon belt, Korea	5	30.2	Jeong, 2006
Metaliferous Black slates	Jogokri, Okcheon belt, Korea	9	9.7	Jeong, 2006
Metaliferous Black slates	Hasodong, Okcheon belt, Korea	4	15.0	Jeong, 2006
Slate	Cunard, Goldenville and Halifax Group, Canada	10	0.56	White and Goodwin, 2011
Marble	Beldens Form., Vt., U.S.A.	1	0.86	Degrazi and Haskin, 1964

Comp* indicates representative composite sampling

Table A.2: Individual Au concentration values for crustal rocks in the literature.

Rock type	Sample No./Location	n	Au (ng/g)	Author, Year
Igneous				
Ultramafic				
Peridotite	Webster, N. Car., U.S.A.	1	2.4	Degrazi and Haskin, 1964
Alpine type dunite	Balsam, N. Car., U.S.A.	1	2.2	Vincent and Crocket, 1960
Dunite	MO 58 Ivrea-Verbano complex, Western Alps	1	4.0	Sighinolfi and Gorgoni, 1977
Dunite	MO 59 Ivrea-Verbano complex, Western Alps	1	3.3	Sighinolfi and Gorgoni, 1977
Lherzolite	MO 5 Ivrea-Verbano complex, Western Alps	1	2.0	Sighinolfi and Gorgoni, 1977
Lherzolite	MO 13 Ivrea-Verbano complex, Western Alps	1	<0.6	Sighinolfi and Gorgoni, 1977
Lherzolite	MO 66 Ivrea-Verbano complex, Western Alps	1	<0.6	Sighinolfi and Gorgoni, 1977
Lherzolite	MO 69 Ivrea-Verbano complex, Western Alps	1	2.1	Sighinolfi and Gorgoni, 1977
Lherzolite	MO 44 Ivrea-Verbano complex, Western Alps	1	1.7	Sighinolfi and Gorgoni, 1977
Harzburgite	MO 74 Ivrea-Verbano complex, Western Alps	1	<0.6	Sighinolfi and Gorgoni, 1977
Pyroxenite	Nir Wandh, Kutch rift basin, India	1	3.1	Crocket, 2008
Pyroxenite	MO 2 Ivrea-Verbano complex, Western Alps	1	4.6	Sighinolfi and Gorgoni, 1977
Pyroxenite	MO 3 Ivrea-Verbano complex, Western Alps	1	4.5	Sighinolfi and Gorgoni, 1977
Pyroxenite	MO 12 Ivrea-Verbano complex, Western Alps Italy	1	3.1	Sighinolfi and Gorgoni, 1977
Pyroxenite	MO 20 Ivrea-Verbano complex, Western Alps	1	1.0	Sighinolfi and Gorgoni, 1977
Pyroxenite	MO 29 Ivrea-Verbano complex, Western Alps	1	3.0	Sighinolfi and Gorgoni, 1977
Pyroxenite	MO 49 Ivrea-Verbano complex, Western Alps	1	10.5	Sighinolfi and Gorgoni, 1977
Shoshonitic Lamprophyre	Z36437, Yilgarn Block, Western Australia	1	3.7	Taylor et al., 1994
Shoshonitic Lamprophyre	Z36438, Yilgarn Block, Western Australia	1	0.7	Taylor et al., 1994
Shoshonitic Lamprophyre	Z36436, Yilgarn Block, Western Australia	1	0.8	Taylor et al., 1994
Shoshonitic Lamprophyre	Z36417, Yilgarn Block, Western Australia	1	2.3	Taylor et al., 1994
Shoshonitic Lamprophyre	Z36414, Yilgarn Block, Western Australia	1	2.3	Taylor et al., 1994

Rock type	Sample No./Location	n	Au (ng/g)	Author, Year
Shoshonitic Lamprophyre	Z36413, Yilgarn Block, Western Australia	1	0.8	Taylor et al., 1994
Shoshonitic Lamprophyre	Z36412, Yilgarn Block, Western Australia	1	0.7	Taylor et al., 1994
Shoshonitic Lamprophyre	Z36408, Yilgarn Block, Western Australia	1	0.6	Taylor et al., 1994
Shoshonitic Lamprophyre	Z18496, Yilgarn Block, Western Australia	1	0.5	Taylor et al., 1994
Shoshonitic Lamprophyre	Z18500, Yilgarn Block, Western Australia	1	0.6	Taylor et al., 1994
Shoshonitic Lamprophyre	Z32680, Yilgarn Block, Western Australia	1	8.7	Taylor et al., 1994
Shoshonitic Lamprophyre	Z27932, Yilgarn Block, Western Australia	1	0.8	Taylor et al., 1994
Shoshonitic Lamprophyre	Z27944, Yilgarn Block, Western Australia	1	0.8	Taylor et al., 1994
Shoshonitic Lamprophyre	Z27949, Yilgarn Block, Western Australia	1	2.6	Taylor et al., 1994
Shoshonitic Lamprophyre	Z15976, Yilgarn Block, Western Australia	1	4.3	Taylor et al., 1994
Shoshonitic Lamprophyre	Z18493, Yilgarn Block, Western Australia	1	0.8	Taylor et al., 1994
Shoshonitic Lamprophyre	Z27928, Yilgarn Block, Western Australia	1	0.4	Taylor et al., 1994
Shoshonitic Lamprophyre	Z18451, Yilgarn Block, Western Australia	1	1800	Taylor et al., 1994
Shoshonitic Lamprophyre	Z18444, Yilgarn Block, Western Australia	1	13.4	Taylor et al., 1994
Shoshonitic Lamprophyre	Z40001, Yilgarn Block, Western Australia	1	2.0	Taylor et al., 1994
Shoshonitic Lamprophyre	Z27962, Yilgarn Block, Western Australia	1	1.2	Taylor et al., 1994
Shoshonitic Lamprophyre	Z19019, Yilgarn Block, Western Australia	1	3.0	Taylor et al., 1994
Shoshonitic Lamprophyre	Z18470, Yilgarn Block, Western Australia	1	1970	Taylor et al., 1994
Shoshonitic Lamprophyre	Z18471, Yilgarn Block, Western Australia	1	63.9	Taylor et al., 1994
Shoshonitic Lamprophyre	Z27969, Yilgarn Block, Western Australia	1	2.3	Taylor et al., 1994
Shoshonitic Lamprophyre	Z40013, Yilgarn Block, Western Australia	1	8.8	Taylor et al., 1994
Shoshonitic Lamprophyre	Z40014, Yilgarn Block, Western Australia	1	3.0	Taylor et al., 1994
Shoshonitic Lamprophyre	Z19027, Yilgarn Block, Western Australia	1	2.0	Taylor et al., 1994
Shoshonitic Lamprophyre	Z32699, Yilgarn Block, Western Australia	1	5.0	Taylor et al., 1994
Shoshonitic Lamprophyre	Z40016, Yilgarn Block, Western Australia	1	3.7	Taylor et al., 1994

Rock type	Sample No./Location	n	Au (ng/g)	Author, Year
Shoshonitic Lamprophyre	47119, Yilgarn Block, Western Australia	1	1.5	Taylor et al., 1994
Shoshonitic Lamprophyre	47121, Yilgarn Block, Western Australia	1	1.0	Taylor et al., 1994
Shoshonitic Lamprophyre	106681, Yilgarn Block, Western Australia	1	1.8	Taylor et al., 1994
Shoshonitic Lamprophyre	16932, Yilgarn Block, Western Australia	1	27.8	Taylor et al., 1994
Shoshonitic Lamprophyre	11707A, Yilgarn Block, Western Australia	1	0.5	Taylor et al., 1994
Shoshonitic Lamprophyre	11693, Yilgarn Block, Western Australia	1	0.4	Taylor et al., 1994
Shoshonitic Lamprophyre	8019, Yilgarn Block, Western Australia	1	5.4	Taylor et al., 1994
Shoshonitic Lamprophyre	8004, Yilgarn Block, Western Australia	1	0.8	Taylor et al., 1994
Shoshonitic Lamprophyre	8012, Yilgarn Block, Western Australia	1	0.8	Taylor et al., 1994
Shoshonitic Lamprophyre	9730, Yilgarn Block, Western Australia	1	0.6	Taylor et al., 1994
Shoshonitic Lamprophyre	9731, Yilgarn Block, Western Australia	1	0.7	Taylor et al., 1994
Shoshonitic Lamprophyre	14096, Yilgarn Block, Western Australia	1	0.5	Taylor et al., 1994
Shoshonitic Lamprophyre	14616, Yilgarn Block, Western Australia	1	1.6	Taylor et al., 1994
Shoshonitic Lamprophyre	15295, Yilgarn Block, Western Australia	1	1.7	Taylor et al., 1994
Shoshonitic Lamprophyre	108846, Yilgarn Block, Western Australia	1	60.4	Taylor et al., 1994
Shoshonitic Lamprophyre	108845, Yilgarn Block, Western Australia	1	10.8	Taylor et al., 1994
Shoshonitic Lamprophyre	108834, Yilgarn Block, Western Australia	1	2.5	Taylor et al., 1994
Shoshonitic Lamprophyre	108847, Yilgarn Block, Western Australia	1	2920	Taylor et al., 1994
Shoshonitic Lamprophyre	108838, Yilgarn Block, Western Australia	1	5.1	Taylor et al., 1994
Shoshonitic Lamprophyre	Z36437, Yilgarn Block, Western Australia	1	<5	Taylor et al., 1994
Shoshonitic Lamprophyre	Z36438, Yilgarn Block, Western Australia	1	<5	Taylor et al., 1994
Shoshonitic Lamprophyre	Z36436, Yilgarn Block, Western Australia	1	<5	Taylor et al., 1994
Shoshonitic Lamprophyre	Z36417, Yilgarn Block, Western Australia	1	<5	Taylor et al., 1994
Shoshonitic Lamprophyre	Z36414, Yilgarn Block, Western Australia	1	<5	Taylor et al., 1994
Shoshonitic Lamprophyre	Z36413, Yilgarn Block, Western Australia	1	<5	Taylor et al., 1994

Rock type	Sample No./Location	n	Au (ng/g)	Author, Year
Shoshonitic Lamprophyre	Z36412, Yilgarn Block, Western Australia	1	<5	Taylor et al., 1994
Shoshonitic Lamprophyre	Z36408, Yilgarn Block, Western Australia	1	<5	Taylor et al., 1994
Shoshonitic Lamprophyre	Z18496, Yilgarn Block, Western Australia	1	<5	Taylor et al., 1994
Shoshonitic Lamprophyre	Z18500, Yilgarn Block, Western Australia	1	<5	Taylor et al., 1994
Shoshonitic Lamprophyre	Z32680, Yilgarn Block, Western Australia	1	<5	Taylor et al., 1994
Shoshonitic Lamprophyre	Z27932, Yilgarn Block, Western Australia	1	<5	Taylor et al., 1994
Shoshonitic Lamprophyre	Z27944, Yilgarn Block, Western Australia	1	<5	Taylor et al., 1994
Shoshonitic Lamprophyre	Z27949, Yilgarn Block, Western Australia	1	<5	Taylor et al., 1994
Shoshonitic Lamprophyre	Z15976, Yilgarn Block, Western Australia	1	<5	Taylor et al., 1994
Shoshonitic Lamprophyre	Z18493, Yilgarn Block, Western Australia	1	<5	Taylor et al., 1994
Shoshonitic Lamprophyre	Z27928, Yilgarn Block, Western Australia	1	<5	Taylor et al., 1994
Shoshonitic Lamprophyre	Z18451, Yilgarn Block, Western Australia	1	2500	Taylor et al., 1994
Shoshonitic Lamprophyre	Z18444, Yilgarn Block, Western Australia	1	12	Taylor et al., 1994
Shoshonitic Lamprophyre	Z40001, Yilgarn Block, Western Australia	1	<5	Taylor et al., 1994
Shoshonitic Lamprophyre	Z27962, Yilgarn Block, Western Australia	1	<5	Taylor et al., 1994
Shoshonitic Lamprophyre	Z19019, Yilgarn Block, Western Australia	1	<5	Taylor et al., 1994
Shoshonitic Lamprophyre	Z18470, Yilgarn Block, Western Australia	1	1545	Taylor et al., 1994
Shoshonitic Lamprophyre	Z18471, Yilgarn Block, Western Australia	1	176	Taylor et al., 1994
Shoshonitic Lamprophyre	Z27969, Yilgarn Block, Western Australia	1	<5	Taylor et al., 1994
Shoshonitic Lamprophyre	Z40013, Yilgarn Block, Western Australia	1	11	Taylor et al., 1994
Shoshonitic Lamprophyre	Z40014, Yilgarn Block, Western Australia	1	<5	Taylor et al., 1994
Shoshonitic Lamprophyre	Z19027, Yilgarn Block, Western Australia	1	<5	Taylor et al., 1994
Shoshonitic Lamprophyre	Z32699, Yilgarn Block, Western Australia	1	<5	Taylor et al., 1994
Shoshonitic Lamprophyre	Z40016, Yilgarn Block, Western Australia	1	<5	Taylor et al., 1994
Shoshonitic Lamprophyre	47119, Yilgarn Block, Western Australia	1	<5	Taylor et al., 1994

Rock type	Sample No./Location	n	Au (ng/g)	Author, Year
Shoshonitic Lamprophyre	47121, Yilgarn Block, Western Australia	1	<5	Taylor et al., 1994
Shoshonitic Lamprophyre	106681, Yilgarn Block, Western Australia	1	<5	Taylor et al., 1994
Shoshonitic Lamprophyre	16932, Yilgarn Block, Western Australia	1	31	Taylor et al., 1994
Shoshonitic Lamprophyre	11707A, Yilgarn Block, Western Australia	1	<5	Taylor et al., 1994
Shoshonitic Lamprophyre	11693, Yilgarn Block, Western Australia	1	<5	Taylor et al., 1994
Shoshonitic Lamprophyre	8019, Yilgarn Block, Western Australia	1	<5	Taylor et al., 1994
Shoshonitic Lamprophyre	8004, Yilgarn Block, Western Australia	1	<5	Taylor et al., 1994
Shoshonitic Lamprophyre	9730, Yilgarn Block, Western Australia	1	<5	Taylor et al., 1994
Shoshonitic Lamprophyre	9731, Yilgarn Block, Western Australia	1	<5	Taylor et al., 1994
Shoshonitic Lamprophyre	14096, Yilgarn Block, Western Australia	1	<5	Taylor et al., 1994
Shoshonitic Lamprophyre	14616, Yilgarn Block, Western Australia	1	<5	Taylor et al., 1994
Shoshonitic Lamprophyre	15295, Yilgarn Block, Western Australia	1	<5	Taylor et al., 1994
Shoshonitic Lamprophyre	108846, Yilgarn Block, Western Australia	1	52	Taylor et al., 1994
Shoshonitic Lamprophyre	108845, Yilgarn Block, Western Australia	1	<5	Taylor et al., 1994
Shoshonitic Lamprophyre	108834, Yilgarn Block, Western Australia	1	10	Taylor et al., 1994
Shoshonitic Lamprophyre	108847, Yilgarn Block, Western Australia	1	10700	Taylor et al., 1994
Shoshonitic Lamprophyre	108838, Yilgarn Block, Western Australia	1	<5	Taylor et al., 1994
Shoshonitic Lamprophyre	Z36437, Yilgarn Block, Western Australia	1	b.d.	Taylor et al., 1994
Shoshonitic Lamprophyre	Z36438, Yilgarn Block, Western Australia	1	b.d.	Taylor et al., 1994
Shoshonitic Lamprophyre	Z36436, Yilgarn Block, Western Australia	1	b.d.	Taylor et al., 1994
Shoshonitic Lamprophyre	Z36417, Yilgarn Block, Western Australia	1	3	Taylor et al., 1994
Shoshonitic Lamprophyre	Z36414, Yilgarn Block, Western Australia	1	b.d.	Taylor et al., 1994
Shoshonitic Lamprophyre	Z36413, Yilgarn Block, Western Australia	1	b.d.	Taylor et al., 1994
Shoshonitic Lamprophyre	Z36412, Yilgarn Block, Western Australia	1	b.d.	Taylor et al., 1994
Shoshonitic Lamprophyre	Z36408, Yilgarn Block, Western Australia	1	b.d.	Taylor et al., 1994

Rock type	Sample No./Location	n	Au (ng/g)	Author, Year
Shoshonitic Lamprophyre	Z18496, Yilgarn Block, Western Australia	1	b.d.	Taylor et al., 1994
Shoshonitic Lamprophyre	Z18500, Yilgarn Block, Western Australia	1	b.d.	Taylor et al., 1994
Shoshonitic Lamprophyre	Z32680, Yilgarn Block, Western Australia	1	3	Taylor et al., 1994
Shoshonitic Lamprophyre	Z27932, Yilgarn Block, Western Australia	1	<2	Taylor et al., 1994
Shoshonitic Lamprophyre	Z27944, Yilgarn Block, Western Australia	1	b.d.	Taylor et al., 1994
Shoshonitic Lamprophyre	Z27949, Yilgarn Block, Western Australia	1	b.d.	Taylor et al., 1994
Shoshonitic Lamprophyre	Z15976, Yilgarn Block, Western Australia	1	b.d.	Taylor et al., 1994
Shoshonitic Lamprophyre	Z18493, Yilgarn Block, Western Australia	1	<2	Taylor et al., 1994
Shoshonitic Lamprophyre	Z27928, Yilgarn Block, Western Australia	1	b.d.	Taylor et al., 1994
Shoshonitic Lamprophyre	Z18451, Yilgarn Block, Western Australia	1	2000	Taylor et al., 1994
Shoshonitic Lamprophyre	Z18444, Yilgarn Block, Western Australia	1	5	Taylor et al., 1994
Shoshonitic Lamprophyre	Z40001, Yilgarn Block, Western Australia	1	<2	Taylor et al., 1994
Shoshonitic Lamprophyre	Z27962, Yilgarn Block, Western Australia	1	b.d.	Taylor et al., 1994
Shoshonitic Lamprophyre	Z19019, Yilgarn Block, Western Australia	1	b.d.	Taylor et al., 1994
Shoshonitic Lamprophyre	Z18470, Yilgarn Block, Western Australia	1	b.d.	Taylor et al., 1994
Shoshonitic Lamprophyre	Z18471, Yilgarn Block, Western Australia	1	260	Taylor et al., 1994
Shoshonitic Lamprophyre	Z27969, Yilgarn Block, Western Australia	1	2	Taylor et al., 1994
Shoshonitic Lamprophyre	Z40013, Yilgarn Block, Western Australia	1	4	Taylor et al., 1994
Shoshonitic Lamprophyre	Z40014, Yilgarn Block, Western Australia	1	b.d.	Taylor et al., 1994
Shoshonitic Lamprophyre	Z19027, Yilgarn Block, Western Australia	1	<2	Taylor et al., 1994
Shoshonitic Lamprophyre	Z32699, Yilgarn Block, Western Australia	1	b.d.	Taylor et al., 1994
Shoshonitic Lamprophyre	Z40016, Yilgarn Block, Western Australia	1	3	Taylor et al., 1994
Shoshonitic Lamprophyre	47119, Yilgarn Block, Western Australia	1	b.d.	Taylor et al., 1994
Shoshonitic Lamprophyre	47121, Yilgarn Block, Western Australia	1	b.d.	Taylor et al., 1994
Shoshonitic Lamprophyre	106681, Yilgarn Block, Western Australia	1	3	Taylor et al., 1994

Rock type	Sample No./Location	n	Au (ng/g)	Author, Year
Shoshonitic Lamprophyre	16932, Yilgarn Block, Western Australia	1	13	Taylor et al., 1994
Shoshonitic Lamprophyre	11707A, Yilgarn Block, Western Australia	1	b.d.	Taylor et al., 1994
Shoshonitic Lamprophyre	11693, Yilgarn Block, Western Australia	1	<2	Taylor et al., 1994
Shoshonitic Lamprophyre	8019, Yilgarn Block, Western Australia	1	3	Taylor et al., 1994
Shoshonitic Lamprophyre	8004, Yilgarn Block, Western Australia	1	b.d.	Taylor et al., 1994
Shoshonitic Lamprophyre	8012, Yilgarn Block, Western Australia	1	b.d.	Taylor et al., 1994
Shoshonitic Lamprophyre	9730, Yilgarn Block, Western Australia	1	b.d.	Taylor et al., 1994
Shoshonitic Lamprophyre	9731, Yilgarn Block, Western Australia	1	b.d.	Taylor et al., 1994
Shoshonitic Lamprophyre	14096, Yilgarn Block, Western Australia	1	b.d.	Taylor et al., 1994
Shoshonitic Lamprophyre	14616, Yilgarn Block, Western Australia	1	b.d.	Taylor et al., 1994
Shoshonitic Lamprophyre	15295, Yilgarn Block, Western Australia	1	2	Taylor et al., 1994
Shoshonitic Lamprophyre	108846, Yilgarn Block, Western Australia	1	b.d.	Taylor et al., 1994
Shoshonitic Lamprophyre	108845, Yilgarn Block, Western Australia	1	11	Taylor et al., 1994
Shoshonitic Lamprophyre	108834, Yilgarn Block, Western Australia	1	6	Taylor et al., 1994
Shoshonitic Lamprophyre	108847, Yilgarn Block, Western Australia	1	4300	Taylor et al., 1994
Shoshonitic Lamprophyre	108838, Yilgarn Block, Western Australia	1	b.d.	Taylor et al., 1994
Shoshonitic Lamprophyre	Z36437, Yilgarn Block, Western Australia	1	<8	Taylor et al., 1994
Shoshonitic Lamprophyre	Z36438, Yilgarn Block, Western Australia	1	<8	Taylor et al., 1994
Shoshonitic Lamprophyre	Z36436, Yilgarn Block, Western Australia	1	<8	Taylor et al., 1994
Shoshonitic Lamprophyre	Z36417, Yilgarn Block, Western Australia	1	<8	Taylor et al., 1994
Shoshonitic Lamprophyre	Z36414, Yilgarn Block, Western Australia	1	<8	Taylor et al., 1994
Shoshonitic Lamprophyre	Z36413, Yilgarn Block, Western Australia	1	b.d.	Taylor et al., 1994
Shoshonitic Lamprophyre	Z36412, Yilgarn Block, Western Australia	1	<8	Taylor et al., 1994
Shoshonitic Lamprophyre	Z36408, Yilgarn Block, Western Australia	1	<8	Taylor et al., 1994
Shoshonitic Lamprophyre	Z18496, Yilgarn Block, Western Australia	1	<8	Taylor et al., 1994

Rock type	Sample No./Location	n	Au (ng/g)	Author, Year
Shoshonitic Lamprophyre	Z18500, Yilgarn Block, Western Australia	1	<8	Taylor et al., 1994
Shoshonitic Lamprophyre	Z32680, Yilgarn Block, Western Australia	1	10	Taylor et al., 1994
Shoshonitic Lamprophyre	Z27932, Yilgarn Block, Western Australia	1	<8	Taylor et al., 1994
Shoshonitic Lamprophyre	Z27944, Yilgarn Block, Western Australia	1	<8	Taylor et al., 1994
Shoshonitic Lamprophyre	Z27949, Yilgarn Block, Western Australia	1	<8	Taylor et al., 1994
Shoshonitic Lamprophyre	Z15976, Yilgarn Block, Western Australia	1	<8	Taylor et al., 1994
Shoshonitic Lamprophyre	Z18493, Yilgarn Block, Western Australia	1	<8	Taylor et al., 1994
Shoshonitic Lamprophyre	Z27928, Yilgarn Block, Western Australia	1	<8	Taylor et al., 1994
Shoshonitic Lamprophyre	Z18451, Yilgarn Block, Western Australia	1	1550	Taylor et al., 1994
Shoshonitic Lamprophyre	Z18444, Yilgarn Block, Western Australia	1	17	Taylor et al., 1994
Shoshonitic Lamprophyre	Z40001, Yilgarn Block, Western Australia	1	<8	Taylor et al., 1994
Shoshonitic Lamprophyre	Z27962, Yilgarn Block, Western Australia	1	<8	Taylor et al., 1994
Shoshonitic Lamprophyre	Z19019, Yilgarn Block, Western Australia	1	<8	Taylor et al., 1994
Shoshonitic Lamprophyre	Z18470, Yilgarn Block, Western Australia	1	215	Taylor et al., 1994
Shoshonitic Lamprophyre	Z18471, Yilgarn Block, Western Australia	1	164	Taylor et al., 1994
Shoshonitic Lamprophyre	Z27969, Yilgarn Block, Western Australia	1	<8	Taylor et al., 1994
Shoshonitic Lamprophyre	Z40013, Yilgarn Block, Western Australia	1	b.d.	Taylor et al., 1994
Shoshonitic Lamprophyre	Z40014, Yilgarn Block, Western Australia	1	<8	Taylor et al., 1994
Shoshonitic Lamprophyre	Z19027, Yilgarn Block, Western Australia	1	11	Taylor et al., 1994
Shoshonitic Lamprophyre	Z32699, Yilgarn Block, Western Australia	1	<8	Taylor et al., 1994
Shoshonitic Lamprophyre	Z40016, Yilgarn Block, Western Australia	1	<8	Taylor et al., 1994
Shoshonitic Lamprophyre	47119, Yilgarn Block, Western Australia	1	<8	Taylor et al., 1994
Shoshonitic Lamprophyre	47121, Yilgarn Block, Western Australia	1	<8	Taylor et al., 1994
Shoshonitic Lamprophyre	106681, Yilgarn Block, Western Australia	1	<8	Taylor et al., 1994
Shoshonitic Lamprophyre	16932, Yilgarn Block, Western Australia	1	30	Taylor et al., 1994

Rock type	Sample No./Location	n	Au (ng/g)	Author, Year
Shoshonitic Lamprophyre	11707A, Yilgarn Block, Western Australia	1	<8	Taylor et al., 1994
Shoshonitic Lamprophyre	11693, Yilgarn Block, Western Australia	1	<8	Taylor et al., 1994
Shoshonitic Lamprophyre	8019, Yilgarn Block, Western Australia	1	<8	Taylor et al., 1994
Shoshonitic Lamprophyre	8004, Yilgarn Block, Western Australia	1	<8	Taylor et al., 1994
Shoshonitic Lamprophyre	8012, Yilgarn Block, Western Australia	1	<8	Taylor et al., 1994
Shoshonitic Lamprophyre	9730, Yilgarn Block, Western Australia	1	<8	Taylor et al., 1994
Shoshonitic Lamprophyre	9731, Yilgarn Block, Western Australia	1	<8	Taylor et al., 1994
Shoshonitic Lamprophyre	14096, Yilgarn Block, Western Australia	1	<8	Taylor et al., 1994
Shoshonitic Lamprophyre	14616, Yilgarn Block, Western Australia	1	<8	Taylor et al., 1994
Shoshonitic Lamprophyre	15295, Yilgarn Block, Western Australia	1	<8	Taylor et al., 1994
Shoshonitic Lamprophyre	108846, Yilgarn Block, Western Australia	1	135	Taylor et al., 1994
Shoshonitic Lamprophyre	108845, Yilgarn Block, Western Australia	1	<8	Taylor et al., 1994
Shoshonitic Lamprophyre	108834, Yilgarn Block, Western Australia	1	<8	Taylor et al., 1994
Shoshonitic Lamprophyre	108847, Yilgarn Block, Western Australia	1	3390	Taylor et al., 1994
Shoshonitic Lamprophyre	108838, Yilgarn Block, Western Australia	1	<8	Taylor et al., 1994
Mafic				
Gabbro	Lakhpa, Kutch rift basin, India	1	5.2	Crocket, 2008
Gabbro	Ironton, Mo., U.S.A.	1	2.4	Degrazi and Haskin, 1964
Gabbro	MO 120 Ivrea-Verbano complex, Western Alps	1	0.6	Sighinolfi and Gorgoni, 1977
Gabbro	MO 126 Ivrea-Verbano complex, Western Alps	1	<0.6	Sighinolfi and Gorgoni, 1977
Gabbro	MO 125 Ivrea-Verbano complex, Western Alps	1	1.6	Sighinolfi and Gorgoni, 1977
Gabbro	MO 127 Ivrea-Verbano complex, Western Alps	1	2.5	Sighinolfi and Gorgoni, 1977
Gabbro	MO 130 Ivrea-Verbano complex, Western Alps	1	2.0	Sighinolfi and Gorgoni, 1977
Gabbro	66GSC-27 Southern California Batholith	1	0.7	Gottfried et al., 1972
Gabbro	66GSC-10 Southern California Batholith	1	2.7	Gottfried et al., 1972

Rock type	Sample No./Location	n	Au (ng/g)	Author, Year
Hornblende gabbro	SLRM-299 Southern California Batholith	1	11.6	Gottfried et al., 1972
Gabbro-norite	MO 18 Ivrea-Verbano complex, Western Alps	1	1.5	Sighinolfi and Gorgoni, 1977
Gabbro-norite	MO 19 Ivrea-Verbano complex, Western Alps	1	1.4	Sighinolfi and Gorgoni, 1977
Norite	MO 23 Ivrea-Verbano complex, Western Alps	1	10.9	Sighinolfi and Gorgoni, 1977
Norite	MO 60 Ivrea-Verbano complex, Western Alps	1	2.7	Sighinolfi and Gorgoni, 1977
Norite	MO 85 Ivrea-Verbano complex, Western Alps	1	0.6	Sighinolfi and Gorgoni, 1977
Norite	Bushveld complex	1	2.9	Degrazi and Haskin, 1964
Olivine norite	SLRM-354 Southern California Batholith	1	0.8	Gottfried et al., 1972
Norite	SLRM-334 Southern California Batholith	1	1.5	Gottfried et al., 1972
Quartz-Biotite norite	SLRM-230 Southern California Batholith	1	9.3	Gottfried et al., 1972
Garnetiferous norite	MO 99 Ivrea-Verbano complex, Western Alps	1	6.1	Sighinolfi and Gorgoni, 1977
Garnetiferous norite	MO 115 Ivrea-Verbano complex, Western Alps	1	4.0	Sighinolfi and Gorgoni, 1977
Garnetiferous norite	MO 116 Ivrea-Verbano complex, Western Alps	1	3.5	Sighinolfi and Gorgoni, 1977
Diabase	W-1	1	8.4	Vincent and Crocket, 1960
Diabase	W-1	1	4.9	Hamaguchi et al., 1961
Dolerite dyke	Diveghat, Deccan Traps, India	1	5.3	Crocket, 2004
Dolerite dyke	8 Panvel, Deccan Traps, India	1	5.0	Crocket, 2004
Dolerite dyke	9 Panvel, Deccan Traps, India	1	1.9	Crocket, 2004
Dolerite dyke	10 Panvel, Deccan Traps, India	1	6.6	Crocket, 2004
Gabbro	Laget,Bamble, Norway	1	0.28	Alirezaei and Cameron, 2002
Gabbro	Laget,Bamble, Norway	1	0.15	Alirezaei and Cameron, 2002
Gabbro	Laget,Bamble, Norway	1	0.50	Alirezaei and Cameron, 2002
Gabbro	Laget,Bamble, Norway	1	0.29	Alirezaei and Cameron, 2002
Gabbro	Laget,Bamble, Norway	1	0.05	Alirezaei and Cameron, 2002
Gabbro	Laget,Bamble, Norway	1	0.15	Alirezaei and Cameron, 2002

Rock type	Sample No./Location	n	Au (ng/g)	Author, Year
Gabbro	Laget,Bamble, Norway	1	0.47	Alirezaei and Cameron, 2002
Gabbro	Laget,Bamble, Norway	1	0.23	Alirezaei and Cameron, 2002
Gabbro	Laget,Bamble, Norway	1	0.13	Alirezaei and Cameron, 2002
Gabbro	Tromsoy, Bamble Belt, Norway	1	0.26	Alirezaei and Cameron, 2002
Gabbro	Tromsoy, Bamble Belt, Norway	1	0.18	Alirezaei and Cameron, 2002
Gabbro	Tromsoy, Bamble Belt, Norway	1	0.29	Alirezaei and Cameron, 2002
Gabbro	Tromsoy, Bamble Belt, Norway	1	0.24	Alirezaei and Cameron, 2002
Gabbro	Tvedstrand, Bamble Belt, Norway	1	0.42	Alirezaei and Cameron, 2002
Gabbro	Tvedstrand, Bamble Belt, Norway	1	0.39	Alirezaei and Cameron, 2002
Gabbro	Tvedstrand, Bamble Belt, Norway	1	0.69	Alirezaei and Cameron, 2002
Gabbro	Tvedstrand, Bamble Belt, Norway	1	0.70	Alirezaei and Cameron, 2002
Gabbro	Tvedstrand, Bamble Belt, Norway	1	0.75	Alirezaei and Cameron, 2002
Gabbro	Hisoy, Bamble Belt, Norway	1	0.44	Alirezaei and Cameron, 2002
Gabbro	Hisoy, Bamble Belt, Norway	1	0.40	Alirezaei and Cameron, 2002
Gabbro	BNH-45 White Mountain Plutonic Series	1	0.3	Gottfried et al., 1972
Gabbro, Concord quad	69G-14 North Carolina	1	0.7	Gottfried et al., 1972
low-Mg Gabbro	Arendal, Bamble Belt, Norway	1	1.05	Alirezaei and Cameron, 2002
low-Mg Gabbro	Arendal, Bamble Belt, Norway	1	0.94	Alirezaei and Cameron, 2002
low-Mg Gabbro	Arendal, Bamble Belt, Norway	1	1.14	Alirezaei and Cameron, 2002
low-Fe Gabbro	Arendal, Bamble Belt, Norway	1	0.47	Alirezaei and Cameron, 2002
low-Fe Gabbro	Arendal, Bamble Belt, Norway	1	0.42	Alirezaei and Cameron, 2002
low-Fe Gabbro	Arendal, Bamble Belt, Norway	1	0.48	Alirezaei and Cameron, 2002
Syenogabbro	S-1419 Boulder batholith, Montana	1	0.6	Gottfried et al., 1972
Post-Archean mafic intrusives	Central East China	276	1.05	Gao et al., 1998
Cafemic rocks	Southwestern Quebec	Comp*	0.49	Shaw et al., 1976

Rock type	Sample No./Location	n	Au (ng/g)	Author, Year
Cafemic rocks	Baffin Island	Comp*	10.1	Shaw et al., 1976
Cafemic rocks	Northern Quebec-Ungava,Canadian Shield	Comp*	3.72	Shaw et al., 1976
Continental Basalts				
Basalt	1 Ambaghat, Deccan Traps, India	1	7.5	Crocket, 2004
Basalt	2 Ambaghat, Deccan Traps, India	1	5.2	Crocket, 2004
Basalt	3 Ambaghat, Deccan Traps, India	1	2.3	Crocket, 2004
Basalt	4 Ambaghat, Deccan Traps, India	1	1.7	Crocket, 2004
Basalt	5 Ambaghat, Deccan Traps, India	1	2.5	Crocket, 2004
Basalt	Rat., Deccan Traps, India	1	5.5	Crocket, 2004
Basalt	7 Panvel, Deccan Traps, India	1	6.3	Crocket, 2004
Basalt	11 Panvel, Deccan Traps, India	1	2.5	Crocket, 2004
Basalt	12 Bhorghat, Deccan Traps, India	1	0.91	Crocket, 2004
Basalt	13 Bhorghat, Deccan Traps, India	1	2.7	Crocket, 2004
Basalt	15 Koyna, Deccan Traps, India	1	5.4	Crocket, 2004
Basalt	16 Koyna, Deccan Traps, India	1	1.5	Crocket, 2004
Basalt	Diveghat, Deccan Traps, India	1	2.3	Crocket, 2004
Basalt	Sing., Deccan traps, India	1	2.8	Crocket, 2004
Basalt	Lintz, Rhenish, Prussia	1	2.6	Degrazi and Haskin, 1964
Alkali basalt	Keera, Kutch rift basin, India	1	0.56	Crocket, 2008
Deccan tholeiite	Pranpur, Kutch rift basin, India	1	5	Crocket, 2008
Deccan tholeiite	Dhanoi, Kutch rift basin, India	1	3.4	Crocket, 2008
Post-Archean mafic volcanics	Central East China	583	1.01	Gao et al., 1998
Oceanic basalts				
Basalt	T-10i Tahiti	1	0.36	Crocket et al., 1973
Basalt	T-10ii Tahiti	1	0.30	Crocket et al., 1973

Rock type	Sample No./Location	n	Au (ng/g)	Author, Year
Basalt	T-10iii Tahiti	1	0.27	Crocket et al., 1973
Basalt	T-14 Tahiti	1	0.29	Crocket et al., 1973
Basalt	T-15 Tahiti	1	1.10	Crocket et al., 1973
Basalt	T-19a Tahiti	1	0.30	Crocket et al., 1973
Basalt	T-7 Tahiti	1	0.48	Crocket et al., 1973
Basalt	T-8 Tahiti	1	0.46	Crocket et al., 1973
Basalt	T-17 Tahiti	1	2.4	Crocket et al., 1973
Basalt	T-19b Tahiti	1	0.93	Crocket et al., 1973
Basalt	T-21a Tahiti	1	0.67	Crocket et al., 1973
Basalt	T-21b Tahiti	1	0.48	Crocket et al., 1973
Basalt	Mid-Atlantic Ridge, GE-159	1	10.6	Degrazi and Haskin, 1964
Basalt	Mid-Atlantic Ridge, GE-160	1	6.3	Degrazi and Haskin, 1964
Basalt	Mid-Atlantic Ridge, GE-260	1	14	Degrazi and Haskin, 1964
Olivine Basalt	Jefferson Co., Colorado, U.S.A.	1	4	Degrazi and Haskin, 1964
Tertiary olivine basalt	Morvern, Scotland	1	2.2	Vincent and Crocket, 1960
Tertiary tholeiitic basalt	N. Ireland	1	2	Vincent and Crocket, 1960
Tholeiitic olivine basalt	Mauna Loa, Hawaii	1	2.6	Vincent and Crocket, 1960
Intermediate				
Post-Archean Diorite	Central East China	243	0.47	Gao et al., 1998
Diorite	CPR-117 Idaho Batholith	1	0.5	Gottfried et al., 1972
Diorite	CPR-118 Idaho Batholith	1	2.6	Gottfried et al., 1972
Quartz diorite	L54-900 Idaho Batholith	1	0.2	Gottfried et al., 1972
Quartz diorite	L54-900A Idaho Batholith	1	1.5	Gottfried et al., 1972
Quartz diorite	47L81 Idaho Batholith	1	2.5	Gottfried et al., 1972
Quartz diorite	47L227 Idaho Batholith	1	6.0	Gottfried et al., 1972
Quartz diorite, Mount Princeton	7395 Rocky Mountains, Colo.	1	0.5	Gottfried et al., 1972

Rock type	Sample No./Location	n	Au (ng/g)	Author, Year
Pyroxene quartz diorite	CL-1 Sierra Nevada, Calif.	1	1.4	Gottfried et al., 1972
Quartz diorite, Bodega Head	Dr-510 Coast Range, Calif.	1	0.5	Gottfried et al., 1972
Monzodiorite	BNH-43 White Mountain Plutonic Series	1	0.3	Gottfried et al., 1972
Green Valley Tonalite	SLR-213 Southern California Batholith	1	10.7	Gottfried et al., 1972
Green Valley Tonalite	SLR-685 Southern California Batholith	1	1.1	Gottfried et al., 1972
Green Valley Tonalite	SLR-582 Southern California Batholith	1	11.3	Gottfried et al., 1972
Lakeview Mountain Tonalite	60-2 Southern California Batholith	1	2.5	Gottfried et al., 1972
Bonsall Tonalite	60-1 Southern California Batholith	1	1.7	Gottfried et al., 1972
Bonsall Tonalite	El 38-28 Southern California Batholith	1	0.8	Gottfried et al., 1972
Tonalite	Ra-3 Southern California Batholith	1	3.7	Gottfried et al., 1972
Tonalite (sphene-rich)	66GSC-20 Southern California Batholith	1	0.5	Gottfried et al., 1972
Tonalite (sphene-rich)	66GSC-18 Southern California Batholith	1	0.8	Gottfried et al., 1972
Archean TTG	Central East China	502	1.05	Gao et al., 1998
Post-Archean TTG	Central East China	596	0.51	Gao et al., 1998
Syenodioritic rocks	Southwestern Quebec	Comp*	0.45	Shaw et al., 1976
Syenodioritic rocks	Northern Quebec-Ungava,Canadian Shield	Comp*	2.42	Shaw et al., 1976
Felsic				
Granodiorite	El 88-126 Southern California Batholith	1	1.2	Gottfried et al., 1972
Woodson Mountain Granodiorite	64GSC-2 Southern California Batholith	1	0.6	Gottfried et al., 1972
Woodson Mountain Granodiorite	64GSC-4 Southern California Batholith	1	0.5	Gottfried et al., 1972
Woodson Mountain Granodiorite (aplite)	64GSC-3 Southern California Batholith	1	0.3	Gottfried et al., 1972
Woodson Mountain Granodiorite	S-11 Southern California Batholith	1	0.5	Gottfried et al., 1972
Woodson Mountain Granodiorite	S-13 Southern California Batholith	1	0.3	Gottfried et al., 1972
Woodson Mountain Granodiorite	S-14 Southern California Batholith	1	0.3	Gottfried et al., 1972
Woodson Mountain Granodiorite	S-12 Southern California Batholith	1	0.4	Gottfried et al., 1972

Rock type	Sample No./Location	n	Au (ng/g)	Author, Year
Woodson Mountain Granodiorite	S-9 Southern California Batholith	1	0.3	Gottfried et al., 1972
Woodson Mountain Granodiorite	S-10 Southern California Batholith	1	0.3	Gottfried et al., 1972
Woodson Mountain Granodiorite	S-15 Southern California Batholith	1	0.2	Gottfried et al., 1972
Woodson Mountain Granodiorite	S-6 Southern California Batholith	1	0.3	Gottfried et al., 1972
Woodson Mountain Granodiorite	Cor-1 Southern California Batholith	1	0.5	Gottfried et al., 1972
Mount Givens Granodiorite	BCc-12 Sierra Nevada, Calif.	1	0.4	Gottfried et al., 1972
Mount Givens Granodiorite	BCa-20 Sierra Nevada, Calif.	1	1.9	Gottfried et al., 1972
Granodiorite of Dinkey Creek type	BCc-13 Sierra Nevada, Calif.	1	1.8	Gottfried et al., 1972
Granodiorite of Dinkey Creek type	SL-18 Sierra Nevada, Calif.	1	0.9	Gottfried et al., 1972
Tinemaha Granodiorite	BP-8 Sierra Nevada, Calif.	1	0.5	Gottfried et al., 1972
Tinemaha Granodiorite	BP-1 Sierra Nevada, Calif.	1	5.2	Gottfried et al., 1972
Granodiorite of the Raymond quarries	FD-4 Sierra Nevada, Calif.	1	1.0	Gottfried et al., 1972
Granodiorite of the Raymond quarries	FD-20 Sierra Nevada, Calif.	1	3.0	Gottfried et al., 1972
Granodiorite of the Goddard pendant	KR Sierra Nevada, Calif.	1	0.8	Gottfried et al., 1972
Granodiorite of the McMurray Meadows	BP-2 Sierra Nevada, Calif.	1	0.8	Gottfried et al., 1972
Lamarck Granodiorite	MG-1 Southern California Batholith	1	0.5	Gottfried et al., 1972
Granodiorite, Red Hills	Dr-100 Coast Range, Calif.	1	0.7	Gottfried et al., 1972
Granodiorite, Long Buttes	Dr-321 Transverse Ranges, Calif.	1	0.7	Gottfried et al., 1972
Granodiorite, Holcomb Ridge	V-4 Transverse Ranges, Calif.	1	0.2	Gottfried et al., 1972
Granodiorite	47L288 Idaho Batholith	1	3.1	Gottfried et al., 1972
Granodiorite	47L70 Idaho Batholith	1	3.2	Gottfried et al., 1972
Granodiorite	L253 Idaho Batholith	1	1.9	Gottfried et al., 1972
Granodiorite	L112 Idaho Batholith	1	2.8	Gottfried et al., 1972
Granodiorite	L255 Idaho Batholith	1	0.8	Gottfried et al., 1972
Granodiorite	L304 Idaho Batholith	1	1.3	Gottfried et al., 1972

Rock type	Sample No./Location	n	Au (ng/g)	Author, Year
Granodiorite	L301 Idaho Batholith	1	5.2	Gottfried et al., 1972
Granodiorite	L295 Idaho Batholith	1	1.4	Gottfried et al., 1972
Granodiorite	L288 Idaho Batholith	1	3.0	Gottfried et al., 1972
Granodiorite	L58-88 Idaho Batholith	1	0.6	Gottfried et al., 1972
Granodiorite	L53-537A Idaho Batholith	1	0.6	Gottfried et al., 1972
Granodiorite	L59-1765 Idaho Batholith	1	0.3	Gottfried et al., 1972
Granodiorite	L61-1182 Idaho Batholith	1	0.2	Gottfried et al., 1972
Granodiorite	L62-1784B Idaho Batholith	1	0.1	Gottfried et al., 1972
Granodiorite	L64-2559 Idaho Batholith	1	2.0	Gottfried et al., 1972
Granodiorite	CPR-123 Idaho Batholith	1	0.9	Gottfried et al., 1972
Unionville Granodiorite	4T-349 Boulder batholith, Montana	1	3.4	Gottfried et al., 1972
Granodiorite of Radar Creek pluton	2T-1065 Boulder batholith, Montana	1	1.0	Gottfried et al., 1972
Clancy Granodiorite	3T-273 Boulder batholith, Montana	1	2.0	Gottfried et al., 1972
Granodiorite	TP-5 Tatoosh pluton, Mount Rainer	1	0.3	Gottfried et al., 1972
Granodiorite	TP-9 Tatoosh pluton, Mount Rainer	1	2.8	Gottfried et al., 1972
Granodiorite	TP-25 Tatoosh pluton, Mount Rainer	1	0.4	Gottfried et al., 1972
Granodiorite	TP-32 Tatoosh pluton, Mount Rainer	1	3.8	Gottfried et al., 1972
Granodiorite	TP-66 Tatoosh pluton, Mount Rainer	1	0.8	Gottfried et al., 1972
Granodiorite	TP-72 Tatoosh pluton, Mount Rainer	1	0.6	Gottfried et al., 1972
Granodiorite	TP-74 Tatoosh pluton, Mount Rainer	1	4.2	Gottfried et al., 1972
Granodiorite	TP-76 Tatoosh pluton, Mount Rainer	1	1.4	Gottfried et al., 1972
Granodiorite	TP-81 Tatoosh pluton, Mount Rainer	1	0.5	Gottfried et al., 1972
Granodiorite	TP-112Tatoosh pluton, Mount Rainer	1	0.7	Gottfried et al., 1972
Granodiorite	TP-152Tatoosh pluton, Mount Rainer	1	0.5	Gottfried et al., 1972
Granodiorite	TP-171Tatoosh pluton, Mount Rainer	1	0.9	Gottfried et al., 1972
Granodiorite	TP-201Tatoosh pluton, Mount Rainer	1	0.9	Gottfried et al., 1972

Rock type	Sample No./Location	n	Au (ng/g)	Author, Year
Granodiorite	TP-211Tatoosh pluton, Mount Rainer	1	0.6	Gottfried et al., 1972
Alaskite of Evolution basin	R-99 Sierra Nevada, Calif.	1	1.3	Gottfried et al., 1972
Alaskite	L62-1784A Idaho Batholith	1	0.3	Gottfried et al., 1972
Alaskite	L58-130 Idaho Batholith	1	0.6	Gottfried et al., 1972
Alaskite	L53-554 Idaho Batholith	1	0.2	Gottfried et al., 1972
Alaskite	L58-1281 Idaho Batholith	1	0.4	Gottfried et al., 1972
Alaskite near Butte Quartz Mozonite	63K-00 Boulder batholith, Montana	1	0.7	Gottfried et al., 1972
Biotite granite of Dinkey Lakes	HL-29 Sierra Nevada, Calif.	1	0.9	Gottfried et al., 1972
Archean granite	Central East China	369	0.41	Gao et al., 1998
Post-Archean granite	Central East China	1140	2.21	Gao et al., 1998
Biotite granite	Stone Mt., GA, U.S.A.	1	1.9	Degrazi and Haskin, 1964
Granite	Bridgelans Still	1	4.7	Degrazi and Haskin, 1964
Aplite	Boulder, Colorado, U.S.A.	1	3.3	Degrazi and Haskin, 1964
Aplite	L64-2609 Idaho Batholith	1	0.8	Gottfried et al., 1972
Red granite	Wausau, Wisconsin, U.S.A.	1	3.3	Degrazi and Haskin, 1964
Standard Granite	G-1	1	4.5	Vincent and Crocket, 1960
Granite (altered)	Cor-3 Southern California Batholith	1	5.6	Gottfried et al., 1972
Granite (fine grained)	L-201 Idaho Batholith	1	0.5	Gottfried et al., 1972
Granite, Mount Antero	7741 Rocky Mountains, Colo.	1	0.4	Gottfried et al., 1972
Granite, Silver Plume quarry	G-78 Rocky Mountains, Colo.	1	0.6	Gottfried et al., 1972
Granite, Pageland S.C.	69G-8 South Carolina	1	0.2	Gottfried et al., 1972
Biotite granite	BNH-5 White Mountain Plutonic Series	1	0.5	Gottfried et al., 1972
Biotite granite	BNH-13 White Mountain Plutonic Series	1	0.9	Gottfried et al., 1972
Biotite granite	BNH-56 White Mountain Plutonic Series	1	0.4	Gottfried et al., 1972
Biotite granite	BNH-68 White Mountain Plutonic Series	1	0.3	Gottfried et al., 1972

Rock type	Sample No./Location	n	Au (ng/g)	Author, Year
Biotite granite	BNH-49 White Mountain Plutonic Series	1	0.5	Gottfried et al., 1972
Biotite granite	BNH-52 White Mountain Plutonic Series	1	0.5	Gottfried et al., 1972
Biotite granite	BNH-36 White Mountain Plutonic Series	1	0.4	Gottfried et al., 1972
Biotite granite	BNH-39 White Mountain Plutonic Series	1	0.8	Gottfried et al., 1972
Biotite granite	BNH-40 White Mountain Plutonic Series	1	0.3	Gottfried et al., 1972
Biotite granite	BNH-57 White Mountain Plutonic Series	1	0.3	Gottfried et al., 1972
Biotite granite	BNH-38 White Mountain Plutonic Series	1	0.2	Gottfried et al., 1972
Biotite granite	55-S-324 White Mountain Plutonic Series	1	0.8	Gottfried et al., 1972
Biotite granite	55-S-307 White Mountain Plutonic Series	1	0.5	Gottfried et al., 1972
Biotite granite	55-S-332 White Mountain Plutonic Series	1	1.6	Gottfried et al., 1972
Biotite granite	55-S-321 White Mountain Plutonic Series	1	1.2	Gottfried et al., 1972
Biotite-amphibole granite	BNH-67 White Mountain Plutonic Series	1	0.3	Gottfried et al., 1972
Biotite-amphibole granite	BNH-64 White Mountain Plutonic Series	1	0.5	Gottfried et al., 1972
Amphibole granite	BNH-60 White Mountain Plutonic Series	1	0.4	Gottfried et al., 1972
Amphibole granite	BNH-25 White Mountain Plutonic Series	1	0.2	Gottfried et al., 1972
Amphibole granite	BNH-28 White Mountain Plutonic Series	1	0.8	Gottfried et al., 1972
Reibeckite granite	BNH-3 White Mountain Plutonic Series	1	0.4	Gottfried et al., 1972
Quartz monzonite (fine phase)	El 38-265 Southern California Batholith	1	0.5	Gottfried et al., 1972
Quartz monzonite (coarse phase)	El 38-167 Southern California Batholith	1	1.9	Gottfried et al., 1972
Hunter Mountain Quartz Monzonite	FD-2 Sierra Nevada, Calif.	1	0.6	Gottfried et al., 1972
Paiute Monument Quartz Monzonite	FD-3 Sierra Nevada, Calif.	1	0.9	Gottfried et al., 1972
Quartz monzonite of Mount Alice mass	BP-3 Sierra Nevada, Calif.	1	0.3	Gottfried et al., 1972
Quartz monzonite, Monterey	Mo-1 Coast Range, Calif.	1	2.1	Gottfried et al., 1972
Quartz monzonite	47L219 Idaho Batholith	1	2.7	Gottfried et al., 1972
Quartz monzonite	L-169 Idaho Batholith	1	1.1	Gottfried et al., 1972

Rock type	Sample No./Location	n	Au (ng/g)	Author, Year
Quartz monzonite	L-84 Idaho Batholith	1	1.1	Gottfried et al., 1972
Quartz monzonite, Mount Princeton	7179 Rocky Mountains, Colo.	1	0.4	Gottfried et al., 1972
Quartz monzonite, Salisbury pluton	A-3 North Carolina	1	0.7	Gottfried et al., 1972
Quartz monzonite, Salisbury pluton	63G-9a North Carolina	1	0.2	Gottfried et al., 1972
Quartz monzonite, Salisbury pluton	69G-9b North Carolina	1	0.5	Gottfried et al., 1972
Quartz monzonite, Salisbury pluton	A-2 North Carolina	1	1.4	Gottfried et al., 1972
Quartz monzonite, Salisbury pluton	E-1 North Carolina	1	1.4	Gottfried et al., 1972
Quartz monzonite, Salisbury pluton	I-1 North Carolina	1	1.8	Gottfried et al., 1972
Quartz monzonite, Salisbury pluton	I-2 North Carolina	1	1.2	Gottfried et al., 1972
Quartz monzonite, Salisbury pluton	69G-11a North Carolina	1	0.2	Gottfried et al., 1972
Quartz monzonite, Salisbury pluton	G-4 North Carolina	1	2.3	Gottfried et al., 1972
Quartz monzonite, Salisbury pluton	69G-11b North Carolina	1	0.2	Gottfried et al., 1972
Quartz monzonite, Salisbury pluton	69G-3 North Carolina	1	0.3	Gottfried et al., 1972
Muscovite quartz monzonite	47-L-272 Idaho Batholith	1	0.6	Gottfried et al., 1972
Muscovite quartz monzonite	L-263 Idaho Batholith	1	0.9	Gottfried et al., 1972
Muscovite quartz monzonite	L-209 Idaho Batholith	1	0.4	Gottfried et al., 1972
Quartz mozonite of Donald pluton	7W-21 Boulder batholith, Montana	1	0.5	Gottfried et al., 1972
Quartz mozonite of Homestake pluton	1K-241 Boulder batholith, Montana	1	0.5	Gottfried et al., 1972
Butte Quartz Mozonite	6K-306 Boulder batholith, Montana	1	0.8	Gottfried et al., 1972
Butte Quartz Mozonite	DDH-B-3 Boulder batholith, Montana	1	0.6	Gottfried et al., 1972
Syenite Concord quadrangle	69G-13 North Carolina	1	0.2	Gottfried et al., 1972
Syenite	BNH-44 White Mountain Plutonic Series	1	0.3	Gottfried et al., 1972
Syenite dyke	BNH-7 White Mountain Plutonic Series	1	0.4	Gottfried et al., 1972
Quartz syenite	BNH-20 White Mountain Plutonic Series	1	0.3	Gottfried et al., 1972
Nepheline syenite	BNH-42 White Mountain Plutonic Series	1	0.3	Gottfried et al., 1972

Rock type	Sample No./Location	n	Au (ng/g)	Author, Year
Nepheline syenite	Bancroft, Ontario, Canada	1	2.6	Degrazi and Haskin, 1964
Nepheline syenite	Wausau, Wisconsin, U.S.A.	1	0.64	Degrazi and Haskin, 1964
Nepheline sodalite syenite	Red Hill, N.H., U.S.A.	1	0.98	Degrazi and Haskin, 1964
Post-Archean felsic volcanics	Central East China	895	0.67	Gao et al., 1998
Carbonatite				
Carbonatite	Panda Hill, Tanganyika	1	1.6	Degrazi and Haskin, 1964
Volcanic glasses and volcaniclastics				
Obsidian	Rotorua, New Zealand	1	21	Degrazi and Haskin, 1964
Perlite	Queensland, Australia	1	1.5	Degrazi and Haskin, 1964
Impact glasses				
Bediasite		1	3	Degrazi and Haskin, 1964
Philippinite	Phillippenes	1	6.7	Degrazi and Haskin, 1964
Sedimentary				
Archean arenaceous rocks	Central East China	110	1.36	Gao et al., 1998
Post-Archean arenaceous rocks	Central East China	2628	2.12	Gao et al., 1998
Archean pelitic rocks	Central East China	60	1.76	Gao et al., 1998
Post-Archean pelitic rocks	Central East China	1238	1.8	Gao et al., 1998
Greywacke	Gowganda Form., Ontario, Canada	1	2.3	Degrazi and Haskin, 1964
Sandstone	Keweenawan, Wisconsin, U.S.A.	1	11.6	Degrazi and Haskin, 1964
Sandstone	Berea Form., Ky. U.S.A.	1	2.6	Degrazi and Haskin, 1964
Tertiary sandstone	1 Kettleman Hills, California, U.S.A.	1	35	Degrazi and Haskin, 1964
Tertiary sandstone	2 Kettleman Hills, California, U.S.A.	1	49	Degrazi and Haskin, 1964
Tertiary sandstone	3 Kettleman Hills, California, U.S.A.	1	44	Degrazi and Haskin, 1964
Tertiary sandstone	4 Kettleman Hills, California, U.S.A.	1	55	Degrazi and Haskin, 1964
Tertiary sandstone	5 Kettleman Hills, California, U.S.A.	1	40	Degrazi and Haskin, 1964
Tertiary sandstone	6 Kettleman Hills, California, U.S.A.	1	57	Degrazi and Haskin, 1964

Rock type	Sample No./Location	n	Au (ng/g)	Author, Year
Tertiary sandstone	7 Kettleman Hills, California, U.S.A.	1	26	Degrazi and Haskin, 1964
Tertiary sandstone	8 Kettleman Hills, California, U.S.A.	1	25	Degrazi and Haskin, 1964
Breccia	TP Tatoosh pluton, Mount Rainer	1	0.6	Gottfried et al., 1972
Quartz-rich sediments	Southwestern Quebec	Comp*	1.37	Shaw et al., 1976
Quartz-rich sediments	Northern Quebec-Ungava,Canadian Shield	Comp*	2.80	Shaw et al., 1976
Quartzofeldspathic	Southwestern Quebec	Comp*	0.41	Shaw et al., 1976
Quartzofeldspathic	Northern Saskatchewan	Comp*	0.3	Shaw et al., 1976
Quartzofeldspathic	Baffin Island	Comp*	2.7	Shaw et al., 1976
Quartzofeldspathic	Northern Quebec-Ungava,Canadian Shield	Comp*	3.97	Shaw et al., 1976
Red clay	Brazil Basin, 343cm core depth	1	31	Degrazi and Haskin, 1964
Red clay	Brazil Basin, 664cm core depth	1	11.6	Degrazi and Haskin, 1964
Red clay	Brazil Basin, 887cm core depth	1	4.2	Degrazi and Haskin, 1964
Lutite	Argentine Basin 100cm core depth	1	10.6	Degrazi and Haskin, 1964
Lutite	Argentine Basin 355cm core depth	1	3.1	Degrazi and Haskin, 1964
Lutite	Argentine Basin 675cm core depth	1	5.2	Degrazi and Haskin, 1964
Lutite	Argentine Basin 1045cm core depth	1	17.3	Degrazi and Haskin, 1964
Limestone	Paola Form., Kans., U.S.A.	1	4.8	Degrazi and Haskin, 1964
Archean carbonate rocks	Central East China	45	0.41	Gao et al., 1998
Post-Archean carbonate rocks	Central East China	1922	1.31	Gao et al., 1998
Carbonates	Southwestern Quebec	Comp*	1.48	Shaw et al., 1976
Carbonates	Northern Quebec-Ungava,Canadian Shield	Comp*	8.75	Shaw et al., 1976
Recent Carbonate	Florida Coast, U.S.A.	1	3.9	Degrazi and Haskin, 1964
Oolite	Cleeve Hill, Cheltenham, England	1	2.3	Degrazi and Haskin, 1964
Recent coral	Florida Keys, U.S.A.	1	0.8	Degrazi and Haskin, 1964
Metaliferous Black slates	Dukpyungri-B, Okcheon belt, Korea	1	71	Jeong, 2006

Rock type	Sample No./Location	n	Au (ng/g)	Author, Year
Metamorphic				
Low Grade				
Intermediate Grade				
Mafic				
Archean amphibolites	Central East China	165	8.21	Gao et al., 1998
Amphibolite	Laget, Bamble Belt, Norway	1	1.25	Alirezaei and Cameron, 2002
Amphibolite	Laget, Bamble Belt, Norway	1	0.20	Alirezaei and Cameron, 2002
Amphibolite	Laget, Bamble Belt, Norway	1	0.32	Alirezaei and Cameron, 2002
Amphibolite	Laget, Bamble Belt, Norway	1	0.78	Alirezaei and Cameron, 2002
Amphibolite	Laget, Bamble Belt, Norway	1	0.75	Alirezaei and Cameron, 2002
Amphibolite	Laget, Bamble Belt, Norway	1	0.42	Alirezaei and Cameron, 2002
Amphibolite	Laget, Bamble Belt, Norway	1	0.20	Alirezaei and Cameron, 2002
Amphibolite	Laget, Bamble Belt, Norway	1	0.13	Alirezaei and Cameron, 2002
Amphibolite	Laget, Bamble Belt, Norway	1	0.27	Alirezaei and Cameron, 2002
Amphibolite	Laget, Bamble Belt, Norway	1	0.18	Alirezaei and Cameron, 2002
Amphibolite	Laget, Bamble Belt, Norway	1	0.07	Alirezaei and Cameron, 2002
Amphibolite	Tvedstrand, Bamble Belt, Norway	1	0.45	Alirezaei and Cameron, 2002
Amphibolite	Tvedstrand, Bamble Belt, Norway	1	0.43	Alirezaei and Cameron, 2002
Amphibolite	Tvedstrand, Bamble Belt, Norway	1	0.32	Alirezaei and Cameron, 2002
Amphibolite	Tvedstrand, Bamble Belt, Norway	1	0.50	Alirezaei and Cameron, 2002
Amphibolite	Hisoy, Bamble Belt, Norway	1	0.42	Alirezaei and Cameron, 2002
Amphibolite	Hisoy, Bamble Belt, Norway	1	0.45	Alirezaei and Cameron, 2002
Amphibolite	Hisoy, Bamble Belt, Norway	1	0.28	Alirezaei and Cameron, 2002
High-Mg Amphibolite	Arendal, Bamble Belt, Norway	1	0.21	Alirezaei and Cameron, 2002
High-Mg Amphibolite	Arendal, Bamble Belt, Norway	1	0.22	Alirezaei and Cameron, 2002
High-Mg Amphibolite	Arendal, Bamble Belt, Norway	1	0.14	Alirezaei and Cameron, 2002

Rock type	Sample No./Location	n	Au (ng/g)	Author, Year
High Grade				
Mafic				
Archean mafic granulites	Central East China	93	0.99	Gao et al., 1998
Mafic granulites	UB 8 Salvador, Bahia State, Brazil	1	<0.4	Sighinolfi and Santos, 1976
Mafic granulites	38 Ilheus, Bahia State, Brazil	1	<0.4	Sighinolfi and Santos, 1976
Mafic granulites	79 Ilheus, Bahia State, Brazil	1	<0.4	Sighinolfi and Santos, 1976
Mafic granulites	NS 5 Rio Salgado, Bahia State, Brazil	1	<0.4	Sighinolfi and Santos, 1976
Intermediate				
Archean intermediate granulites	Central East China	115	1.35	Gao et al., 1998
Acid-intermediate granulites	1 Ilheus, Bahia State, Brazil	1	<0.4	Sighinolfi and Santos, 1976
Acid-intermediate granulites	6 Ilheus, Bahia State, Brazil	1	<0.4	Sighinolfi and Santos, 1976
Acid-intermediate granulites	7 Ilheus, Bahia State, Brazil	1	0.8	Sighinolfi and Santos, 1976
Acid-intermediate granulites	8 Ilheus, Bahia State, Brazil	1	2	Sighinolfi and Santos, 1976
Acid-intermediate granulites	9 Ilheus, Bahia State, Brazil	1	0.9	Sighinolfi and Santos, 1976
Acid-intermediate granulites	10 Ilheus, Bahia State, Brazil	1	2.8	Sighinolfi and Santos, 1976
Acid-intermediate granulites	12 Ilheus, Bahia State, Brazil	1	1.2	Sighinolfi and Santos, 1976
Acid-intermediate granulites	14 Ilheus, Bahia State, Brazil	1	0.7	Sighinolfi and Santos, 1976
Acid-intermediate granulites	17 Ilheus, Bahia State, Brazil	1	<0.4	Sighinolfi and Santos, 1976
Acid-intermediate granulites	18 Ilheus, Bahia State, Brazil	1	<0.4	Sighinolfi and Santos, 1976
Acid-intermediate granulites	19 Ilheus, Bahia State, Brazil	1	<0.4	Sighinolfi and Santos, 1976
Acid-intermediate granulites	24 Ilheus, Bahia State, Brazil	1	<0.4	Sighinolfi and Santos, 1976
Acid-intermediate granulites	25 Ilheus, Bahia State, Brazil	1	3.1	Sighinolfi and Santos, 1976
Acid-intermediate granulites	26 Ilheus, Bahia State, Brazil	1	0.8	Sighinolfi and Santos, 1976
Acid-intermediate granulites	27 Ilheus, Bahia State, Brazil	1	<0.4	Sighinolfi and Santos, 1976
Acid-intermediate granulites	28 Ilheus, Bahia State, Brazil	1	1.6	Sighinolfi and Santos, 1976
Acid-intermediate granulites	29 Ilheus, Bahia State, Brazil	1	1.3	Sighinolfi and Santos, 1976

Rock type	Sample No./Location	n	Au (ng/g)	Author, Year
Acid-intermediate granulites	30 Ilheus, Bahia State, Brazil	1	0.9	Sighinolfi and Santos, 1976
Acid-intermediate granulites	31 Ilheus, Bahia State, Brazil	1	1.3	Sighinolfi and Santos, 1976
Acid-intermediate granulites	32 Ilheus, Bahia State, Brazil	1	4.2	Sighinolfi and Santos, 1976
Acid-intermediate granulites	33 Ilheus, Bahia State, Brazil	1	1.6	Sighinolfi and Santos, 1976
Acid-intermediate granulites	34 Ilheus, Bahia State, Brazil	1	0.7	Sighinolfi and Santos, 1976
Acid-intermediate granulites	36 Ilheus, Bahia State, Brazil	1	0.5	Sighinolfi and Santos, 1976
Acid-intermediate granulites	39 Ilheus, Bahia State, Brazil	1	1.8	Sighinolfi and Santos, 1976
Acid-intermediate granulites	40 Ilheus, Bahia State, Brazil	1	2.0	Sighinolfi and Santos, 1976
Acid-intermediate granulites	41 Ilheus, Bahia State, Brazil	1	2.0	Sighinolfi and Santos, 1976
Acid-intermediate granulites	42 Ilheus, Bahia State, Brazil	1	<0.4	Sighinolfi and Santos, 1976
Acid-intermediate granulites	43 Ilheus, Bahia State, Brazil	1	1.9	Sighinolfi and Santos, 1976
Acid-intermediate granulites	44 Ilheus, Bahia State, Brazil	1	0.6	Sighinolfi and Santos, 1976
Acid-intermediate granulites	45 Ilheus, Bahia State, Brazil	1	0.8	Sighinolfi and Santos, 1976
Acid-intermediate granulites	46 Ilheus, Bahia State, Brazil	1	2.2	Sighinolfi and Santos, 1976
Acid-intermediate granulites	47 Ilheus, Bahia State, Brazil	1	2.0	Sighinolfi and Santos, 1976
Acid-intermediate granulites	50 Ilheus, Bahia State, Brazil	1	0.4	Sighinolfi and Santos, 1976
Acid-intermediate granulites	52 Ilheus, Bahia State, Brazil	1	<0.4	Sighinolfi and Santos, 1976
Acid-intermediate granulites	53 Ilheus, Bahia State, Brazil	1	<0.4	Sighinolfi and Santos, 1976
Acid-intermediate granulites	54 Ilheus, Bahia State, Brazil	1	0.5	Sighinolfi and Santos, 1976
Acid-intermediate granulites	55 Ilheus, Bahia State, Brazil	1	0.5	Sighinolfi and Santos, 1976
Acid-intermediate granulites	56 Ilheus, Bahia State, Brazil	1	2.9	Sighinolfi and Santos, 1976
Acid-intermediate granulites	57 Ilheus, Bahia State, Brazil	1	0.5	Sighinolfi and Santos, 1976
Acid-intermediate granulites	58 Ilheus, Bahia State, Brazil	1	0.6	Sighinolfi and Santos, 1976
Acid-intermediate granulites	59 Ilheus, Bahia State, Brazil	1	1.0	Sighinolfi and Santos, 1976
Acid-intermediate granulites	60 Ilheus, Bahia State, Brazil	1	1.5	Sighinolfi and Santos, 1976
Acid-intermediate granulites	61 Ilheus, Bahia State, Brazil	1	1.4	Sighinolfi and Santos, 1976

Rock type	Sample No./Location	n	Au (ng/g)	Author, Year
Acid-intermediate granulites	62 Ilheus, Bahia State, Brazil	1	<0.4	Sighinolfi and Santos, 1976
Acid-intermediate granulites	63 Ilheus, Bahia State, Brazil	1	8.1	Sighinolfi and Santos, 1976
Acid-intermediate granulites	64 Ilheus, Bahia State, Brazil	1	0.8	Sighinolfi and Santos, 1976
Acid-intermediate granulites	66 Ilheus, Bahia State, Brazil	1	2.3	Sighinolfi and Santos, 1976
Acid-intermediate granulites	67 Ilheus, Bahia State, Brazil	1	1.4	Sighinolfi and Santos, 1976
Acid-intermediate granulites	68 Ilheus, Bahia State, Brazil	1	1.4	Sighinolfi and Santos, 1976
Acid-intermediate granulites	70 Ilheus, Bahia State, Brazil	1	<0.4	Sighinolfi and Santos, 1976
Acid-intermediate granulites	71 Ilheus, Bahia State, Brazil	1	16.0	Sighinolfi and Santos, 1976
Acid-intermediate granulites	72 Ilheus, Bahia State, Brazil	1	0.5	Sighinolfi and Santos, 1976
Acid-intermediate granulites	73 Ilheus, Bahia State, Brazil	1	0.5	Sighinolfi and Santos, 1976
Acid-intermediate granulites	76 Ilheus, Bahia State, Brazil	1	<0.4	Sighinolfi and Santos, 1976
Acid-intermediate granulites	77 Ilheus, Bahia State, Brazil	1	2.8	Sighinolfi and Santos, 1976
Acid-intermediate granulites	78 Ilheus, Bahia State, Brazil	1	16.2	Sighinolfi and Santos, 1976
Acid-intermediate granulites	82 Ilheus, Bahia State, Brazil	1	1.4	Sighinolfi and Santos, 1976
Acid-intermediate granulites	83 Ilheus, Bahia State, Brazil	1	0.8	Sighinolfi and Santos, 1976
Acid-intermediate granulites	1 Itabuna, Bahia State, Brazil	1	18.4	Sighinolfi and Santos, 1976
Acid-intermediate granulites	UB 2 Salvador, Bahia State, Brazil	1	<0.4	Sighinolfi and Santos, 1976
Acid-intermediate granulites	UB 10 Salvador, Bahia State, Brazil	1	<0.4	Sighinolfi and Santos, 1976
Acid-intermediate granulites	UB 16 Salvador, Bahia State, Brazil	1	0.6	Sighinolfi and Santos, 1976
Acid-intermediate granulites	P 136 Salvador, Bahia State, Brazil	1	2.3	Sighinolfi and Santos, 1976
Acid-intermediate granulites	RP 1 Itaberaba-Seabra, Bahia State, Brazil	1	1.0	Sighinolfi and Santos, 1976
Acid-intermediate granulites	RP 1A Itaberaba-Seabra, Bahia State, Brazil	1	1.0	Sighinolfi and Santos, 1976
Acid-intermediate granulites	RP 2 Itaberaba-Seabra, Bahia State, Brazil	1	<0.4	Sighinolfi and Santos, 1976
Acid-intermediate granulites	RP 3 Itaberaba-Seabra, Bahia State, Brazil	1	0.5	Sighinolfi and Santos, 1976
Acid-intermediate granulites	RP 3A Itaberaba-Seabra, Bahia State, Brazil	1	1.0	Sighinolfi and Santos, 1976
Acid-intermediate granulites	RP 3B Itaberaba-Seabra, Bahia State, Brazil	1	0.5	Sighinolfi and Santos, 1976

Rock type	Sample No./Location	n	Au (ng/g)	Author, Year
Acid-intermediate granulites	RP 4 Itaberaba-Seabra, Bahia State, Brazil	1	0.6	Sighinolfi and Santos, 1976
Acid-intermediate granulites	RP 5 Itaberaba-Seabra, Bahia State, Brazil	1	0.9	Sighinolfi and Santos, 1976
Acid-intermediate granulites	RP 6 Itaberaba-Seabra, Bahia State, Brazil	1	2.3	Sighinolfi and Santos, 1976
Acid-intermediate granulites	RP 7 Itaberaba-Seabra, Bahia State, Brazil	1	<0.4	Sighinolfi and Santos, 1976
Acid-intermediate granulites	RB 5 Itaberaba-Iacu, Bahia State, Brazil	1	0.5	Sighinolfi and Santos, 1976
Acid-intermediate granulites	RB 5B Itaberaba-Iacu, Bahia State, Brazil	1	0.5	Sighinolfi and Santos, 1976
Acid-intermediate granulites	RB 53 Itaberaba-Iacu, Bahia State, Brazil	1	<0.4	Sighinolfi and Santos, 1976
Acid-intermediate granulites	RB 78 Itaberaba-Iacu, Bahia State, Brazil	1	<0.4	Sighinolfi and Santos, 1976
Acid-intermediate granulites	RB 253 Itaberaba-Iacu, Bahia State, Brazil	1	1.5	Sighinolfi and Santos, 1976
Acid-intermediate granulites	RB 254 Itaberaba-Iacu, Bahia State, Brazil	1	4.4	Sighinolfi and Santos, 1976
Acid-intermediate granulites	RB 266 Itaberaba-Iacu, Bahia State, Brazil	1	1.7	Sighinolfi and Santos, 1976
Acid-intermediate granulites	CQ 3 Senhor do Bonfim, Bahia State, Brazil	1	1.1	Sighinolfi and Santos, 1976
Acid-intermediate granulites	CQ 5 Senhor do Bonfim, Bahia State, Brazil	1	<0.4	Sighinolfi and Santos, 1976
Acid-intermediate granulites	ES 13 Nanuque, Bahia State, Brazil	1	0.8	Sighinolfi and Santos, 1976
Acid-intermediate granulites	ES 35 Nanuque, Bahia State, Brazil	1	0.9	Sighinolfi and Santos, 1976
Acid-intermediate granulites	NP 1 Rio Pardo, Bahia State, Brazil	1	1.0	Sighinolfi and Santos, 1976
Acid-intermediate granulites	NP 13 Rio Pardo, Bahia State, Brazil	1	0.8	Sighinolfi and Santos, 1976
Acid-intermediate granulites	NP 14 Rio Pardo, Bahia State, Brazil	1	0.4	Sighinolfi and Santos, 1976
Acid-intermediate granulites	NP 15 Rio Pardo, Bahia State, Brazil	1	0.5	Sighinolfi and Santos, 1976
Acid-intermediate granulites	NS 4 Rio Salgado, Bahia State, Brazil	1	0.7	Sighinolfi and Santos, 1976
Acid-intermediate granulites	NS 7 Rio Salgado, Bahia State, Brazil	1	1.2	Sighinolfi and Santos, 1976
Acid-intermediate granulites	NS 10 Rio Salgado, Bahia State, Brazil	1	<0.4	Sighinolfi and Santos, 1976
Acid-intermediate granulites	NS 11 Rio Salgado, Bahia State, Brazil	1	0.4	Sighinolfi and Santos, 1976
Acid-intermediate granulites	NS 12 Rio Salgado, Bahia State, Brazil	1	0.5	Sighinolfi and Santos, 1976
Acid-intermediate granulites	NS 14 Rio Salgado, Bahia State, Brazil	1	0.7	Sighinolfi and Santos, 1976
Acid-intermediate granulites	JP 48 Bahia State, Brazil	1	1.0	Sighinolfi and Santos, 1976

Rock type	Sample No./Location	n	Au (ng/g)	Author, Year
Acid-intermediate granulites	GH 17 Bahia State, Brazil	1	1.4	Sighinolfi and Santos, 1976
Acid-intermediate granulites	P 323 Bahia State, Brazil	1	1.1	Sighinolfi and Santos, 1976
Acid-intermediate granulites	RP 8 Bahia State, Brazil	1	0.8	Sighinolfi and Santos, 1976
Acid-intermediate granulites	RP 10 Bahia State, Brazil	1	<0.4	Sighinolfi and Santos, 1976
Acid-intermediate granulites	P 127 Bahia State, Brazil	1	3.0	Sighinolfi and Santos, 1976
Acid-intermediate granulites	P 129 Bahia State, Brazil	1	<0.4	Sighinolfi and Santos, 1976
Felsic				
Porphyritic tonalite gneiss	47L113 Idaho Batholith	1	2.1	Gottfried et al., 1972
Charnokite, flesic granulite	A 8 Ivrea-Verbano complex, Western Alps	1	<0.6	Sighinolfi and Gorgoni, 1977
Charnokite, flesic granulite	MO 307 Ivrea-Verbano complex, Western Alps	1	<0.6	Sighinolfi and Gorgoni, 1977
Charnokite, flesic granulite	MO 105 Ivrea-Verbano complex, Western Alps	1	2.1	Sighinolfi and Gorgoni, 1977
Charnokite, flesic granulite	B 2 Ivrea-Verbano complex, Western Alps	1	2.2	Sighinolfi and Gorgoni, 1977
Charnokite, flesic granulite	DB 17 Ivrea-Verbano complex, Western Alps	1	4.6	Sighinolfi and Gorgoni, 1977
Stronalithes, flesic granulite	MO 41 Ivrea-Verbano complex, Western Alps	1	1.4	Sighinolfi and Gorgoni, 1977
Stronalithes, flesic granulite	MO 88 Ivrea-Verbano complex, Western Alps	1	2.2	Sighinolfi and Gorgoni, 1977
Stronalithes, flesic granulite	MO 202 Ivrea-Verbano complex, Western Alps	1	2.0	Sighinolfi and Gorgoni, 1977
Stronalithes, flesic granulite	MO 316 Ivrea-Verbano complex, Western Alps	1	3.5	Sighinolfi and Gorgoni, 1977
Stronalithes, flesic granulite	09 V Ivrea-Verbano complex, Western Alps	1	6.7	Sighinolfi and Gorgoni, 1977
Metasediments				
Aluminous schist, gneiss	Baffin Island	Comp*	2.4	Shaw et al., 1976
Aluminous schist, gneiss	Northern Quebec-Ungava,Canadian Shield	Comp*	2.80	Shaw et al., 1976
Mica-garnet gneiss	New York City, U.S.A.	1	1.8	Degrazi and Haskin, 1964
Unknown Grade				
Felsic				
Archean metafelsic volcanics	Central East China	38	0.25	Gao et al., 1998

Rock type	Sample No./Location	n	Au (ng/g)	Author, Year
Metasediments				
Quartzite	Rib Mt., Wisconsin, U.S.A.	1	7.3	Degrazi and Haskin, 1964
Quartzite	Devils' Lake, Wisconsin, U.S.A.	1	2.4	Degrazi and Haskin, 1964

b.d. = below detection
Comp* indicates representative composite sampling

Bibliography

Ague, J.J. 2003. Fluid Flow in the Deep Crust. In: Rudnick, R., ed. Volume 3 The Crust, *Treatise on Geochemistry* (Holland, H. D., and Turekian, K. K. Eds.), Elsevier-Pergamon, Oxford, p.195-228.

Alirezaei, S. and Cameron, E. M., 2002. Mass balance during gabbro-amphibolite transition, Bamble Sector, Norway: implications for petrogenesis and tectonic setting of the gabbros. *Lithos* **60**, 21-45.

Asif, M. and Parry, S. J., 1989. Elimination of Reagent Blank Problems in the Fire-Assay Pre-Concentration of the Platinum Group Elements and Gold with a Nickel Sulfide Bead of Less Than One Gram Mass. *Analyst* **114**, 1057-1059.

Binns, R.A., Gunthorpe, R.J., and Groves, D.I., 1976. Metamorphic patterns and development of greenstone belts in the eastern Yilgarn block, Western Australia. In: *The Early History of the Earth* (ed. Windley, B.F.), pp. 303-313. Wiley, London.

Blondes, M. S., Brandon, M. T., Reiners, P. W., Page, F. Z., and Kita, N. T., 2013. Generation of Forsteritic Olivine (Fo 99.8) by Subsolidus Oxidation in Basaltic Flows. *J. Petrol.* **53**, 971-984.

Borisov, A. & Palme, H. 1996. Experimental determination of the solubility of Au in silicate melts. Mineral. Petrol. 56: 297-312.

Boyle, R.W., and Jonasson, L.R., 1984. The geochemistry of antimony and its use as an indicator element in geochemical prospecting. *Journal of Geochemical Exploration,* **20**, 223-302.

Brenan, J. M. and McDonough, W. F., 2009. Core formation and metal-silicate fractionation of osmium and iridium from gold. *Nature Geoscience* **2**, 798-801.

Brenan, J. M., McDonough, W. F., and Ash, R., 2005. An experimental study of the solubility and partitioning of iridium, osmium and gold between olivine and silicate melt. *Earth Planet. Sci. Lett.* **237**, 855-872.

Brugmann, G. E., Naldrett, A. J., Asif, M., Lightfoot, P. C., Gorbachev, N. S., and Fedorenko, V. A., 1993. Siderophile and Chalcophile Metals as Tracers of the Evolution of the Siberian Trap in the Norilsk Region, Russia. *Geochim. Cosmochim. Acta* **57**, 2001-2018.

Cameron, E. M., 1988. Archean Gold - Relation to Granulite Formation and Redox Zoning in the Crust. *Geology* **16**, 109-112.

Cameron, E. M., 1989. Scouring of Gold from the Lower Crust. *Geology* **17**, 26-29.

Cameron, E. M., 1994. Mobilization of gold in the deep crust: evidence from mafic intrusions in the Bamble belt, Norway. *Lithos* **30**, 151-166.

Candela, P.A. 2003. Ores in the Earth's Crust. In: Rudnick, R., ed. Volume 3 The Crust, *Treatise on Geochemistry* (Holland, H.D. and Turekian, K.K., eds.), Elsevier-Pergamon, Oxford, p. 411-432.

Cartwright, I., and Oliver, N.H.S., 2000. Metamorphic fluids and their relationship to the formation of metamorphosed and metamorphogenic ore deposits. *Reviews in Economic Geology,* **11**, 81-96.

Chyi, L. L., 1982. The Distribution of Gold and Platinum in Bituminous Coal. *Economic Geology* **77**, 1592-1597.

Clough, P.W.L., and Field, D., 1980. Chemical variation in metabasites from a Proterozoic amphibolite-granulite transition zone, south Norway. *Contributions Min. and Pet.* **73**, 277-286.

Condie, K.C. 1993. Chemical composition and evolution of the upper continental crust: Contrasting results from surface samples and shales. *Chemical Geology*, **104**, 1-37.

Coveney, R. M. and Glascock, M. D., 1989. A Review of the Origins of Metal-Rich Pennsylvanian Black Shales, Central USA, with an Inferred Role for Basinal Brines. *Applied Geochemistry* **4**, 347-367.

Coveney, R. M., Murowchick, J. B., Grauch, R. I., Glascock, M. D., and Denison, J. R., 1992. Gold and Platinum in Shales with Evidence against Extraterrestrial Sources of Metals. *Chem. Geol.* **99**, 101-114.

Crocket, J. H., Macdougall, J.D., and Harriss, R. C., 1973. Gold, Palladium and Iridium in Marine Sediments. *Geochim. Cosmochim. Acta* **37**, 2547-2556.

Crocket, J. H. and Paul, D. K., 2004. Platinum-group elements in Deccan mafic rocks: a comparison of suites differentiated by Ir content. *Chem. Geol.* **208**, 273-291.

Crocket, J. H. and Paul, D. K., 2008. Platinum-group elements in igneous rocks of the Kutch rift basin, NW India: Implications for relationships with the Deccan volcanic province. *Chem. Geol.* **248**, 239-255.

Danielson, L., Sharp, T. & Hervig, R. L. 2005. Implications for core formation of the Earth from high pressure temperature Au partitioning experiments. Lunar and Planetary Science Conference XXXVI (2005) 1955.pdf

Degrazia, A. R. and Haskin, L., 1964. On the Gold Contents of Rocks. *Geochim. Cosmochim. Acta* **28**, 559-564.

DePaolo, D.J., Linn, A.M., and Schubert, G., 1991. The continental crustal age distribution: Methods of determining mantle separation ages from Sm-Nd isotopic data and application to the southwestern U.S. *Journal of Geophysical Research,* **96**, 2071-2088.

Dissanayake, C. B., Kritsotakis, K., and Tobschall, H. J., 1984. The Abundance of Au, Pt, Pd, and the Mode of Heavy-Metal Fixation in Highly Polluted Sediments from the Rhine River near Mainz, West-Germany. *International Journal of Environmental Studies* **22**, 109-119.

Etheridge, M.A., Wall, V.J., Cox, S.F., and Vernon, R.J., 1984. High fluid pressure during regional metamorphism and deformation. *Journal of Geophysical Research,* **89**, 4344-4358.

Fan, D., 1983. Polyelements in the Lower Cambrian black shale series in southern China. In: S.S. Augustithis (Editor), The Significance or Trace Metals in Solving Petrogenetic Problems and Controversies. Theophrastus, Athens, pp. 447-474.

Ferry, J.M., 1980. A case study of the amount and distribution of heat and fluid during metamorphism. *Contributions to Mineralogy and Petrology,* **71**, 373-385.

Ferry, J.M, 1981. Petrology of graphitic sulfide-rich schists from south-central Maine: an example of desulfidation during prograde regional metamorphism. *American Mineralogist,* **66**, 908-930.

Fyfe, W. S., 1973. The granulite facies, partial melting and the Archean crust. *Phil. Trans., R. Soc. London, Ser.* **A 273**, 457-461.

Fyfe, W. S., Price, N., Thompson, A.B., 1978. Fluids in the Earth's crust. *Amsterdam, Elsevier,* 383 p.

Gao, S., Luo, T. C., Zhang, B. R., Zhang, H. F., Han, Y. W., Zhao, Z. D., and Hu, Y. K., 1998. Chemical composition of the continental crust as revealed by studies in East China. *Geochim. Cosmochim. Acta* **62**, 1959-1975.

Glassley, W.E., 1982. Fluid evolution and graphite genesis in the deep continental crust. *Nature,* **295**, 229-231.

Glassley, W.E., 1983. The role of CO_2 in the chemical modification of deep continental crust. *Geochimica et Cosmochimica Acta,* **47**, 597-616.

Gottfried, D., Rowe, J.J. and Tilling, R.I., 1972. Distribution of gold in igneous rocks. *U.S. Geol. Surv., Prof. Pap*., 727, 42 pp.

Groves, D.I., Phillips, G.N., Ho, S.E., Henderson, C.A., Clark, M.E., and Woad, G.M., 1984. Controls on distribution of Archaean hydrothermal gold deposits in Western Australia. In: *Gold 82: The Geology, Geochemistry, and Genesis of Gold Deposits* (ed. Foster, R.P.), pp. 689-712. Balkema, Rotterdam.

Hamaguchi, H., Kuroda, R., Tomura, K., Osawa, M., Watanabe, K., Onuma, N., Yasunaga, T., Hosohara, K., and Endo, T., 1961. Values for Trace Elements in G-1 and W-1 with Neutron Activation Analysis. *Geochim. Cosmochim. Acta* **23**, 296-299.

Harlov, D.E., Newton, R.C., Hansen, E.C., and Janardhan, A.S., 1997. Oxide and sulphide minerals in highly oxidized, Rb-depleted, Archaean granulites of the Shevaroy Hills Massif, South India: Oxidation states and the role of metamorphic fluids. *Journal of Metamorphic Geology,* **15**, 701-717.

Harris, P.G., Reay, A., and White, I.G., 1967. Chemical composition of the upper mantle. *Jour. Geophys. Research*. **72**, 6359 – 6369.

Ho, S.E., 1984. Alternative host rocks for Archaean gold deposits: nature and genesis of hydrothermal gold deposits, Kanowna, Western Australia. *Proceedings of the Regional Conference on Gold-Mining, Metallurgy and Geology,* October, Kalgoorlie, Eastern Australia, AusIMM, Perth, pp. 405-415.

Ho, S.E., Groves, D.I., and Phillips, G.N., 1985. Fluid inclusions as indicators of the nature and source of ore fluids and ore depositional conditions for Archaean gold deposits of the Yilgarn Block, Western Australia. *Transactions of the Geological Society of South Africa,* **88**, 149-158.

Hughes, M.J., Phillips, G.N., and Gregory, L.M., 1997. Mineralogical domains in the Victorian gold province, Maldon, and Carlin-style potential. Australian Institute of Mining and Metallurgy, Annual Conference, Melbourne, pp. 215-227.

Jeong, G. Y., 2006. Mineralogy and geochemistry of metalliferous black slates in the okcheon metamorphic belt, Korea: a metamorphic analogue of black shales in the South China block. *Mineralium Deposita* **41**, 469-481.

Katz, O., Beyth, M., Miller, N., Stern, R., Avigad, D., Basu, A, and Anbar, A., 2004. A late Neoproterozoic (630 Ma) high-magnesium andesite suite from southern

Israel: implications for the consolidation of Gondwanaland. *Earth Planet Sci. Lett.,* **218**, 475-490.

Kerrich, R. and Wyman, D., 1990. Geodynamic Setting of Mesothermal Gold Deposits - an Association with Accretionary Tectonic Regimes. *Geology* **18**, 882-885.

Ketris, M. P. and Yudovich, Y. E., 2009. Estimations of Clarkes for Carbonaceous biolithes: World averages for trace element contents in black shales and coals. *International Journal of Coal Geology* **78**, 135-148.

Koide, M., Hodge, V.F., Yang, J.S., Stallard, M., Goldberg, E.G., Calhoun, J. and Bertine, K.K., 1986. Some comparative marine chemistries of rhenium, gold, silver and molybdenum. *Appl. Geochem*., 1:705-714.

Korobeynikov, A. F., 1986. Gold Distribution in Products of Differentiation of Basic and Acid Magmas of Various Geologic Epochs. *Geokhimiya*, 328-338.

Maier, W.D., Barnes, S.-J., Marsh, J.S., 2001. PGE in southern African flood basalts: implications for magmatic sulphide exploration. In: Piestrzynski, A. (Eds.), Mineral Deposits at the Beginning of the 21st Century. A.A.Balkema, Lisse, pp. 665– 668.

Manning, C. E., and Ingebritsen, S. E., 1999. Permeability of the continental crust: Implications of geothermal data and metamorphic systems. *Reviews of Geophysics*, **37**, 127-150.

Mansur, A.T. 2008. Age, Composition, and Origin of the Lower Continental Crust, Northern Tanzania. M.S. dissertation, Univeristy of Maryland, College Park.

Manya, S., 2004. Geochemistry and petrogenesis of volcanic rocks of the Neoarchaean Sukumaland Greenstone Belt, northwestern Tanzania. *Journal of African Earth Sciences* **40**, 877-900.

Manya, S., and Maboko, M. A. H., 2003. Dating basaltic volcanism in the Neoarchaean Sukumaland Greenstone Belt of the Tanzania Craton using the Sm-Nd method: implications for the geological evolution of the Tanzania Craton. *Precambrian Research* **121**, 35-45.

Manya, S., Kobayashi, K., Maboko, M. A. H., and Nakamura, E., 2006. Ion microprobe zircon U-Pb dating of the late Archaean metavolcanics and associated granites of the Musoma-Mara Greenstone Belt, Northeast Tanzania: Implications for the geological evolution of the Tanzania Craton. *Journal of African Earth Sciences* **45**, 355-366.

Manya, S., Maboko, M. A. H., and Nakamura, E., 2007. The geochemistry of high-Mg andesite and associated adakitic rocks in the Musoma-Mara Greenstone Belt, northern Tanzania: Possible evidence for Neoarchaean ridge subduction? *Precambrian Research,* **159**, 241-259.

Martin, H., 1999. Adakitic magmas: modern analogue to Archaean granitoids. *Lithos*, **46**, 411-429.

McDonough, W. F., 1990. Constraints on the composition of the continental lithospheric mantle. *Earth Planet. Sci. Lett.* **101**, 1-18.

McDonough, W. F. and Sun, S. S., 1995. The Composition of the Earth. *Chem. Geol.* **120**, 223-253.

McDonough, W.F. 2003. Compositional Model for The Earth's Core, pp547-568. In The Mantle and Core (ed. R. W. Carlson.) Vol. 2 Treatise on Geochemistry (eds. H.D. Holland and K.K. Turekian), Elsevier-Pergamon, Oxford.

Meisel, T., Moser, J., Wegscheider, W. 2001. "Recognizing heterogeneous distribution of platinum group elements (PGE) in geological materials by means of the Re-Os isotope system. 370: 566-572.

Mikucki, E.J., and Ridley, J.R., 1993. The hydrothermal fluid of Archaean lode-gold deposits at different metamorphic grades: compositional constraints from ore and wallrock alteration assemblages. *Mineralium Deposita,* **28**, 469-481.

Morgan, J.W. 1986. Ultramafic xenoliths: Clues to Earth's late accretionary history. *Journal of Geophysical Research* **91**, 12,375-12,387.

Morrison, G. H. and Freiser, H., 1962. Extraction. *Analytical Chemistry* **34**, R64-&.

Mtoro, M., Maboko, M. A. H., and Manya, S., 2009. Geochemistry and geochronology of the bimodal volcanic rocks of the Suguti area in the southern part of the Musoma-Mara Greenstone Belt, Northern Tanzania. *Precambrian Research* **174**, 241-257.

Naylor, W.I., 1961. Geology of the Geita district, Quarter degree sheet 20 and 32. *Geological Survey of Tanganyika, Dar es Salaam,* **9**, 13-18.

Neall, F.B., and Phillips, G.N., 1987. Fluid-wallrock interaction around Archean hydrothermal gold deposits: a thermodynamic model. *Economic Geology,* **82**, 1679-1694.

Newton, R. C., Smith, J. V., and Windley, B. F., 1980. Carbonic Metamorphism, Granulites and Crustal Growth. *Nature* **288**, 45-50.

Nielsen, T. F. D. and Brooks, C. K., 1995. Precious metals in magmas of East Greenland: Factors important to the mineralization in the Skaergaard intrusion. *Economic Geology and the Bulletin of the Society of Economic Geologists* **90**, 1911-1917.

Natural Resources Canada, 1994. Certificate of Analysis: TDB-1 Diabase Rock PGE Material http://www.nrcan.gc.ca/sites/www.nrcan.gc.ca.minerals-metals/files/pdf/mms-smm/tect-tech/ccrmp/cer-cer/tdb-1-eng.pdf

Orth, C. J., Quintana, L. R., Gilmore, J. S., Barrick, J. E., Haywa, J. N., and Spesshardt, S. A., 1988. Pt-Group Metal Anomalies in the Lower Mississippian of Southern Oklahoma. *Geology* **16**, 627-630.

Peach, C. L., Mathez, E. A., and Keays, R. R., 1990. Sulfide Melt Silicate Melt Distribution Coefficients for Noble-Metals and Other Chalcophile Elements as Deduced from Morb - Implications for Partial Melting. *Geochim. Cosmochim. Acta* **54**, 3379-3389.

Phillips, G. N., 1993. Metamorphic Fluids and Gold. *Mineralogical Magazine* **57**, 365-374.

Phillips, G.N., Groves, D.I., 1983. The nature of Archaean gold-bearing fluids as deduced from gold deposits of Western Australia. *Journal Geological Society of Australia,* **30**, 25-39.

Phillips, G.N., and Powell, R., 2009. Formation of gold deposits: review and evaluation of the continuum model. *Earth-Science Reviews,* **94**, 1-21.

Phillips, G.N., and Powell, R., 2010. Formation of gold deposits: a metamorphic devolatilization model. *Journal of Metamorphic Geology,* **28**, 689-718.

Pitcairn, I. K., Warwick, P. E., Milton, J. A., and Teagle, D. A. H., 2006a. Method for ultra-low-level analysis of gold in rocks. *Analytical Chemistry* **78**, 1290-1295.

Pitcairn, I. K., Teagle, D. A. H., Craw, D., Olivo, G. R., Kerrich, R., and Brewer, T. S., 2006b. Sources of metals and fluids in orogenic gold deposits: Insights from the Otago and Alpine schists, New Zealand. *Economic Geology* **101**, 1525-1546.

Quennell, A.M., McKinlay, A.C.M., and Aitken, W.G., 1956. Summary of the geology of Tanganyika: Part I; Introduction and stratigraphy. *Geological Survey of Tanganyika, Dar es Salaam, Memoir* **1**, 1-264.

Ridley, J., 1995. Archaean gold deposits in amphibolite-facies terranes, with special reference to the Southern Cross greenstone belt. In: Schwebel, P.J., ed.

Southern Cross Greenstone Belt: Geology and Gold Mines, Extended Abstracts, pp. 17-20.

Robert, F., and Kelly, W.C., 1987. Ore-forming fluids in Archean gold-bearing quartz veins at the Sigma mine, Abitibi Greenstone Belt, Quebec, Canada. *Economic Geology,* **82**, 1464-1482.

Rudnick, R. L. and Gao, S., 2003. Composition of the Continental Crust. In: Rudnick, R., ed. Volume 3 The Crust, *Treatise on Geochemistry,* (Holland, H. D., and Turekian, K. K. Eds.), Elsevier-Pergamon, Oxford, p. 1-64.

Ryabchikov, I. D., Baranova, N. N., Zotov, A. V., and Orlova, G. P., 1985. Stability of $Au(OH)^0$ in Supercritical Phase of Water and Metal-Bearing Capacity of Magmatic Fluids Being in Equilibrium with Granite Magma. *Geokhimiya*, 267-268.

Seward, T. M., 1973. Thio Complexes of Gold and Transport of Gold in Hydrothermal Ore Solutions. *Geochim. Cosmochim. Acta* **37**, 379-399.

Shaw, D. M., Dostal, J., and Keays, R. R., 1976. Additional Estimates of Continental Surface Precambrian Shield Composition in Canada. *Geochim. Cosmochim. Acta* **40**, 73-83.

Sighinolfi, G. P. and Gorgoni, C., 1977. Gold Distribution in Ivrea - Verbano Gabbroic Complex. *Chem. Geol.* **20**, 99-107.

Sighinolfi, G. P. and Santos, A. M., 1976a. Determination of Gold in Geological Samples at Parts Per Milliard Levels by Flameless Atomic-Absorption Spectroscopy. *Mikrochimica Acta* **2**, 33-40.

Sighinolfi, G. P. and Santos, A. M., 1976b. Geochemistry of Gold in Archean Granulite Facies Terrains. *Chem. Geol.* **17**, 113-123.

Taylor, S.R. and McLennan, S.M. 1985. The continental crust and its composition and evolution. Oxford-Blackwell.

Taylor, W. R., Rock, N. M. S., Groves, D. I., Perring, C. S., and Golding, S. D., 1994. Geochemistry of Archean Shoshonitic Lamprophyres from the Yilgarn Block, Western-Australia - Au Abundance and Association with Gold Mineralization. *Applied Geochemistry* **9**, 197-222.

Terashima, S., Nakao, S., Mita, N., Inouchi, Y., and Nishimura, A., 1995. Geochemical Behavior of Au in Terrigenous and Pelagic Marine-Sediments. *Applied Geochemistry* **10**, 35-44.

Theriault, R. D., Barnes, S. J., and Severson, M. J., 1997. The influence of country-rock assimilation and silicate to sulfide ratios (R factor) on the genesis of the Dunka road Cu-Ni-platinum-group element deposit, Duluth complex, Minnesota. *Canadian Journal of Earth Sciences* **34**, 375-389.

Togashi, S. and Terashima, S., 1997. The behavior of gold in unaltered island arc tholeiitic rocks from Izu-Oshima, Fuji, and Osoreyama volcanic areas, Japan. *Geochim. Cosmochim. Acta* **61**, 543-554.

Vincent, E. A. and Crocket, J. H., 1960. Studies in the Geochemistry of Gold .2. The Gold Content of Some Basic and Ultrabasic Rocks and Stone Meteorites. *Geochim. Cosmochim. Acta* **18**, 143-148.

Walther, J.P., and Orville, P.M., 1982. Volatile transport and production in regional metamorphism. *Contributions to Mineralogy and Petrology,* **79**, 252-257.

Wedepohl, K. H., 1995. The Composition of the Continental-Crust. *Geochim. Cosmochim. Acta* **59**, 1217-1232.

White, C. E. and Goodwin, T. A., 2011. Lithogeochemistry, petrology, and the acid-generating potential of the Goldenville and Halifax groups and associated granitoid rocks in metropolitan Halifax Regional Municipality, Nova Scotia, Canada. *Atlantic Geology* **47**, 158-184.

Yardley, B.W.D., 1986. Fluid migration and veining in the Connemara schists. *Advances in Physical Geochemistry*, **5**, 109-131.

Yogodzinski, G.M., Kay, R.W., Volynets, O.N., Koloskov, A.V., and Kay, S.M., 1995. Magnesian andesite in the western Aleutian Komandorosky region: Implications for slab melting and processes in the mantle wedge. *Geol. Soc. Am. Bull.,* **107**, 505-519.

Zajacz, Z., Seo, J. H., Candela, P. A., Piccoli, P. M., Heinrich, C. A., and Guillong, M., 2010. Alkali metals control the release of gold from volatile-rich magmas. *Earth Planet. Sci. Lett.* **297**, 50-56.

Zentilli, M., Brooks, R. R., Helgason, J., Ryan, D. E., and Zhang, H., 1985. The Distribution of Gold in Volcanic-Rocks of Eastern Iceland. *Chem. Geol.* **48**, 17-28.